

SJCE
SCIENTIFIC
JOURNAL
OF CIVIL
ENGINEERING

Volume 10
Issue 2
December 2021

ISSN - 1857 - 839X

SJCE
SCIENTIFIC
JOURNAL
OF CIVIL
ENGINEERING



EDITORIAL - Preface to Volume 10 Issue 2 of the Scientific Journal of Civil Engineering (SJCE)

Marijana Lazarevska EDITOR - IN - CHIEF

Dear Readers,

Scientific Journal of Civil Engineering (SJCE) is an international, peer-reviewed, open access journal published bi-annually since December 2012. As of December 2021, SJCE has its own web page and offers a completely digital submission, review, and publication process. For more information regarding the online version of the Journal, please visit www.sjce.gf.ukim.edu.mk.

This Journal is committed to publish and disseminate high quality and novel scientific research work in the broad field of engineering sciences. SJCE is designed to advance technical knowledge and to foster innovative engineering solutions in the field of civil engineering, geotechnics, survey and geo-spatial engineering, environmental protection, construction management etc.

Our aim is to provide the best platform for the researchers to publish their work with transparency and integrity with the open-access model, and to provide a forum for original papers on theoretical and practical aspects of civil engineering and related sub-topics.

As an editor-in-chief of the Scientific Journal of Civil Engineering, it is my great pleasure to present you the **Second Issue of Volume 10**, an open-subject issue that contains ten scientific-research papers that have passed the double-blind, external peer review.

These papers cover various advanced scientific topics. The first paper presents the results of the hydrological analysis conducted for Vardar River section. The second paper deals with the heavy rainfall as an extremely stochastic phenomenon, describing the importance of quality data measurement and data updating for climate studies, water resources evaluation, drainage designs etc. The development of real estate mass valuation model for condominiums in Skopje is shown in the third

paper. The fourth paper presents the basic settings and measures for achieving a safe intersection with a roundabout, in terms of pedestrian and bicycle traffic. The main subject of the fifth paper is comparison of the results obtained from linear and non-linear seismic analysis of concrete frame structure designed according to principles of Eurocode 8 and capacity design method. The design of steel frame with variable cross-section considering stability using general method is explained in detail in the sixth paper of the Journal. The next paper presents the results from structural analysis performed on twelve models of T-joints from hollow cross sections reinforced with welded flange plate on the chord. This eighth paper deals with the identification of chemical anchors embedded in reinforced concrete slab under tension load. The next paper shows one example of civil engineering research conducted with the Delphi method, as one of the most popular scientific research methods used for problems that lack known data. The last paper describes a creation of the information system that gives an insight into the critical bridge infrastructure network elements and can identify the losses that can be caused by earthquake.

I sincerely hope that all papers published in this issue will encourage further researches on the fields.

I thank all the authors for contributing to this Issue and all the reviewers for providing detailed and timely evaluations of the submitted manuscripts. Furthermore, I would like to express my sincere gratitude to all editor members for their excellent work, remarkable contribution, enthusiasm and support.

Sincerely Yours,
Assoc. Prof. Dr. Marijana Lazarevska
December, 2021

FOUNDER AND PUBLISHER

Faculty of Civil Engineering
Partizanski odredi 24, 1000
Skopje, N. Macedonia

PRINT

This Journal is printed in Mar-saz
DOOEL Skopje

EDITORIAL OFFICE

Faculty of Civil Engineering
Partizanski odredi 24, 1000
Skopje, N. Macedonia
tel. +389 2 3116 066
fax. +389 2 3118 834
prodekan.nauka@gf.ukim.edu.mk

EDITOR IN CHIEF

Assoc. Prof. PhD **Marijana Lazarevska**
University "Ss. Cyril and Methodius"
Faculty of Civil Engineering
Partizanski odredi 24, 1000
Skopje, N. Macedonia
marijana@gf.ukim.edu.mk

EDITORIAL ADVISORY BOARD

Prof. PhD **Elena Dumova-Jovanoska**
University "Ss. Cyril and Methodius", Skopje, N. Macedonia

Assoc. Prof. PhD **Zlatko Bogdanovski**
University "Ss. Cyril and Methodius", Skopje, N. Macedonia

TECHNICAL EDITORS

MSc **Milica Jovanoska**
Assistant, University "Ss. Cyril and Methodius", Skopje, N. Macedonia

PhD **Kristina Milkova**
Assistant, University "Ss. Cyril and Methodius", Skopje, N. Macedonia

MSc **Riste Volcev**
Assistant, University "Ss. Cyril and Methodius", Skopje, N. Macedonia

ISSN: 1857-839X

EDITORIAL BOARD

Rita Bento, PhD
Instituto Superior Técnico,
Universidade de Lisboa,
Department of Civil Engineering,
Architecture and Georesources,
Lisbon, Portugal

Zlatko Bogdanovski, PhD
University "Ss. Cyril and Methodius", Faculty of Civil Engineering, Skopje, N. Macedonia

Heinz Brandl, PhD
Vienna University of Technology,
Institute for Geotechnics, Vienna,
Austria

Maosen Cao, PhD
Hohai University, Department of Engineering Mechanics, Nanjing, China

Eleni Chatzi, PhD
ETH Zurich, Chair of Structural Mechanics & Monitoring, Zurich, Switzerland

Tina Dasic, PhD
University of Belgrade, Faculty of Civil Engineering, Belgrade, R. Serbia

Ljupco Dimitrievski, PhD
University "Ss. Cyril and Methodius", Faculty of Civil Engineering, Skopje, N. Macedonia

Katerina Donevska, PhD
University "Ss. Cyril and Methodius", Faculty of Civil Engineering, Skopje, N. Macedonia

Elena Dumova-Jovanoska, PhD
University "Ss. Cyril and Methodius", Faculty of Civil

Engineering, Skopje, N. Macedonia

Michael Havbro Faber, PhD
Aalborg University, Department of Civil Engineering, Aalborg, Denmark

Massimo Fragiaco, PhD
University of L'Aquila, Department of Civil, Construction-Architectural & Environmental Engineering, L'Aquila, Italy

Tomas Hanak, PhD
Brno University of Technology, Faculty of Civil Engineering, Brno, Czech Republic

Nenad Ivanisevic, PhD
University of Belgrade, Faculty of Civil Engineering, Belgrade, R. Serbia

Milos Knezevic, PhD
University of Montenegro, Faculty of Civil Engineering, Podgorica, Montenegro

Andrej Kryzanowski, PhD
University of Ljubljana, Faculty of Civil and Geodetic Engineering, Ljubljana, Slovenia

Stjepan Lakusic, PhD
University of Zagreb, Faculty of Civil Engineering, Zagreb, Croatia

Marijana Lazarevska, PhD
University "Ss. Cyril and Methodius", Faculty of Civil Engineering, Skopje, N. Macedonia

Peter Mark, PhD
Ruhr University, Faculty of Civil and Environmental Engineering, Bochum, Germany

Marc Morell
Institute des Sciences de l'Ingénieur de Montpellier, France

Vlastimir Radonjanin, PhD

University of Novi Sad, Faculty of
Technical Sciences, Novi Sad,
R. Serbia

Marina Rakocevic, PhD

University of Montenegro, Faculty
of Civil Engineering, Podgorica,
Montenegro

Resat Ulusay, PhD

Hacettepe University, Faculty of
Engineering, Ankara, Turkey

Joost C. Walraven, PhD

Delft University of Technology,
Department of Civil Engineering,
Delft, Netherlands

Zlatko Zafirovski, PhD

University "Ss. Cyril and
Methodius", Faculty of Civil
Engineering, Skopje, N.
Macedonia

Ales Znidaric, PhD

ZAG – Slovenian National Building
and Civil Engineering Institute,
Ljubljana, Slovenia

COVER DESIGN:

Prof. PhD **Mitko Hadzi Pulja**

Mr. Arh **Darko Draganovski**

Faculty of Architecture, University
"Ss. Cyril and Methodius", Skopje,
N. Macedonia

ORDERING INFO

SJCE is published bi-annually.

All articles published in the journal
have been reviewed.

Edition: 100 copies

SUBSCRIPTIONS

Price of a single copy:
for Macedonia (500 den);
for abroad (10 EUR + shipping
cost).

**BANKING DETAILS
(NORTH MACEDONIA)**

Narodna banka na RNM
Account number:
160010421978815
Prihodno konto 723219,
Programa 41

**BANKING DETAILS
(INTERNATIONAL)**

Correspond bank details:
Deutsche Bundesbank Zentrale
Address: Wilhelm Epstein Strasse
14 Frankfurt am Main, Germany
SWIFT BIC: MARK DE FF
Bank details:
National Bank of the RNM
Address: Kompleks banki bb 1000
Skopje North Macedonia
SWIFT BIC: NBRM MK 2X
IBAN: MK 07 1007 0100 0036 254
Name: Gradezen fakultet Skopje

HOW WOULD YOU TAKE YOUR STUDYING?

STAY IN



TAKEOUT



ON THE GO



CONTENTS

V. Gjesovska, B. Ilioski APPLICATION OF HEC-RAS FOR ANALYSIS OF FLOOD ZONES	5
V. Gjesovska, G. Taseski, B. Ilioski HEAVY RAINFALL IN THE R.N. MACEDONIA	19
Gj. Gjorgjiev, V. Gjorgjiev, N. Malijanska DEVELOPMENT OF REAL ESTATE MASS VALUATION MODEL FOR CONDOMINIUMS IN SKOPJE	31
K. Harapovic SAFETY OF PEDESTRIANS AND CYCLISTS AT ROUNDABOUTS	41
I. Mrdak, M. Rakocevic EUROCODE - BASED SEISMIC ASSESSMENT OF FRAME STRUCTURE WITH NON - LINEAR DYNAMIC ANALYSIS	51
H. Pasternak, Z. Li DESIGN OF STEEL FRAME WITH VARIABLE CROSS-SECTION CONSIDERING STABILITY USING GENERAL METHOD ACCORDING TO EN 1993-1-1	59
E. Popovska, M. Partikov, D. Popovski STIFFNESS COMPARISON OF UNSTIFFENED AND STIFFENED T - JOINTS OF HOLLOW SECTIONS	65
D. Popovski, M. Partikov, I. Micevski PULL-OUT TEST FOR CHEMICAL ANCHORS	71
J. Topalic Markovic, V. Mucenski, I. Pesko ONE EXAMPLE OF CIVIL ENGINEERING RESEARCH CONDUCTED WITH THE DELPHI METHOD	77
M. Vitanova, J. Bojadjeva, S. Micajkov REGIONAL INFRASTRUCTURE INVENTORY TOWARD SEISMIC NETWORK SAFETY	83



SELECT A PROFESSION

CREATIVE	SOPHISTICATED	RECOGNIZED	RESPONSIBLE
ENDURING	UP-TO-DATE	WORLWIDE	IMPORTANT

WWW.GF.UKIM.EDU.MK



OUR FACULTY CAN GIVE YOU

IMPULSE !	SCHOLARSHIPS FOR THE BEST	ASSURANCE !	COOPERATION WITH INDUSTRY AND INTERNATIONAL UNIVERSITIES
SIMPLE ENROLLMENT	MOTIVATION !	100% EMPLOYMENT AND INTERNATIONALLY RECOGNIZED DIPLOMA	SUPPORT !

WWW.GF.UKIM.EDU.MK

Violeta Gjeshovska

PhD, Associate Professor
University "Ss. Cyril and Methodius"
Faculty of Civil Engineering - Skopje,
N. Macedonia
violetag@gf.ukim.edu.mk

Bojan Ilioski

MSc, Civil engineer
University "Ss. Cyril and Methodius"
Faculty of Civil Engineering - Skopje,
N. Macedonia
bojaniloski@hotmail.com

APPLICATION OF HEC-RAS FOR ANALYSIS OF FLOOD ZONES

Timely forecasting of floods and floodplains allows measures to be taken to prevent or reduce their occurrence and/or to provide protection against their harmful effects. The flood wave from increase of the water level and the flow in the riverbed is defined as a non-stationary flow, which results in flooding of riverbeds. The use of hydraulic models to conduct flood simulations is a common practice and widely accepted for rapid and accurate definition of flood zones.

In the investigations presented in this paper, the HEC-RAS (1D, 2D, 1D / 2D) software package has been used to simulate different flood scenarios related to Vardar River.

Using the HEC-RAS software package, 1D, 2D and a combination of 1D and 2D models of a non-stationary flow have been formulated by defining the initial and the boundary conditions separately for each model. As a result of the simulation of the flood wave propagation through the riverbed, the flood zones and the most endangered areas have been defined. The obtained results and the differences among the considered models have been analyzed in order to see which model is the most appropriate for the case of a flood wave.

From the hydraulic analyses carried out by use of all three models, it is concluded that the riverbed of the Vardar river in the considered section has a very low transportation capacity and that there are flood zones along the entire length of the river. The riverbed of the Vardar river in the analyzed region, from the village Tudence to the village Jegunovce, can safely transform flows up to $Q=62 \text{ m}^3/\text{s}$.

Keywords: flood, flood wave, flood zones, HEC-RAS.

1. INTRODUCTION

Floods are among the most devastating natural disasters affecting people and infrastructure. It is therefore not surprising that modeling and predicting such events is becoming a high priority in many countries, [1]. Flood modeling involves simulation of the processes of transformation of precipitation in the hydrograph of a flood wave and its propagation through the catchment area or the river bed, [2].

In this way, flood processes consisting of upstream systems with hydrological processes and river and flood zones with hydraulic processes - are described physically or mathematically (through the use of appropriate mathematical equations) by presentation of relationships between the state of the system, the input and the output.

To analyze the morphology of the Tigris River in Baghdad and determine the capability of the riverbed, A. A. Ali et al (2012) analyzed a section with a length of 49 km, with transverse profiles at intervals of 250 meters, [3]. For this purpose, they developed a one-dimensional hydraulic model with the help of the HEC-RAS software and calibrated the obtained results according to a 10-year analysis of data from the measuring station in Baghdad, whereat they concluded that the one-dimensional model is a good method for predicting the bandwidth of a riverbed. The hydraulic model developed by use of the HEC-RAS software proved to be a good way of modeling a flood wave that provides fast and accurate data. Santillan J.R. and Dr. Paringit E.C (2013) analyzed the floods from the Marikina River in the Philippines that occurred as a result of the heavy rainfall in the river basin, [4]. Hong Quang Nguyen (2015) used the HEC-RAS software bundled with KINEROS2 software for the floods in the tropical regions of northern Vietnam, [5]. With the final results of the research, he came to the conclusion that the HEC-RAS software works well with other software.

Thaileng Thol et al. (2016) presented an analysis of flood zones for the Mekong River in Cambodia using HEC-RAS, [6]. The results of the analysis with the model from HEC-RAS were compared with the measured data for that section of the river and these agreed with each other. The authors believe that HEC-RAS analyzes are a good way of timely predicting flood zones.

With the analysis for modeling and forecasting of flood zones, Vassiliki Terezinha Galvao Boulomytis (2017) came to the conclusion that poorly performed hydrological analysis is one of the biggest reasons for poor modeling of flood wave transformation, [7]. Romali, N. et al. (2018) applied the HEC-RAS model in flood mapping and simulation of a flood map for different return periods for an urban area in the town of Segamat in Malaysia, [8]. To calculate the extreme flows with different return periods, five distribution models were tested during the flood frequency analysis. The results showed that most of the flooded areas in the simulated 100-year return period were also affected by

the historic 2011 floods. Khalfallah and Saidi (2018) presented spatial-temporal mapping and flood forecasting by using HEC-RAS-GIS for the Meyerda River, Tunisia, [9]. The authors found that obtaining information about floods in regions with poor data is a difficult and uncertain task, but it is very valuable for flood risk management in order to protect human civilization and the environment. In order to find an effective model for analyzing flood wave transformation and perform flood zone analysis, Lea Dasallas et al. (2019) developed a combined one-dimensional and two-dimensional model for the 2011 Baeksan River flood case in South Korea. The results obtained from the model show great similarities with the measured data and data from different methods of analysis, which proves that the HEC-RAS software is an excellent method for analysis of this issue, [10]. Diedhiou, R. et al. (2020) performed hydraulic modeling of the Senegal River Basin downstream the Diamond Dam using the HEC-RAS software, [11]. The results obtained by the HEC-RAS simulations refer to variations of water level, maximum flow velocities and flood propagation time. These results suggest that HEC-RAS is a useful tool for making quick and timely flood management decisions in times of crisis.

Huțanu, E. et al. (2020) developed a one-dimensional model for analysis of flood zones for the Jijia River in Romania using HEC-RAS in order to compare the results of the model with those of the model already developed in the MIKE SHE software. The comparison of the models by the authors led to the conclusion that the model based on HEC-RAS gave better results and that the software itself provided a better display of the final results, [12].

Presented in this paper is a description of the development, calibration and validation of the flood model for the Vardar river basin (R. North Macedonia) by the widely used hydraulic modeling systems HEC-RAS, [13]. Hydraulic models 1D, 2D and a combination of 1D and 2D models of a non-stationary flow have been formulated by defining the initial and boundary conditions separately for each model. The differences between these models in terms of defining flood zones as well as the advantages of applying HEC-RAS in solving such problems are discussed.

2. STUDY AREA

The river Vardar is the largest river in the R.N. Macedonia. It is 388 km long, of which 301 km are located in the Republic of Macedonia. Its

basin covers approximately 25,000 km², with a river basin area of 20,535 km² in the Macedonia. In this paper, the watershed of upper Vardar is analyzed, which extends upstream from the village of Radusa in the northwestern part of RN Macedonia, Figure 1. The catchment area of the river Vardar, opposite the village of Radusa, covers an area of 1489.19 km². In height, the catchment area extends from elevation 2747.03 m above sea level to elevation 317.57 m asl. The terrain topography data around the Vardar River used in this analysis are in digital form (DTM-Digital Terrain Model). Using the SWAT model of the Geographic Information System (GIS) for spatial analysis (SA), [14], the watershed is drawn and the shape and size of the catchment area of the river Vardar to the village Radusa is determined, Figure 2. Characteristics of the watershed upstream of the village Radusa and the village of Jegunovce are shown in Table 1.



Figure 1. Location of the upper Vardar watershed



Figure 2. Form and size of upper Vardar watershed

Table 1. Geometrical characteristics of the upper Vardar watershed

Profile	A [km ²]	O [km]	Ssr [%]	Hsr [m asl]	L [km]
Radusa	1489.1	232.2	9.37	1138.8	101.4
Jegunov	1336.6	217.3	9.24	1152.8	94.55

2.1 LAND USE

For the needs of hydrological modeling of the Vardar river basin in the upper course to the village Radusa, analysis of land use and the representation of certain classes, was done accordance with the data from CORINE Layer Classification, [15]. The data are processed and interpreted by means of the GIS software moduli, Figure 3. Table 2 shows the land use of the basin of Goren Vardar to the village Radusa according to the CORINE classification.

The most present within the watershed, accounting for more than 1031 km² (69.3%), are forests and semi-natural areas. Out of these, forests account for 516 km² (34.51%). Dominant forests are the broadleaved ones, with minor presence of mixed forests and very little, almost negligible presence of coniferous forests. Coppice forests and grass vegetation is present both in the transition areas and the higher parts of the watershed. The most present in this group is natural grass accounting for 292.87km² (19.7%) of the total watershed area, then the coppice bush vegetation covering about 148.1 km². Within the total area covered by coppice and grass vegetation amounting to 503.29 km² (33.86% of the watershed), wastelands or sclerophyllous vegetation are present to a minor scope. This category also includes open areas with little or no vegetation, accounting for about 1% of the watershed. Agricultural areas accounting for 408.0 km² (27,4%) are considerably present within the watershed and include arable land of 133.93 km², some perennial plantations accounting for 4.48 km², pastures accounting for 10.20 km², and dominant 261.81km² (17.61%) of different agricultural areas (agricultural land and complex crop rotation lands). Within the watershed, artificial areas (urban areas, industrial, commercial and transportation structures, mines, landfills and construction sites) cover 49.5 km² (3.26%) of the total watershed area.

The scale of the used network (250x250 m) does not allow accurate definition of individual categories pertaining to the third level, for example, roads and railways that exist within

the watershed. This was probably the reason for not detecting marshes and swamps as well as water bodies (small lakes on Shar Mountain and along the water courses within the watershed). Hence, this analysis of presence of individual categories of land use should be considered only indicative and done for the purposes of hydrological analysis of the watershed.

Table 2. Geometrical characteristics of the upper Vardar watersheds

Category	Area A [km ²]
Artificial surfaces	49.5
Agricultural areas	409.0
Forests	1031.0
Wetlands	0.0
Water bodies	0.0
Total	1486.1

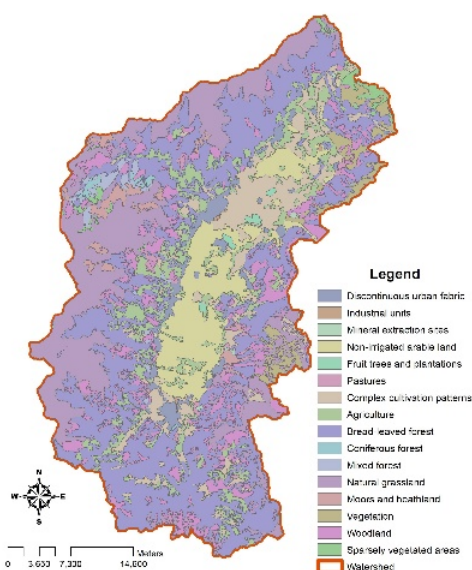


Figure 3. Land use classification

2.2 HYDROGRAPHIC CHARACTERISTICS

The river Vardar from the village Tudence to the village Jegunovce, in a total length of about 7 km, is located in the basin of Goren Vardar or in the lower part of the Polog valley. Dominant participation in the outflow and formation of flows in the river Vardar have surface waters coming from the northwestern massif, ie from the left tributaries of the river Vardar. These rivers come from the highlands of Shar Mountain, have a torrential character, carry a significant amount of sediment and flood and

degrade the fertile agricultural areas along the river Vardar. The Vardar river basin in this part is hydrographically more developed on the left side, where the larger tributaries are: Pena, Porojska / Dzepechka, Bistrica and Vratnicka.

The length of the river Vardar to the profile in Radusa is 82.33 km, and the equivalent length of the watershed is 101.43 km. The maximum altitude in the watershed is 2746 m above sea level, while the minimum altitude curve of the Vardar river basin upstream of Radusa and the summary line of the altitude distribution are shown in Figure 4. Larger tributaries of the Vardar river in this part of the watershed are the rivers Pena, Vratnicka and Bistrica. The basic characteristics of these sub watersheds are shown in Table 3.

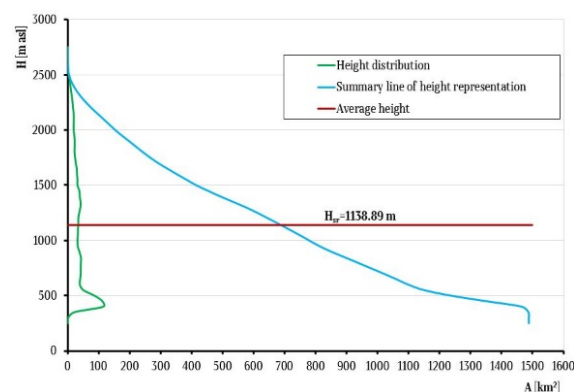


Figure 4. Hypsogram curve of the upper Vardar watershed

Table 3. Geometrical characteristics of the sub watersheds

Profile	A [km ²]	O [km]	Ssr [%]	Hsr [m H.B.]	L [km]
Pena	173.03	93.91	13.49	1681.65	39.35
Vratnicka	30.62	32.70	12.72	1393.26	13.28
Bistrica	39.30	44.35	15.02	1629.66	21.20

2.3 GEOLOGICAL AND HYDROGEOLOGICAL CHARACTERISTICS

The section of Vardar River to be regulated represents a part of the Polog valley and belongs to the Vardar tectonic zone. The geological structure of this valley is composed from sedimentary, magmatic and metamorphic rocks dating back to the Paleozoic and Mesozoic as well as Tertiary and Quaternary. The Paleozoic rocks are represented by albite-phyllite mikaschists and green shales, meta-sandy rocks, metaconglomerates, metadiabases, carbonate shales and marbles.

Mesozoic rocks are mainly represented by granites, granodiorites, massive marbleized limestone, diabases, spilites and dunites. Tertiary rocks are developed in the south part of the Polog depression and are represented by pliocene sandy layers with a thickness of 250 m. Quaternary rocks are represented by alluvial sediments, proluvial terraces, fluvio-glacial sediments and disintegrated/moraine materials.

The hydrogeological characteristics of the region can be described by the investigated and recorded aquifers. Phreatic and artesian aquifers are formed in intergranular and unconsolidated sediments. Phreatic aquifers are found in alluvial and proluvial sediments, marbles as well as in the upper Pliocene deposits at the bottom of Shar Mountain. The wells in Tetovo, Gostivar and Miletino belong to these aquifers. Phreatic aquifers belong to the group of aquifers with good yield, $1 \div 10$ l/s and > 10 l/s. The artesian aquifer is representative for Lower Polog (Dolen Polog) (village Zhilche, village Janchishte, village Jegunovce and village Raotince) and belongs to the upper Pliocene sandy/lacustrine sediments with a thickness of about 40 m. The yield of this aquifer amounts to $1 \div 10$ l/s.

3. HYDROLOGICAL ANALYSIS

Available data for the hydrological study have been found only for the station in Jegunovce (1951-2008) and the station in Radusha (1961-2008). The registered data at both stations are incomplete and they have been completed by correlation links between these two arrays of data. In the series referring to Radusha, there are interruptions in the measured data in the period from 1961 to 1968, while in the series referring to Jegunovce, there are interruptions in the period from 2001 to 2003. In order to determine the characteristic flow values for the Vardar river and define the referent discharge for proportioning the regulated river bed and facilities, hydrological analyses have been conducted for both stations at the downstream/outlet profile of the considered section, v. Jegunovtse and v. Radusha. For analysis of the flood waters, the dates of maximum annual flow have been used, specifically for the period 1951-2008 for Jegunovce and the period 1961-2008 for Radusha. To determine the flow with different return periods, several theoretical distribution functions have been applied: Gumbel, Pearson III type distribution, Log Normal distribution, Log Pearson III type distribution. The graphical presentation of the empirical and theoretical

lines of distribution of the probability of occurrence of the referent flow are shown in Figure 5 for Radusha and in Figure 6 for Jegunovce. The referent flow of the Vardar river at profiles Radusha and Jegunovce determined by the theoretical distribution functions for different probabilities of occurrence is shown in Table 4. For the theoretical distribution functions, adjustment tests have been performed with a 0.05 probability for a test overlap. The testing of the applied theoretical distribution functions has proved the best adjustments for the Gumbel distribution for both profiles.

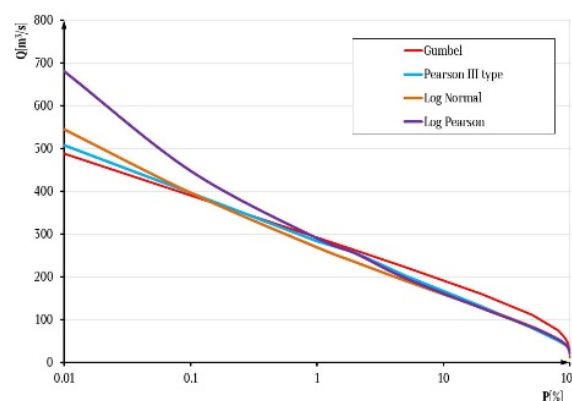


Figure 5. Lines of distribution for Radusha

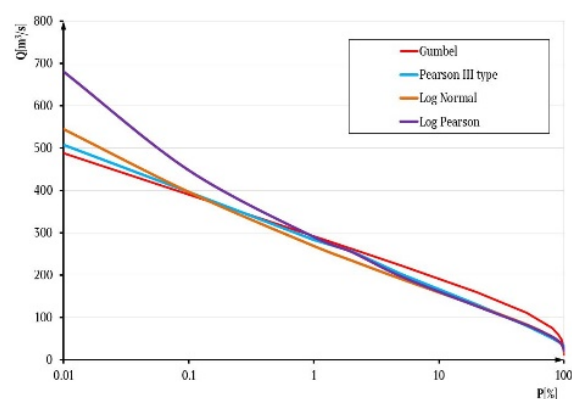


Figure 6. Lines of distribution for Jegunovce

Down to the Radusha profile, the measured flows in the observed period (1951-2008) cover all the upstream tributaries, as well as the released installed quantities from the HPP Raven (in operation for more than 40 years) whose maximum capacity is $Q=32$ m³/s. The defined characteristic flows for the Radusha profile are not much different from those at Jegunovce profile, which is, in fact, a downstream profile or a downstream boundary condition for the analyzed section. According to these statements, the characteristic flows defined for the Radusha profile have been adopted in modeling the flood zones in this part of the Vardar river.

Table 4. Flow determined by the theoretical distribution functions

T [years]	Probability p	p [%]	Radusa				Jegunovce			
			Gumbel	Pearson III type	Log- normal	Log Pearson	Gumbel	Pearson III type	Log- normal	Log Pearson
10000	0.0001	0.01	491.40	498.24	549.45	679.81	487.71	507.18	544.99	680.64
1000	0.0010	0.10	394.13	393.14	405.08	454.96	389.54	395.65	396.44	447.54
100	0.0100	1.00	296.61	285.88	279.08	300.09	291.13	283.04	268.69	289.84
50	0.0200	2.00	267.11	259.61	244.90	265.25	261.36	255.70	234.43	254.81
20	0.0500	5.00	227.73	208.41	200.83	206.75	221.62	202.67	190.58	196.44
10	0.1000	10.00	198.15	174.28	168.73	170.37	191.77	167.14	158.89	167.74
5	0.2000	20.00	165.62	143.72	136.37	135.71	158.94	131.06	127.22	126.58
2	0.5000	50.00	117.74	139.07	90.82	89.52	110.63	80.22	83.23	81.98
1.25	0.8000	80.00	82.12	88.69	60.49	60.20	74.68	50.70	54.45	54.18
1.11	0.9000	90.00	66.99	58.35	48.89	49.37	59.41	41.95	43.60	44.04
1.05	0.9500	95.00	55.88	48.60	41.07	42.28	48.20	37.03	36.35	37.47
1.01	0.9900	99.00	37.71	42.64	29.56	31.63	29.86	32.66	25.78	27.67
1.001	0.9990	99.90	20.56	37.23	20.36	23.32	12.55	31.02	17.47	20.13

4. HYDRAULIC ANALYSIS

The hydraulic analysis of the natural riverbed and the solution for the transformation of the flood wave in the investigated Vardar river section, from the bridge in the village of Jegunovce to the bridge in the village of Radusha, have been performed and obtained by using the HEC-RAS software, [16]. The riverbed has a non-prismatic cross-section, almost no straight sections and passes from one meander to another. From field prospecting

and photo documentation, it can be concluded that the river banks are overgrown with dense vegetation and that the riverbed is a recipient of significant amounts of solid and organic waste, which interfere with the flow and cause the river to overflow even in the case of small quantities of water, Figure 7. The bottom of the riverbed is variable, with a reverse slope and expressed erosive deepenings in places, especially in front of bridges. Using the photo documentation from the field, the roughness coefficient of the riverbed has been determined to amount to $n=(0.030\div 0.040) \text{ m}^{-1/3}\text{s}$ and $n=0.050\div 0.100\text{ m}^{-1/3}\text{s}$ for the flooded areas.



Figure 7. Photographs from site (field)

4.1 ONE-DIMENSIONAL MODEL (1D)

The hydraulic model for simulation of the stationary variable flow in the Vardar riverbed at the analyzed section, in addition to the information on the geometric characteristics of the riverbed, has been defined by the boundary conditions of the flow, upstream and downstream, respectively. For that purpose, the riverbed of the Vardar river has been

modeled from the bridge in the village of Jegunovce to the bridge in the village of Tudence, with a total length of 8504.41 km and a total of 80 cross-sections, Figure 8. The cross-sections have been positioned at different distances from each other, having several different lengths. The analyzed section of the Vardar river starts at chainage km 0+000.00 near the bridge in the village of Jegunovce and extends to chainage km 8+504.41 to a profile at a distance of 500 m

upstream the Tudence bridge. Assigned for the boundaries of the modeled section have been the riverbed slope in the most upstream profile at chainage km 8+504.41, $S_o = 1.5\%$ and in the lowest downstream profile at chainage km 0+000.00, $S_o = 1.47\%$, assuming that the flow in these profiles is even and gradually variable. The hydraulic analysis has been performed for 6 valid flows, namely $Q=24.2 \text{ m}^3/\text{s}$ (average multi-year flow), $Q=46.1 \text{ m}^3/\text{s}$ (average multi-year flow determined by the maximum monthly flows), $Q=62 \text{ m}^3/\text{s}$ (critical flow according to UHMR), $Q=102 \text{ m}^3/\text{s}$ (average multi-year flow determined by the maximum yearly flows), $Q=227 \text{ m}^3/\text{s}$ ($Q_{0,05}$) and $Q=267 \text{ m}^3/\text{s}$ ($Q_{0,02}$). In order to determine the impact of the bridges on the propagation of the flood wave in the riverbed and the shape of the water surface, the bridge structures have been modeled with their basic characteristics: type of structure, number of openings, number of piers, width of piers, width of openings, elevation of the

superstructure, elevation of the substructure and angle of the bridge axis in relation to the riverbed, Table 5.



Figure 8. Situation with cross sections of 1D modelling

Table 5. Basic characteristics of the bridges (Source: [17])

Bridge	Type	Stationing [km]	Number of openings	Number of piers	Width of openings [m]	Elev. of upper constr. [m asl]	Elev. of lower constr. [m asl]	Axis
Jegunovce	steel	0+030.39	1	/	38	385.74	384.01	/
Raotince	concrete	2+248.00	3	2	3/13/7.63	386.37	385.39	126
Kopance	concrete	4+262.00	2	3	8.24/7.98	388.67	388.07	65
Tudence	concrete	7+707.00	3	2	6.6/13.5/6	393.43	392.56	66

4.2 COMBINATION OF ONE AND TWO-DIMENSIONAL MODEL (1D/2D)

In the combined model of 1D and 2D, the riverbed is considered as one-dimensional element, while the inundations or flood zones are considered as two-dimensional. This means that the flow in the riverbed is a stationary variable flow, while in the inundations, there is a non-stationary flow. For that purpose, the riverbed has been modeled with the characteristic cross-sections and their characteristics, while a georeferenced topographic map has been elaborated for the inundations based on the Photogrammetric Map of Macedonia by use of the ArcMap software, [18]. In order to consider the flow in the inundations and the bank zones as two-dimensional, a 2D network has been generated for the left side of the riverbed with a total of 2407 cells sized 50x50 m and for the right side of the riverbed with a total of 2111 cells sized 50x50 m.



Figure 9. Calculation zone of 1D/2D hydraulic model of the river Vardar

The width of the net depends on the geometry of the terrain and it is usually plotted up to the assumed flood area. The riverbed and these two-dimensional flow zones are interconnected by lateral structures. The lateral structures are positioned along the entire length of the riverbed, starting from the river banks (left and right).

Assigned at the boundaries of the modeled section have been the slope of the river bottom in the most upstream profile at chainage km 8+504.41, $S_0 = 1.5\text{‰}$ and in the lowest downstream profile at chainage km 0+000.00, $S_0 = 1.47\text{‰}$. The roughness coefficient according to Manning for the riverbed is $n=0.030 \text{ m}^{-1/3}\text{s}$, while for the two-dimensional surface, it is $n=0.060 \text{ m}^{-1/3}\text{s}$. Figure 9 shows the layout of the two-dimensional computational networks and side structures in the hydraulic model.

4.3 TWO-DIMENSIONAL MODEL (2D)

In the two-dimensional model of analysis of transformation of the flood wave in the Vardar river, from the bridge in the village of Jegunovce to the bridge in the village of Tudence, the entire analyzed section, the river bed, the inundations and the bank zones are considered as two-dimensional. The flow in this model is non stationary. For that purpose, a georeferenced topographic map has been elaborated for the analyzed section of the Vardar river and a two-dimensional calculation network (area) has been generated for the riverbed, the inundations and the bank zones with a total of 38663 cells of a different size. For better results of the analysis of transformation of the flood wave in the model, the size of the cells in the 2D surface have been variable as follows: in the mid zone of the riverbed, the cells have been sized 2x4 m, in the heel zone of the river bed, the cell size has been 3x5 m, in the bank zone, the cell size has been 5x10 m, in the zone of the inundations, the cell size has been 10x30 m, at a distance of 150 m from the riverbed, the cells have been sized 30x50 m and to the end of the surface, the cells have been sized 100x100 m, Figure 10.

Due to variation of the roughness coefficients in different parts of the surface, 3 zones of variable values have been established, or more precisely, a zone in the riverbed with a roughness coefficient according to Manning of $n=0.030 \text{ m}^{-1/3}\text{s}$, an inundation zone with a roughness coefficient of $n=0.035 \text{ m}^{-1/3}\text{s}$ and bank zones with a roughness coefficient of $n=0.060 \text{ m}^{-1/3}\text{s}$.

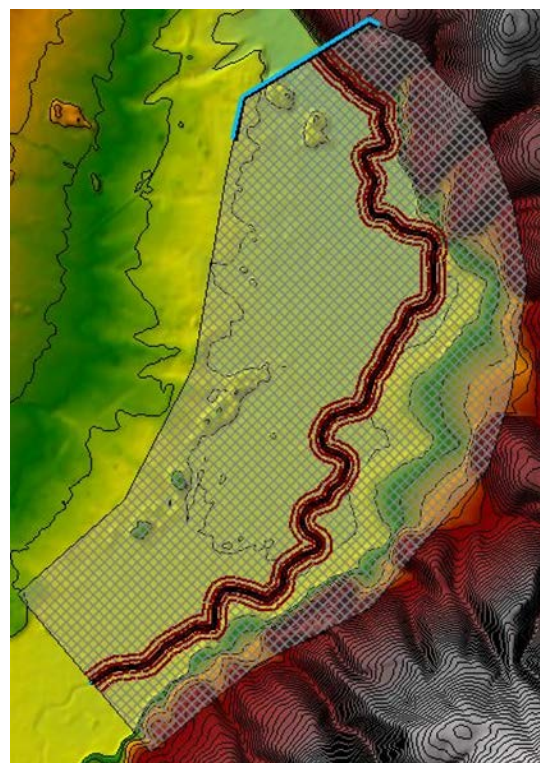


Figure 10. Calculation zone of 2D hydraulic model of the river Vardar

At the boundaries of the modeled section, boundary conditions have been assigned by means of a BC Line (Boundary condition line). In front of the very entry into the surface (according to the river flow), at the village of Tudence, a boundary condition for the beginning of the flow, namely, a flow hydrograph has been assigned, whereas, at the end of the surface, at v. Jegunovce, a boundary condition for the flow end in the form of a slope at normal depth (energy line slope) has been assigned to amount to $S=1.5 \text{‰}$.

The inlet flow hydrograph has been generated by means of flows defined during the hydrological analysis. To determine the inflow and outflow time of the hydrograph, the flood wave of Vardar river registered by UHMR at Jegunovce profile for the period 06.05.2005 to 10.05.2005 has been used. The inflow time of the hydrograph has been calculated to amount to $T_b=30 \text{ hrs}$, while the outflow time has been calculated to amount to $T_r=60 \text{ hrs}$. The construction of the curvilinear hydrograph has been based on the Gauss distribution curve. The established curvilinear hydrograph for the profile near the village of Jegunovce is shown in Figure 11.

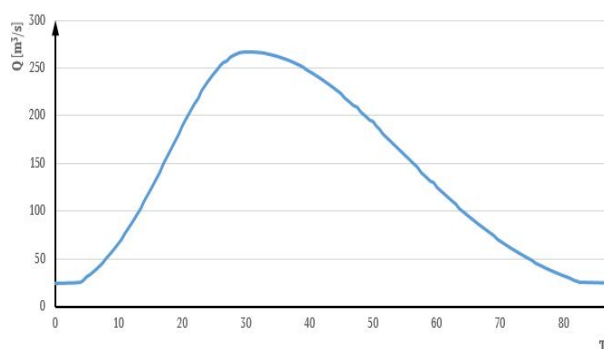


Figure 11. Flow hydrograph for the profile at v.Jegunovce

5. ANALYSIS OF RESULTS

The hydraulic analysis conducted by use of the one-dimensional model has shown that, for the flows of $Q=24.2 \text{ m}^3/\text{s}$ and $Q=46.1 \text{ m}^3/\text{s}$, there will be no overflow in any part of the analyzed river section. For flows close to the critical $Q=62 \text{ m}^3/\text{s}$, the first overflows occur as presented in Table 6. The same table contains a description of the location of the cross-sections with chainage and lateral (left/right) overflow for the registered critical flow $Q=62 \text{ m}^3/\text{s}$.

Table 6. Critical cross sections of overflow

Profile	Stationing [km]	Overflow		Profile	Stationing [km]	Overflow	
		left	right			left	right
5	0+213.92	✓		23	2+102,01		✓
6	0+288.49	✓		28	2+378.25	✓	✓
8	0+610.81	✓		29	2+447.72		✓
9	0+711.52	✓		32	2+733.78	✓	
10	0+819.91	✓		35	3+034.39	✓	
11	0+910.90	✓		36	3+125.80	✓	
12	1+050.71	✓		37	3+251.29	✓	
13	1+205.63	✓	✓	42	3+919.02	✓	✓
14	1+331.20		✓	52	5+035.67		✓
15	1+413.10		✓	62	6+512.07	✓	
16	1+536.07	✓		69	7+586.88	✓	
17	1+652.77	✓	✓	72	7+806.71	✓	
18	1+780.17	✓	✓	73	7+878.63	✓	
19	1+854.71	✓	✓	74	7+956.86	✓	
20	1+913.68	✓	✓	75	8+108.79	✓	
21	1+992.00	✓	✓	76	8+198.70	✓	
22	2+065.49		✓	77	8+265.40		✓

From the conducted hydraulic analysis, it can be concluded that the riverbed of the Vardar river in the analyzed region, from the village Tudence to the village Jegunovce, can safely transform flows up to $Q=62 \text{ m}^3/\text{s}$. Larger flows cause the river to overflow, with the first flooded zones appearing upstream from the village Raotince. With the increase of the water level, the overflow intensifies and the flooded zones become bigger, Figure 12. The flow regime for all characteristic flows is subcritical and the Froude numbers are less than the critical value, $Fr < 1$. Small and medium flows pass through the bridge openings without any problems. However, the observed deepening of the bottom in the area of the bridges, indicates the

presence of erosion of the bridge piers even at these small flows. The position of the bridges and the layout of the bridge piers are hydraulically unfavorable and cause flow slow down, raising the level in the riverbed upstream the bridges. The bridges in the analyzed region generally sustain flows of up to $Q=100 \text{ m}^3/\text{s}$ without any overflow. The bridge near the village of Tudence safely sustains a flow of $Q=102 \text{ m}^3/\text{s}$. At $Q=228 \text{ m}^3/\text{s}$, no overflow is registered, but the flow is under pressure, endangering the bridge. The bridge in the village of Kopance has the smallest capacity, meaning that the flow is under pressure at $Q=102 \text{ m}^3/\text{s}$, while in the case of bigger flows, there is an overflow outside the riverbed. The

bridge in the village of Raotince safely sustains a flow of $Q=102 \text{ m}^3/\text{s}$, while there are signs of flow under pressure at around $Q=130 \text{ m}^3/\text{s}$. At the maximum flows with a return period of 20 and 50 years, $Q=228 \text{ m}^3/\text{s}$ and $Q=267 \text{ m}^3/\text{s}$, there is an overflow in the riverbed in inhabited places. The bridge near the village of Jegunovce can be said to be the safest compared to the other bridges. The bridge has a sufficient capacity to sustain all of the analyzed flows. At a flow of $Q=62 \text{ m}^3/\text{s}$, the velocities in the riverbed are in the range of $V=0.83 \text{ m/s}$ to $V=2.27 \text{ m/s}$. The flow velocities in the riverbed at a flow of $Q=102 \text{ m}^3/\text{s}$ are in the range of $V=1.08 \text{ m/s}$ to $V=2.66 \text{ m/s}$. At a flow of $Q=228 \text{ m}^3/\text{s}$, the velocities in the riverbed are in the range of $V=1.17 \text{ m/s}$ to $V=3.36 \text{ m/s}$. In the analysis done for the maximum flow of $Q=267 \text{ m}^3/\text{s}$, the biggest values for the flow velocity occur and they are in the range of $V=1.21 \text{ m/s}$ to $V=3.51 \text{ m/s}$.

From the analysis of flood wave transformation by use of the combined model of one- and two-dimensional flow, it has been concluded that, at small flows of $Q=24.2 \text{ m}^3/\text{s}$ and $Q=46.1 \text{ m}^3/\text{s}$, there is no overflow in the riverbed. The first overflows occur at a flow of $Q=62 \text{ m}^3/\text{s}$, in the left inundation, near the village of Raotince, Figure 13-a. From the conducted hydraulic analysis by use of the combined model, it can be concluded that, at a flow of $Q=102 \text{ m}^3/\text{s}$, there are overflows in the following cross-sections of the analyzed river: km 0+950.00 to km 2+120.00, km 2+350.00 to km 3+250.00, km 3+900.00 to km 4+200.00, km 4+500.00 to km 4+700.00, km 5+000.00 to km 5+250.00, km 5+570.00 to km 6+500.00, km 6+800.00 to km 7+020.00 and from km 8+100.00 to km 8+427.61, Figure 13-b. The flooded area during this flow covers about 35 ha. At a flow of $Q=228 \text{ m}^3/\text{s}$, an overflow occurs along the entire length of Vardar river, from the village of Tudence to the village of Jegunovce, Figure 13-c, the flooded agricultural area covering 510 ha, while at a flow of $Q=267 \text{ m}^3/\text{s}$, the flooded area increases to about 600 ha, Figure 13-d. At a flow of $Q=62 \text{ m}^3/\text{s}$, the flow velocities in the riverbed are in the range of $V=0.88 \text{ m/s}$ to $V=4.21 \text{ m/s}$, while the flow velocities in the flooded areas are in the range of $V=0.03 \text{ m/s}$ to $V=0.83 \text{ m/s}$. The maximum amount of flow that occurs in the flooded areas is $Q=4.56 \text{ m}^3/\text{s}$. Flow velocities in the riverbed at a flow of $Q=102 \text{ m}^3/\text{s}$ are in the range of $V=1.03 \text{ m/s}$ to $V=4.71 \text{ m/s}$, while the flow velocities in the flooded areas are in the range of $V=0.10 \text{ m/s}$ to $V=0.91 \text{ m/s}$. The maximum amount of flow that occurs in the flooded areas is $Q=37.83 \text{ m}^3/\text{s}$. At a flow of $Q=228 \text{ m}^3/\text{s}$, the flow velocities in the

riverbed are in the range of $V=1.24 \text{ m/s}$ to $V=5.73 \text{ m/s}$, while the flow velocities in the flooded areas are in the range of $V=0.28 \text{ m/s}$ to $V=1.00 \text{ m/s}$. The maximum amount of flow that occurs in the flooded areas is $Q=121.19 \text{ m}^3/\text{s}$. In the analysis for the maximum flow of $Q=267 \text{ m}^3/\text{s}$, the biggest flow velocities occur and they are in the range of $V=1.26 \text{ m/s}$ to $V=5.99 \text{ m/s}$ for the riverbed and in the range of $V=0.14 \text{ m/s}$ to $V=1.00 \text{ m/s}$ for the flooded areas. The maximum amount of overflow is $Q=156.25 \text{ m}^3/\text{s}$.

As in the case of the previous two models, the conclusion from the analysis done by use of the two-dimensional model is that, at small flows of $Q=24.2 \text{ m}^3/\text{s}$ and $Q=46.1 \text{ m}^3/\text{s}$, there is no overflow in the riverbed. The first overflow occurs at a flow of $Q=62 \text{ m}^3/\text{s}$ along the entire river, Figure 14. From the hydraulic analysis conducted by use of the two-dimensional model, it is concluded that, at a flow of $Q=62 \text{ m}^3/\text{s}$, the flow velocities in the riverbed are in the range of $V=0.75 \text{ m/s}$ to $V=3.92 \text{ m/s}$, while the flow velocities in the flooded areas are in the range of $V=0.03 \text{ m/s}$ to $V=0.76 \text{ m/s}$, Figure 16-a. The maximum depth in the flooded areas is $H=0.62 \text{ m}$, Figure 15-a. The flow velocities at a flow of $Q=102 \text{ m}^3/\text{s}$ are in the range from $V=0.91 \text{ m/s}$ to $V=4.22 \text{ m/s}$ in the riverbed and in the range of $V=0.08 \text{ m/s}$ to $V=0.83 \text{ m/s}$ in the flooded areas, Figure 16-b. The maximum depth in the flooded areas is $H=0.75 \text{ m}$, Figure 15-b. At a flow of $Q=228 \text{ m}^3/\text{s}$, the flow velocities in the riverbed are in the range of $V=1.04 \text{ m/s}$ to $V=5.18 \text{ m/s}$, while the flow velocities in the flooded areas are in the range of $V=0.19 \text{ m/s}$ to $V=0.95 \text{ m/s}$, Figure 16-c. The maximum depth in the flooded areas is $H=1.27 \text{ m}$, Figure 15-c. In the analysis for the maximum flow of $Q=267 \text{ m}^3/\text{s}$, the biggest flow velocities occur and they are in the range of $V=1.08 \text{ m/s}$ to $V=5.64 \text{ m/s}$ in the riverbed and in the range of $V=0.20 \text{ m/s}$ to $V=1.01 \text{ m/s}$ in the flooded areas, Figure 16-d. The maximum depth in the flooded areas is $H=1.48 \text{ m}$, Figure 15-d.

6. CONCLUSION

From the hydraulic analyses carried out by use of all three models, it is concluded that the riverbed of the Vardar river in the considered section has a very low transportation capacity and that there are flood zones along the entire length of the river. The most critical points in this section are located near the village of Raotince, the village of Kopance and the village of Tudence, where flood zones occur in

agricultural lands and inhabited places under a slight increase of flood waters.

The research that has been done so far points out the importance of having high quality input data such as high quality field documentation, high quality hydrological and hydraulic analyses, available public data for the conducting of high quality analyses of flood wave propagation and determination of flood zones. The time frame for calculations and analysis of hydraulic parameters is significantly shortened by using the HEC-RAS software. The software enables fast, accurate and precise modeling of the riverbed with all the

accompanying facilities, which is extremely important in determining the flood zones and their prevention. The ability to create different types of models such as one-dimensional, two-dimensional or a combination of both is a step forward in the analysis of flood zones.

The high quality results from the hydraulic models can be used as input parameters in preparation of maps of critical zones in floodplains. These maps can be used for analysis of flood zones, flood disaster prevention preparedness and management of the affected areas in the event of a major flood wave.

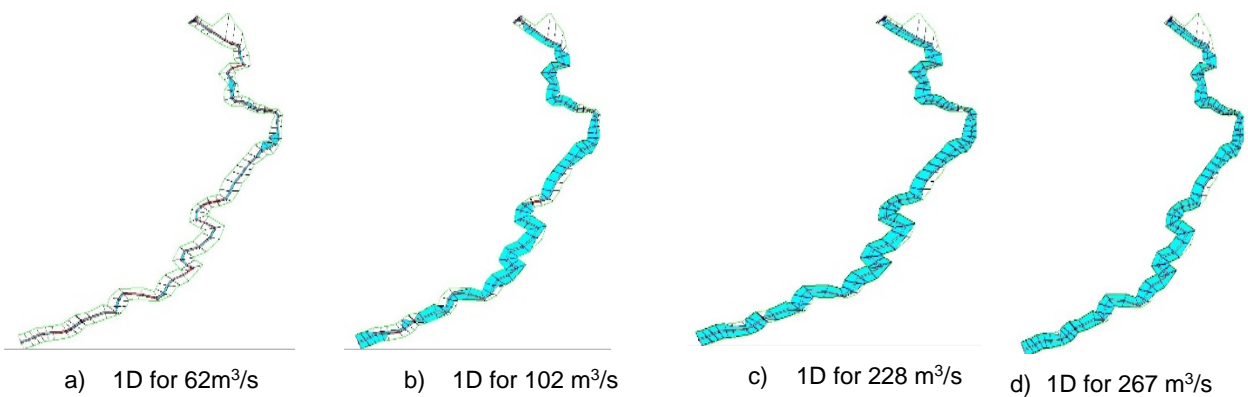


Figure 12. Flood area of 1D model

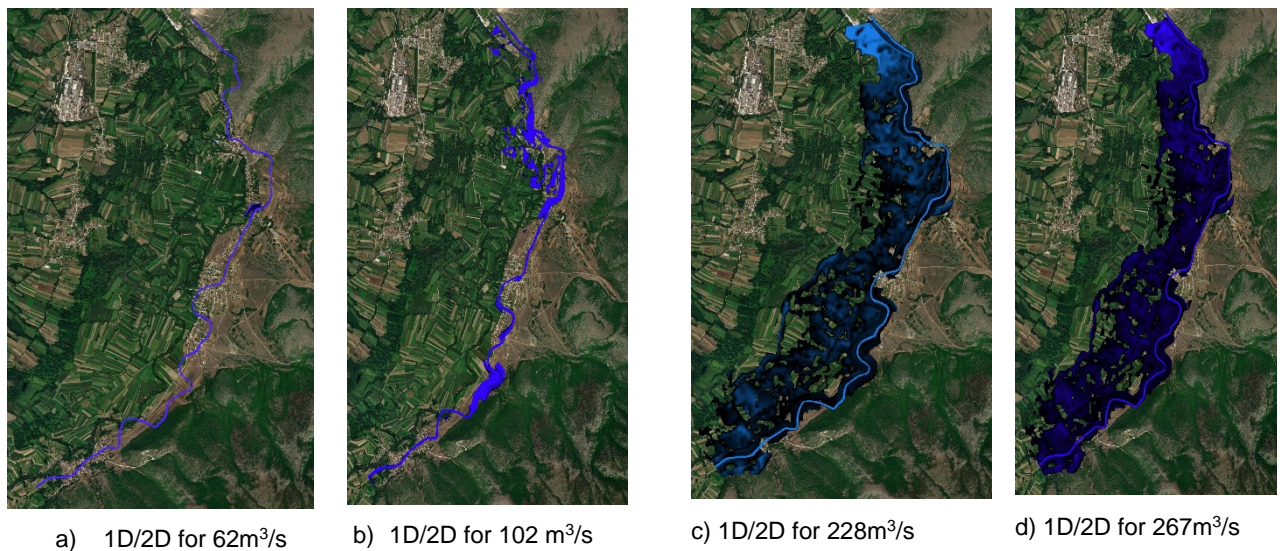


Figure 13. Flood area of 1D/2D model

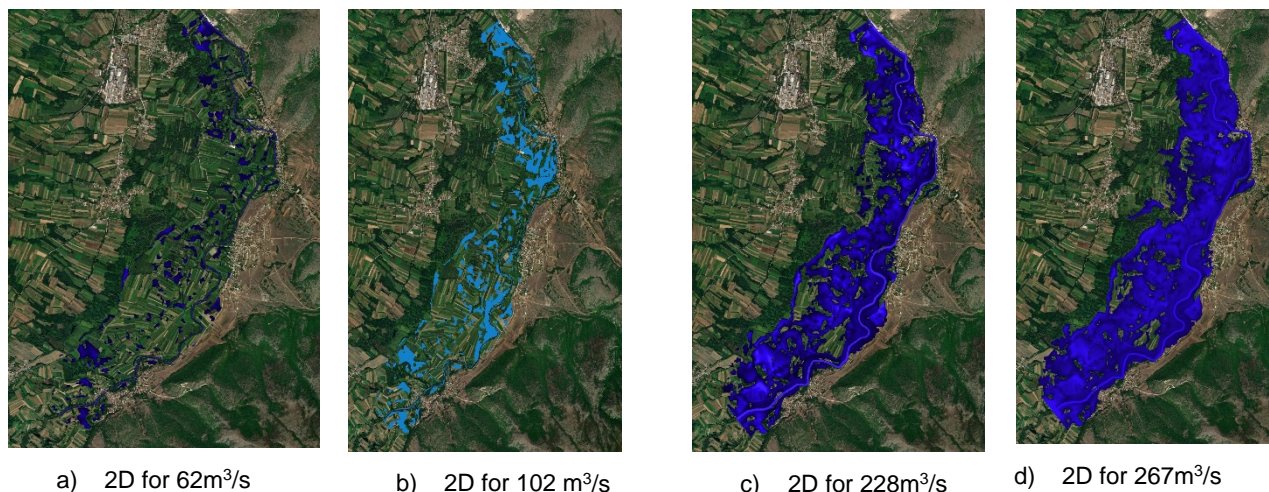


Figure 14. Flood area of 2D model

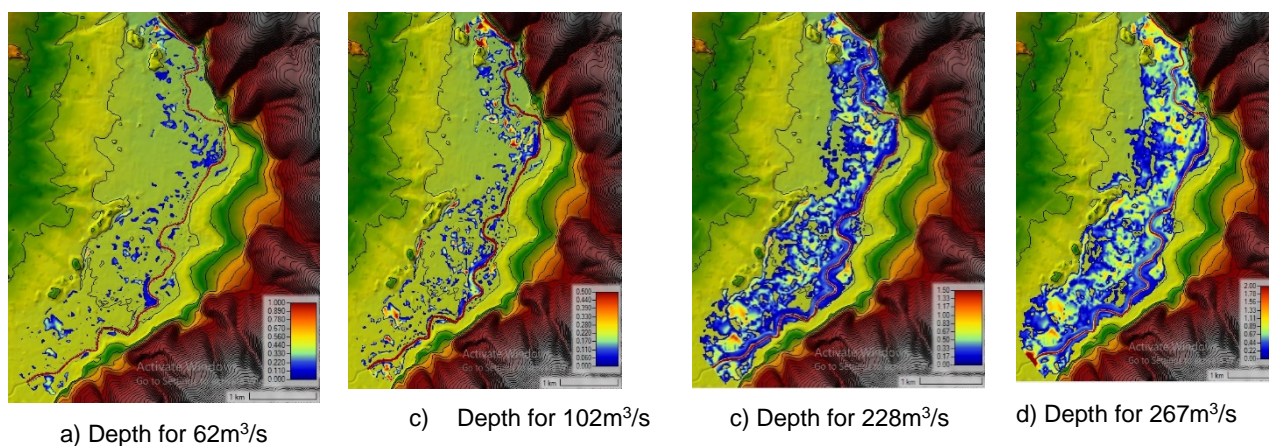


Figure 15. Water depth of 2D model

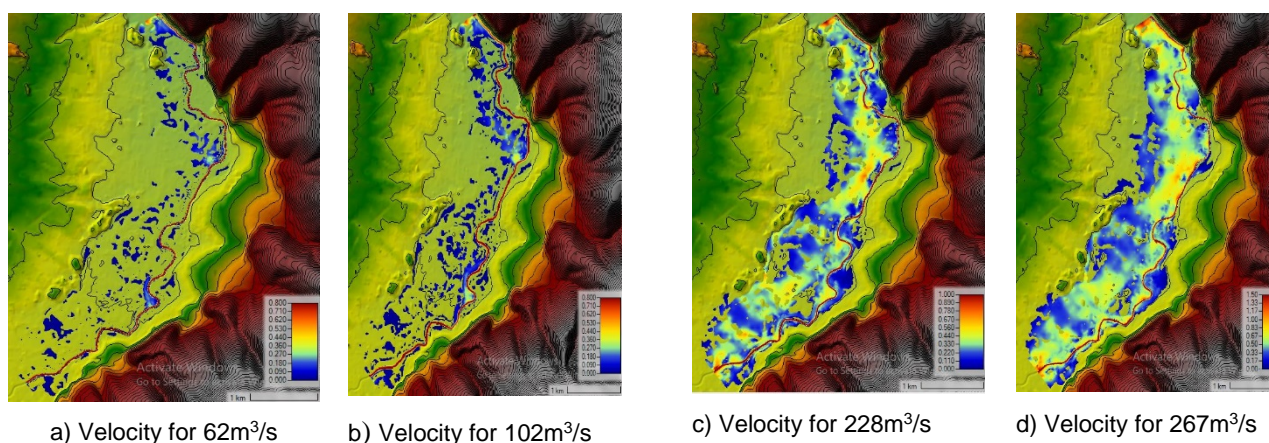
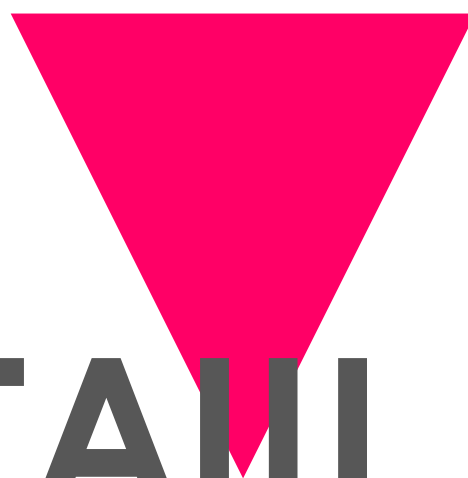
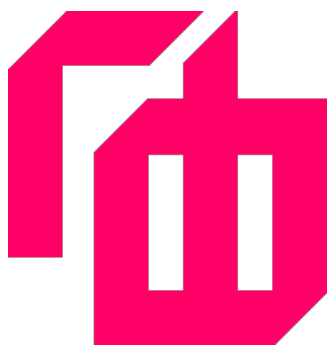


Figure 16. Water velocity of 2D model

REFERENCES

- [1] E. Morin, Y Jabocy, S Navon, and E Bet-Halachmi, "Towards flash-flood prediction in the dry Dead Sea region utilizing radar rainfall information," *Advances in Water Resources*, vol.32, pp. 1066-1076, 2009.
- [2] C. C. Abon, C P David, and N B Pellejera, "Reconstructing the Tropical Storm Ketsana flood event in Marikina River, Philippines," *Hydrology and Earth System Sciences*, vol. 15, no. 4, pp. 1283-1289, 2011.
- [3] Ali, A. A., Al-Ansari, N. A., and Knutsson, S., (2012): Morphology of Tigris River within Baghdad City, *Hydrol. Earth Syst. Sci.*, 16, 3783–3790, <https://doi.org/10.5194/hess-16-3783-2012>.
- [4] Santillan J.R., Dr. Paringit E.C., (2013): Modeling of Flash-flood Events using Integrated GIS and Hydrological Simulations. SMTFCMMS, Philippines.
- [5] Hong Q. N., et al., (2015): „Flash flood prediction by coupling KINEROS2 and HEC-RAS models for tropical regions of Northern Vietnam". *Hydrology* 2015, 2, 242-265; doi:10.3390/hydrology2040242.
- [6] Thaileng T.; et al., (2016): „Application of HEC-RAS for a flood study of a river reach in Cambodia". *Vietnam*, pp. 16-20.
- [7] Vassiliki T. G. B., et al., (2017): „Hydrological impacts of urban developments: modelling and decision-making concepts". *Theoretical and Empirical Resesources in Urban Management*, v 12 i 4.
- [8] Romali, N., Yusop, Z. and Ismail, A., 2018. Application of HEC-RAS and arcGIS for floodplain mapping in Segamat town, Malaysia. *International Journal of GEOMATE*, 15(47).
- [9] Ben Khalfallah, C. and Saidi, S., (2018). Spatiotemporal floodplain mapping and prediction using HEC-RAS - GIS tools: Case of the Mejerda river, Tunisia. *Journal of African Earth Sciences*, 142, pp.44-51.
- [10] Dasallas, L.; Kim, Y.; An, H., (2019): Case Study of HEC-RAS 1D–2D Coupling Simulation: 2002 Baeksan Flood Event in Korea., 11, 2048.
- [11] Diedhiou, R., et al., (2020). Calibration of HEC-RAS Model for One Dimensional Steady Flow Analysis—A Case of Senegal River Estuary Downstream Diama Dam. *Open Journal of Modern Hydrology*, 10(03), pp.45-64.
- [12] Huțanu, E.; et al., (2020): Using 1D HEC-RAS Modeling and LiDAR Data to Improve Flood Hazard Maps Accuracy: A Case Study from Jijia Floodplain (NE Romania)., 12, 1624.
- [13] Ilioski B., (2021): "Application of HEC-RAS for analysis of flooding areas", Master thesis, Faculty of Civil Engineering, Skopje, Macedonia.
- [14] Grassland, Soil & Water Research Laboratory, Temple, Texas (2012): Soil and Water Assessment Tool User's Manual.
- [15] Copernicus Land Monitoring Service (CLMS) & European Environmental Agency (EEA), (2012): Corine Land Cover.
- [16] US Army Corps of Engineers, Hydrologic Engineering Center, (February 2016): Hydraulic Reference Manual Version 5.0.
- [17] Faculty of Civil Engineering, (2016): „Regulation of the river Vardar in the Polog region ". Skopje, Macedonia.
- [18] Tiffany Schanatre, MGEO (2014): ESRI ArcMap 10.1 Manual For Hydrography & Survey Use. www.Geo-Tiff.com.



СЕКОГАШ

БИДИ

ИН

WWW.GF.UKIM.EDU.MK

Violeta Gjeshovska

PhD, Associate Professor
University “Ss. Cyril and Methodius”
Faculty of Civil Engineering - Skopje,
N. Macedonia
violetag@gf.ukim.edu.mk

Goce Taseski

PhD, Associate Professor
University “Ss. Cyril and Methodius”
Faculty of Civil Engineering - Skopje,
N. Macedonia
taseski@gf.ukim.edu.mk

Bojan Ilioski

MSc, Civil engineer
University “Ss. Cyril and Methodius”
Faculty of Civil Engineering - Skopje,
N. Macedonia
bojaniloski@hotmail.com

HEAVY RAINFALL IN THE R.N. MACEDONIA

Information on maximum precipitation of a short duration, i.e., knowledge of intensity-duration-probability (i-T-p) curves is highly important for various studies in the field of surface water hydrology, generally in hydrotechnics, water management, traffic, etc. However, such crucial data are often unavailable in different parts of the world due to lack of sufficient measuring stations and also due to unprocessed, raw data.

In R.N. Macedonia, data on heavy rainfall that took place in the period from 1956 to 1988 are still in use in practice. The need for updating these data is more than necessary, given that rainfall is an extremely stochastic phenomenon.

Annual maximum precipitation registered on pluviographic strips in the period from 1989 to 2020 at eight measuring stations has been analyzed in this paper. Maximum precipitation series with a duration of 5, 10, 20, 40, 60, 90, 150, 300, 720 and 1440 minutes have been established for the entire period from 1956 to 2020. All these arrays of data have been tested for homogeneity and statistically processed. The probability of occurrence of maximum annual precipitation has been defined according to the adopted mathematical probability function and the i-T-p curves have been constructed. The results of the analysis are presented in a tabular and graphical form.

Key words: maximum precipitation, intensity, time duration, probability of occurrence.

1. INTRODUCTION

Rainfall data are very important for climate study, water resources evaluation, drainage design (Desa and Rakhecha 2004; Wang 1987), environmental studies and many other purposes. To have high quality data on measured precipitation at many measuring stations means a higher degree of quality of conducted hydrological analysis. Unfortunately, it often happens that these data are not available due to lack of a metering network and often due to unprocessed, raw data.

When designing hydraulic facilities, the realistically estimated flood waters are the basic parameter on which depend the necessary investments in construction of these facilities and their maintenance. For the purpose of construction of small reservoirs and sizing of spillway facilities of dams, construction of sewerage systems for

drainage of atmospheric waters, regulation of rivers with small catchment areas, regulation of torrents and sizing of anti-erosion protection measures in erosive areas, hydro melioration systems, dimensioning of drainage systems in road construction, dimensioning of bridges and culverts and in many other cases, the competent flood waters are determined by applying methods that enable establishment of a connection between intense rainfall and direct surface runoff.

Defining real quantities of flood waters that can be expected in certain small catchment areas is necessary in order to know the possible occurrences of intense rainfall of a short duration [1]. Data on intense precipitations of maximum intensity and short duration are needed to solve various technical and scientific problems in the field of surface water hydrology, generally in hydrotechnics, water management, traffic and alike.

Intensive precipitation represents a random variable regarding time and space. To explore precipitation as a stochastic process in hydrology, mathematical methods, i.e., methods of statistics and theory of probability are used. These are based on data on this stochastic process of precipitation registered in a certain period. These data are obtained based on an established meteorological network of metering stations for continuous measurement of precipitation and systematic acquisition of data on measured precipitation for the purpose of establishment of a sound database. Based on this database obtained on the basis of a sufficiently long period of measurement, knowledge on occurrence of intensive precipitation in a certain area can be gathered.

In the R.N. Macedonia, data on intensive precipitation obtained by processing precipitation registered in the period from 1956 to 1988 are used for this purpose in practice [16]. Given that precipitation is an extremely stochastic phenomenon, variable in time and space, there is a need to renew the research by extending the data series up to the current period. It is important to note that, for the last thirty years, there has been a change in the precipitation regime in terms of intensity and duration, both globally and regionally as a result of climate change. The importance of the need for re-analysis of the curves of intensity, duration and recurrence of intense rainfall has also been confirmed in the Climate Change Strategy for the City of Skopje (2017) in which it is indicated, within the Action Plan, that there is a need for preparation of a Study on Innovated Curves of Intensity, Duration and Recurrence of Intense

Rainfall in the Skopje Region in Conditions of Climate Change [18].

The purpose of the investigations presented in this paper has been to innovate data on intensive precipitation with different recurrence period and short time duration through analysis of data on precipitation obtained at eight measuring stations in the R. N. Macedonia in the period 1959 – 2020 and thus enable definition of the competent real flood waters in proportioning hydrotechnical structures.

2. METHODOLOGY

2.1 OVERVIEW OF METEOROLOGICAL STATIONS FOR MEASURING PRECIPITATION

Meteorological observations in R.N. Macedonia are performed at 19 main meteorological stations, 7 climatological, 24 phenological, 87 rain gauge stations and 55 automatic meteorological stations (AMS), Figure 1.



Figure 1. Network of meteorological stations in R.N. Macedonia (Source: UHMR)

Within the network of meteorological stations, short-term precipitation is measured by pluviographs at a number of measuring points. Depending on the possibilities, conditions and the need for information, the number of these measuring stations was decreased or increased in the past period. Permanent monitoring of intense rainfall in the R. N. Macedonia is carried out at the meteorological stations shown in Table 1.

Pluviographic, short-term, rainfall strips registered at measuring stations Skopje (SK), Shtip (SH), Prilep (P), Bitola (B), Ohrid (O), Kriva Palanka (KP), Demir Kapija (DK) and Lazaropole (L) have been processed and analysed within the investigations presented in this paper.

In Skopje, precipitation is measured at three locations: Skopje - Old airport-(SK-1), Skopje-Petrovec (SK-2) and Skopje-Zajchev rid (SK-3)

Measurement of short-term precipitation is performed mainly by use of three types of instruments: (1) Pluviograph produced by Lambrecht- a German instrument with one-day, weekly and monthly pluviographs. The aperture area of the pluviograph is 200 cm², (2) Pluviograph produced by R FRUESS- a German instrument with one-day pluviograph and (3). Pluviograph type P-2- a Russian instrument, one-day

pluviograph with forced discharge. The aperture area of this pluviograph is 500 cm². Given the technical possibilities for observations of precipitation by pluviographs, the measurements were performed only in the warm period of the year (from April to November). In winter, the so-called pluviographs with heaters were used (to prevent freezing under negative temperatures), in which case, not one-day pluviograph tapes were used, but mostly seven-day ones. Such records referring to the period from 1956 to 1988 have not been analysed, while those from the period from 1989 to 2020 have been processed and analysed.

Table 1. Overview of analyzed meteorological stations

station	H [ma.s.l.]	position		pluviograf	measurement period	notes
		latitude	longitude			
SK-1	240	41°59'	20°28'	R FRUESS	1956-66	stopped working
SK-2	239	41°57'42"	021°37'17"	R FRUESS	1967-75	
SK-3	302	42°00'59"	021°12'59"	R FRUESS	1978-1988	with interruption
					1989-2020	
Shtip	336	41°45'13"	022°21'49"	П-2	1963-1988	with interruption
					1988-2020	
Prilep	675	41°20'02"	021°13'14"	П-2	1959-1988	with interruption
					1989-2020	
Bitola	590	41°02'30"	021°12'13"	П-2	1956-1988	with interruption
					1989-2019	with interruption
Ohrid	757	41°06'53"	020°04'50"	Lambrecht	1956-1988	
					1989-2020	with interruption
Kriva Palanka	693	42°12'13"	022°21'52"	П-2	1959-1988	
					1989-2020	
Demir Kapija	112	41°24'34"	022°21'14"	Lambrecht	1957-1979	with interruption
					1987-2020	
Lazaropole	1340	41°32'15"	020°04'45"	П-2	1964-1988	with interruption
					1988-2012	with interruption

2.2 AVAILABLE DATA

For the measuring stations for which there are data on at least 10 years of continuous measurement and registration of amount of precipitation, i.e., for which there is a pluviographic record of precipitation, the intensity of precipitation of a certain duration can be determined. In this paper, precipitation for the period from 1956 to 2020 has been analyzed for the measuring stations: Skopje, Shtip, Prilep, Bitola, Ohrid, Demir Kapija and Lazaropole. An overview of the processed pluviographic diagrams for all analysed stations for the period from 1956 to 1988 is shown in Table 2. For the period from 1989 to 2020, it is

shown in Table 3. Pluviographic diagrams for the period from 1989 to 2020 that have been available (source: UHMR) for the meteorological stations are mainly one-day, but there are also weekly and monthly tapes. Based on detailed review of all pluviographic records obtained each year (daily, weekly and monthly) selection of diagrams of all recorded episodes of precipitation and torrents in the course of each month and then in the course of each year has been made. The diagrams with recorded illogical values of precipitation (unreliable diagrams controlled by the UHMR staff) have not been taken into account in the analyses.

Table 2. Overview of available pluviographic diagrams for the period 1956 to 1988

station	1956	1957	1958	1959	1960	1961	1962	1963	1964	1965	1966	1967	1968	1969	1970	1971	1972	1973	1974	1975	1976	1977	1978	1979	1980	1981	1982	1983	1984	1985	1986	1988	1989			
Skopje																																				
Shtip																																				
Prilep																																				
Bitola																																				
Ohrid																																				
Kriva Palanka																																				
Demir Kapija																																				
Lazaropole																																				

Table 3. Overview of available pluviographic diagrams for the period 1989 to 2020

station	1989	1990	1991	1992	1993	1994	1995	1996	1997	1998	1999	2000	2001	2002	2003	2004	2005	2006	2007	2008	2009	2010	2011	2012	2013	2014	2015	2016	2017	2018	2019	2020				
Skopje																																				
Shtip																																				
Prilep																																				
Bitola																																				
Ohrid																																				
Kriva Palanka																																				
Demir Kapija																																				
Lazaropole																																				

2.3 READING PLUVIOGRAPHIC DIAGRAMS AND FORMING A TABLE WITH BASIC DATA FOR PROCESSING

The procedure of processing pluviographic tapes in order to define the intensity of the maximum precipitation of a certain duration can be done by the method of characteristic (transitional) points or the method of five-minute period of discretization ($\Delta t = 5\text{min}$). In the investigations presented in this paper, the second method has been used, i.e., the method of five-minute period of discretization ($\Delta t = 5\text{min}$) for which the period of discretizing is constant ($\Delta t = 5\text{min}$) and, for the total duration of precipitation, a chronological series of average five-minute intensities of precipitation has been obtained. The maximum values of intensity of precipitation have been obtained by extraction-separation of the largest value in the series of average five-minute precipitation, or the median value of precipitation of a certain duration. An online **graphreader** tool has been used to read the values from the pluviographic diagrams. For that purpose, all the tapes have, first of all, been scanned, the diagrams have been digitized and the values of the highest precipitation heights with a duration of 5, 10, 20, 40, 60, 90, 150, 300, 720 and 1440 minutes have been determined.

2.4 DETERMINATION OF ANNUAL MAXIMUM PRECIPITATION WITH A CERTAIN DURATION

For the analysed meteorological stations, all pluviographic diagrams in which precipitation has

been registered for all years for the period from 1989 to 2020, have been processed. Based on these data, chronological series of data on annual maximum precipitation with a duration of 5 minutes to 1440 minutes have been established. For each year, a series of maximum daily precipitation measured by an ordinary rain gauge has also been established (source: UHMR).

When establishing the series of annual maximum precipitations, the processed data have been controlled and the following principles have been followed: 1) the height of the annual maximum precipitations of a certain duration must be greater than the annual maximum precipitation of a shorter duration, 2) the annual maximum precipitations with a duration of 1440 minutes must be greater and/or possibly equal to the maximum daily rainfall. In case this condition is not met by processing the pluviographic diagrams, the annual maximum precipitation with a duration of 1440 minutes is equal to the maximum daily precipitation (for these, there is a complete sequence for the analysed period), 3) in case of two or more separate shorter precipitations between which there is a period without precipitation, the maximum precipitation of a certain duration is determined on the basis of precipitation for the entire period, from the beginning of the precipitation to its cessation.

Based on the previously explained procedure, for the analysed meteorological stations (Skopje, Shtip, Prilep, Bitola, Ohrid, Kriva Palanka, Demir Kapija and Lazaropole), unique series of data on

annual maximum precipitations with a duration of 5, 10, 20, 40, 60, 90, 150, 300, 720 and 1440 minutes have been established for the period from 1989 to 2020.

2.5 ADDING INCOMPLETE ARRAYS

Due to the interruptions of the precipitation measurements at certain measuring stations (Bitola, Lazaropole and Ohrid) and for the purpose of completing the series of annual maximum precipitation of a certain duration, the need to supplement the series has been imposed. The completing of the arrays has been done by establishing correlations between the arrays of annual maximum precipitations of a certain duration and the array of maximum daily precipitations which are complete for all stations. When establishing these correlation links, the

strength of the connection has been controlled according to the basic criterion for correlation links, i.e., the correlation coefficient (r) has been calculated and controlled, Table 4.

For the measuring stations Bitola and Ohrid, this coefficient has lower values of precipitation of a shorter duration and higher values of precipitation of a longer duration. For the measuring station Lazaropole, these values have been relatively small, indicating weak connections, wherefore a spatial correlation has been made with the stations: Prilep, Demir Kapija, Ohrid and Bitola. From the comparative analysis of the obtained correlation links, the highest coefficients have been obtained when establishing a correlation relationship of precipitation of a certain duration for m.s. Lazaropole with precipitation of the same duration for m.s. Ohrid.

Table 4. Correlation coefficients

r	5'	10'	20'	40'	60'	90'	150'	300'	720'	1440'
Bitola										
24h	0.297	0.356	0.417	0.435	0.467	0.490	0.498	0.502	0.590	0.560
Ohrid										
24h	0.165	0.206	0.157	0.130	0.128	0.142	0.295	0.418	0.638	0.933
Lazaropole										
24h	0.161	0.106	0.028	-0.003	-0.028	-0.045	-0.057	-0.037	0.029	0.087
Prilep	0.213	0.076	0.052	-0.117	-0.157	-0.122	-0.173	0.049	0.295	0.396
Demir Kapija	0.298	0.244	0.074	0.000	-0.043	-0.095	-0.098	-0.197	-0.037	-0.031
Ohrid	0.666	0.585	0.788	0.623	0.435	0.414	0.443	0.379	0.064	0.162
Bitola	0.324	0.429	0.510	0.343	0.222	0.172	0.126	0.025	0.013	0.003

2.7 DEFINING THE FUNCTIONS OF PROBABILITY OF HEAVY RAINFALL

The statistical processing of the established series of data on annual maximum precipitation of a certain duration for all measuring stations consists of determination of the basic statistical parameters: mean arithmetic value (P_{avr}), mean square deviation (σ), coefficient of variation (C_v), coefficient of asymmetry (C_s) [2], Table 5.

The theoretical probability density function, which is adequate to the empirical frequency, and the probability distribution function apply to the whole population, i.e., the existing arrays of limited data ($n=65$) are treated as arrays of unlimited data ($n=\infty$), which cover all possible future occurrences.

Several probability density functions have been analysed: Gumble distribution, Pearson type III, Log-normal two-parameter, and Log-Pearson. By testing the adaptability of these functions to the empirical frequency of the random variable by applying the χ^2 -test at a test significance of $\alpha = 5\%$, the best adjustment has been shown by the Gumble function.

The probability of occurrence of maximum intensive precipitation for all rain gauges and duration of precipitation has been defined by applying the Gumble distribution. The established graphical dependencies between precipitation intensity, duration and probability of occurrence (i-T-p curve) for all measuring stations and short-term precipitation (5, 10, 20, 40, 60, 150, 300, 720, 1440 minutes) are shown graphically, Figure 2-9.

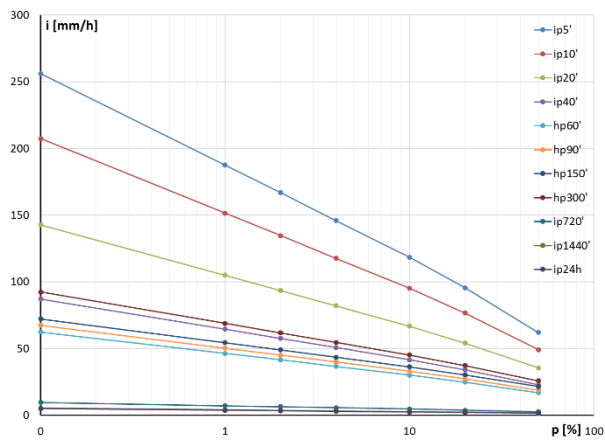


Figure 2. i-T-p curves for Skopje

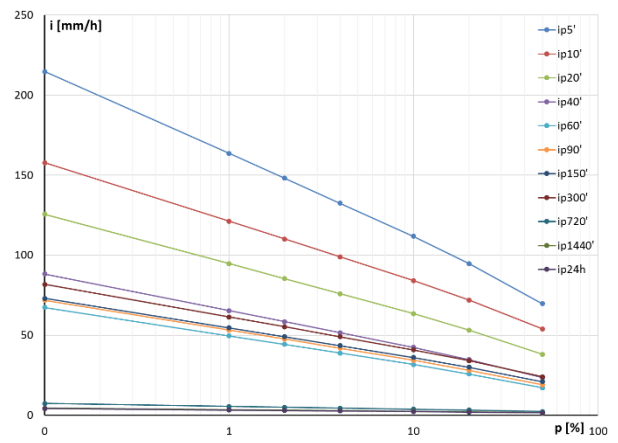


Figure 3. i-T-p curves for Shtip

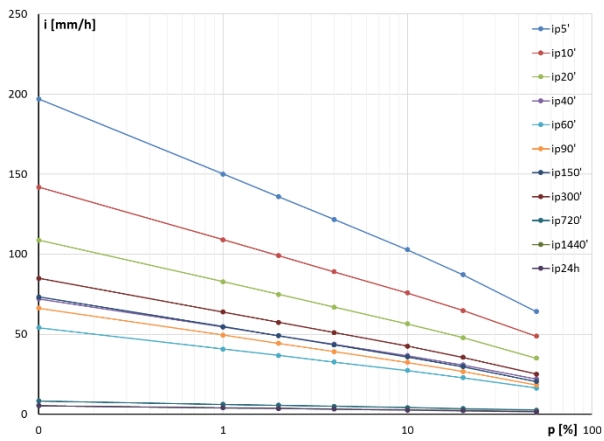


Figure 4. i-T-p curves for Prilep

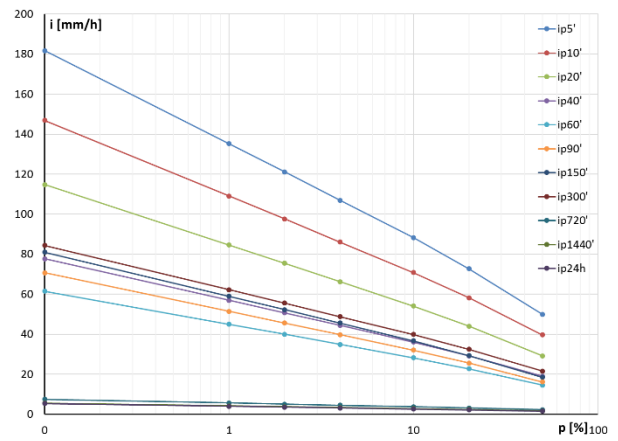


Figure 5. i-T-p curves for Bitola

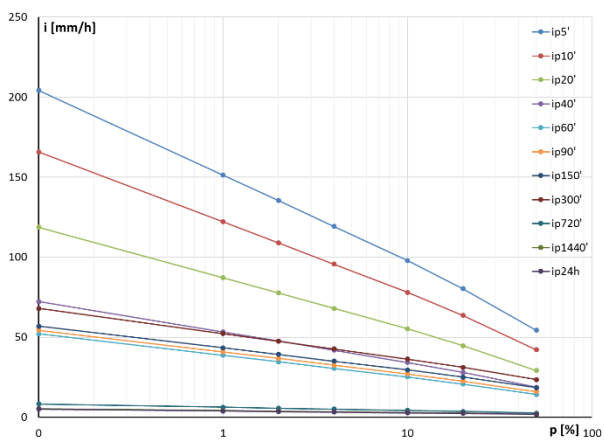


Figure 6. i-T-p curves for Ohrid

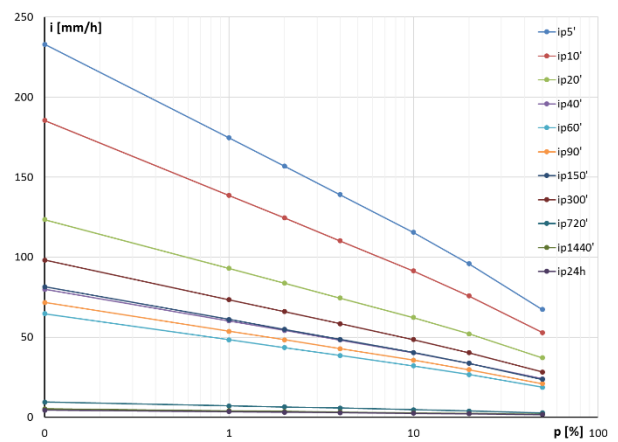


Figure 7. i-T-p curves for Kriva Palanka

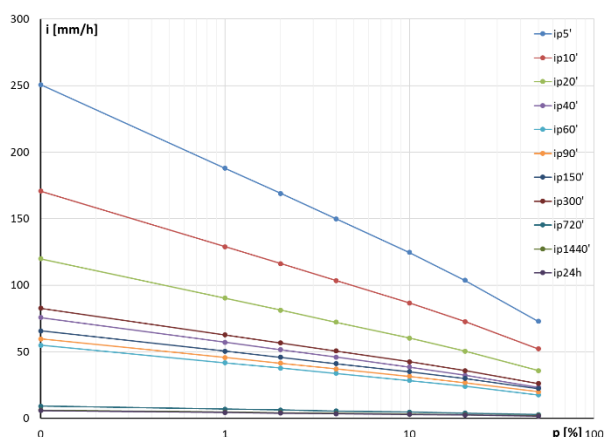


Figure 8. i-T-p curves for Demir Kapija

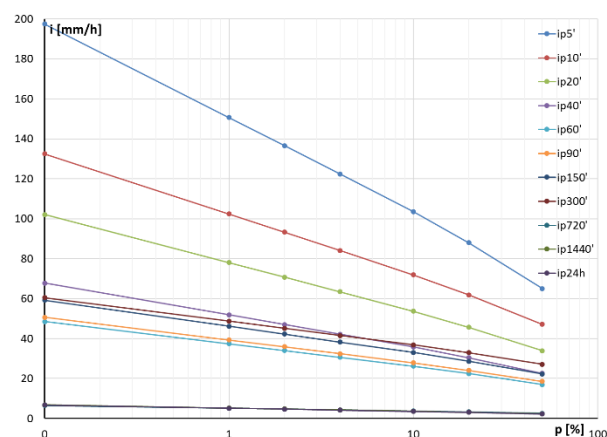


Figure 9. i-T-p curves for Lazaropole

Heavy rainfall in the R. N. Macedonia

3. ANALYSIS OF RESULTS AND DISCUSSION

In terms of available information on heavy rainfall, the following main advantages or disadvantages can be noted:

- the measuring points where the measurements were performed in the past period may have spatial variability and temporal inconsistency,
- observations of precipitation by means of a pluviograph were performed only in the warm period of the year (from April to November). In winter, the so-called pluviographs with heaters were used (to prevent freezing under negative temperatures),
- during measurements of precipitation by use of the mentioned "Helman pluviograph", frequent cases of malfunction of the pluviograph (incorrect discharge, lack of ink, defective feather, etc.) were noticed. This often happened on the days with maximum amount of precipitation according to the 24 hour measurements done by an ordinary rain gauge,
- the processing of the pluviographic tapes was done by their digitization, while the reading of the precipitations of a short duration was done with a great accuracy,
- the established series with a total of 65 data on maximum annual precipitations of different duration (5, 10, 20, 40, 60, 150, 300, 720, 1440 minutes) are long enough to define curves with a high degree of reliability.

The established correlations between the series of data on annual maximum precipitations of a certain duration and the series of data on

maximum daily precipitations for the measuring stations Bitola and Ohrid, have a correlation coefficient with relatively lower values for the precipitations of a shorter duration and higher values for the precipitations of a longer duration.

The established correlation of precipitation of a certain duration for m.s. Lazaropole with precipitation of the same duration for m.s. Ohrid is characterized by relatively higher values of the correlation coefficient and it can be used to supplement the sequence of maximum precipitation in m.s. Lazaropole.

The calculated statistical parameters show small variability of the variation coefficient (C_v): (0.4 ÷ 0.56) for Skopje, (0.33 ÷ 0.53) for Shtip, (0.35 ÷ 0.47) for Prilep, (0.43 ÷ 0.60) for Bitola, (0.32 ÷ 0.55) for Ohrid, (0.31 ÷ 0.45) for Kriva Palanka, (0.36 ÷ 0.45) for Demir Kapija and (0.23 ÷ 0.37) for Lazaropole. The coefficient of asymmetry (C_s) shows a great variability: (0.69 ÷ 2.02) for Skopje, (0.08 ÷ 2.48) for Shtip, (0.04 ÷ 2.21) for Prilep, (1.00 ÷ 3.40) for Bitola, (0.55 ÷ 2.055) for Ohrid, (0.46 ÷ 2.23) for Kriva Palanka, (0.03 ÷ 1.71) for Demir Kapija and (0.12 ÷ 1.85) for Lazaropole.

The comparative analysis of the graphical dependencies between the intensity of precipitation and the probability of occurrence (i-p) for all measuring stations, for a certain short duration of precipitation of 5, 10, 20, 40, 60, 150, 300, 720, 1440 minutes, is shown in Figure 10-19.

Comparing the maximum values of precipitation intensity for $p = 0.1\%$, it can be noticed that the probability lines for different durations have different positions in relation to the other stations.

Table 5. Statistical parameters for the series of annual maximum precipitation with a certain duration

param-eters	5'	10'	20'	40'	60'	90'	150'	300'	720'	1440'	24h
Skopje											
P _{SR}	5.69	9.05	13.00	16.63	18.41	20.40	23.17	27.90	33.80	42.31	38.97
P _{MIN}	0.67	1.33	2.66	4.10	4.10	4.10	5.90	7.30	7.30	14.30	14.20
P _{MAX}	14.00	25.00	33.00	38.00	42.00	45.75	51.02	91.90	92.55	92.55	92.90
σ	3.17	5.17	7.01	8.41	8.91	9.54	9.94	13.06	16.41	16.98	16.26
C _V	0.56	0.57	0.54	0.51	0.48	0.47	0.43	0.47	0.49	0.40	0.42
C _S	0.69	1.10	0.91	0.74	0.78	0.80	0.97	2.02	1.25	0.94	1.28
C _{S2}	1.26	1.34	1.36	1.34	1.25	1.17	1.15	1.27	1.24	1.21	1.31
Shtip											
P _{SR}	6.19	9.55	13.62	17.09	18.70	20.73	22.63	25.92	30.00	40.12	38.44
P _{MIN}	0.50	0.80	1.40	1.90	2.20	2.85	3.50	7.60	15.80	21.00	18.20
P _{MAX}	11.80	20.00	34.82	50.00	67.00	70.17	70.82	71.36	72.20	86.90	86.90
σ	2.37	3.39	5.72	8.45	9.85	10.36	10.20	11.31	11.64	13.39	12.84
C _V	0.38	0.35	0.42	0.49	0.53	0.50	0.45	0.44	0.39	0.33	0.33
C _S	0.08	0.44	1.34	1.94	2.48	2.40	2.30	2.18	1.53	1.21	1.24
C _{S2}	0.83	0.77	0.94	1.11	1.19	1.16	1.07	1.23	1.64	1.40	1.27
Prilep											
P _{SR}	5.70	8.62	12.47	15.78	17.56	19.94	22.21	27.06	32.46	42.40	40.14
P _{MIN}	1.59	2.00	2.60	4.80	4.90	5.00	5.00	7.00	7.00	17.80	17.80
P _{MAX}	10.00	16.31	23.50	29.66	39.88	52.00	58.00	65.83	78.01	120.00	120.20
σ	2.17	3.04	4.82	6.54	7.40	9.39	10.35	11.72	13.46	17.79	17.79
C _V	0.38	0.35	0.39	0.41	0.42	0.47	0.47	0.43	0.41	0.42	0.44
C _S	0.04	0.06	0.32	0.54	0.74	1.27	1.52	1.42	1.38	2.01	2.21
C _{S2}	1.05	0.92	0.98	1.19	1.17	1.26	1.20	1.17	1.06	1.45	1.59
Bitola											
P _{SR}	4.51	7.19	10.66	13.91	16.09	17.83	20.46	23.56	28.98	43.29	39.93
P _{MIN}	0.59	1.19	2.37	4.59	4.96	5.06	6.26	7.70	8.90	2.90	17.80
P _{MAX}	11.95	23.90	39.40	54.70	69.10	78.00	90.80	92.50	93.00	116.00	120.20
σ	2.15	3.50	5.60	7.68	9.21	10.72	12.27	12.34	12.33	18.48	17.71
C _V	0.48	0.49	0.53	0.55	0.57	0.60	0.60	0.52	0.43	0.43	0.44
C _S	1.00	1.66	2.32	2.64	3.29	3.20	3.40	3.06	2.57	1.78	2.27
C _{S2}	1.10	1.17	1.35	1.65	1.65	1.68	1.73	1.56	1.23	0.91	1.60
Ohrid											
P _{SR}	4.93	7.69	10.70	13.62	15.40	17.13	19.69	24.87	33.93	49.42	46.48
P _{MIN}	1.05	2.10	3.00	4.20	5.12	6.11	7.24	8.67	9.53	26.20	25.80
P _{MAX}	15.10	26.20	39.90	45.10	46.20	46.20	48.70	49.50	67.50	95.10	90.40
σ	2.45	4.03	5.85	6.99	7.42	7.54	7.53	8.73	13.23	15.78	15.16
C _V	0.50	0.52	0.55	0.51	0.48	0.44	0.38	0.35	0.39	0.32	0.33
C _S	1.39	2.01	2.38	2.05	1.98	1.88	1.57	0.70	0.55	0.95	1.22
C _{S2}	1.26	1.44	1.52	1.48	1.44	1.37	1.21	1.08	1.08	1.36	1.47
Kriva Palanka											
P _{SR}	6.05	9.52	13.31	17.26	20.21	22.56	25.51	30.47	35.91	45.46	42.30
P _{MIN}	2.25	3.10	4.90	7.81	7.82	9.16	9.40	9.50	9.80	22.10	22.10
P _{MAX}	11.50	20.00	30.10	41.04	50.00	70.00	81.20	91.30	111.20	113.90	97.00
σ	2.71	4.33	5.64	7.29	9.00	9.94	11.35	13.71	15.89	16.20	13.05
C _V	0.45	0.45	0.42	0.42	0.45	0.44	0.44	0.45	0.44	0.36	0.31
C _S	0.46	0.89	0.82	1.38	1.55	2.06	2.31	2.23	2.07	1.49	1.31
C _{S2}	1.42	1.35	1.34	1.54	1.45	1.48	1.41	1.31	1.22	1.39	1.29
Demir Kapija											
P _{SR}	6.55	9.34	12.86	16.68	18.78	21.24	23.76	27.90	35.63	49.49	44.95
P _{MIN}	0.65	1.29	2.55	4.84	6.13	8.75	10.38	10.58	10.58	20.00	13.70
P _{MAX}	15.10	19.70	25.60	34.10	35.10	37.49	41.20	58.90	97.21	122.25	121.90
σ	2.90	3.87	5.49	6.84	7.32	7.78	8.50	11.09	14.98	19.72	18.87
C _V	0.44	0.41	0.43	0.41	0.39	0.37	0.36	0.40	0.42	0.40	0.42
C _S	0.03	0.29	0.34	0.53	0.36	0.29	0.32	0.68	1.47	1.53	1.71
C _{S2}	0.98	0.96	1.07	1.15	1.16	1.25	1.27	1.28	1.20	1.34	1.21
Lazaropole											
P _{SR}	5.78	8.31	12.02	16.05	17.98	19.57	23.45	28.23	32.87	59.75	58.75
P _{MIN}	0.73	1.47	2.93	5.86	6.30	7.90	11.17	16.30	17.00	31.00	31.00
P _{MAX}	12.50	17.00	31.50	34.50	40.20	40.20	42.90	46.20	66.00	154.40	154.40
σ	2.16	2.79	4.46	5.91	6.19	6.29	7.25	6.53	9.07	21.03	20.60
C _V	0.37	0.34	0.37	0.37	0.34	0.32	0.31	0.23	0.28	0.35	0.35
C _S	0.35	0.12	1.29	0.90	1.21	1.16	0.80	0.32	1.47	1.72	1.85
C _{S2}	0.86	0.81	0.98	1.16	1.06	1.08	1.18	1.09	1.14	1.46	1.48

Thus, for the rains with a duration of 5 minutes, the lowest intensity is observed at station Bitola, then Prilep, Ohrid, Lazaropole, Shtip, Kriva Palanka, Demir Kapija, while the highest intensity is observed at m.s. Skopje. As to the precipitation with a duration of 10 minutes, the lowest intensity of precipitation is observed at m.s Lazaropole, then Bitola, Shtip, Prilep, Ohrid; Demir Kapija, Kriva Palanka, while the greatest intensity of precipitations is observed at m.s. Skopje. Regarding the rains with duration of 20 minutes, the intensity is the lowest at Lazaropole station, then Prilep, Bitola, Ohrid, Demir Kapija; Kriva Palanka, Shtip, while the greatest intensity of precipitation is observed at m.s. Skopje.

As to the rains with a duration of 40 minutes, the lowest intensity is observed at m.s Lazaropole, then Ohrid, Prilep, Demir Kapija, Bitola, Kriva Palanka, Skopje, while the highest intensity of rains is observed at m.s. Shtip. For the rains with duration of 60 minutes, the lowest intensity is observed at Lazaropole station, then Ohrid, Prilep, Demir Kapija, Bitola, Skopje, Kriva Palanka, while the highest intensity of rain is observed at m.s. Shtip. Regarding the rains with a duration of 90 minutes, the lowest intensity is observed at Lazaropole station, then Ohrid, Demir Kapija, Prilep, Skopje, Bitola, Shtip, while the highest intensity of rain is observed at m.s. Kriva Palanka.

Concerning the rains with a duration of 150 minutes, the lowest intensity is observed at Ohrid station, then Lazaropole, Demir Kapija, Skopje, Shtip, Prilep, Bitola, while the highest intensity of rain is observed at m.s. Kriva Palanka.

As to the rains with a duration of 300 minutes, the lowest intensity is observed at Lazaropole station, then Ohrid, Shtip, Demir Kapija, Bitola, Prilep, Skopje, while the highest intensity of rain is observed at m.s. Kriva Palanka. Regarding the rains with a duration of 720 minutes, the lowest intensity is observed at Lazaropole station, then Shtip, Bitola, Prilep, Ohrid, Demir Kapija, Skopje, while the highest intensity of rain is observed at m.s. Kriva Palanka.

Finally, as to the rains with a duration of 1440 minutes, the lowest intensity is observed at m.s. Shtip, then Skopje, Kriva Palanka, Prilep, Ohrid, Bitola, Demir Kapija, while the highest intensity of rain is observed at m.s. Lazaropole.

The complex orographic structure of the R.N. Macedonia conditions an uneven spatial distribution of precipitation and affects the pluviometric regime. One of the most important conditions that has an impact on the amount of precipitation is the geographical location of the considered place, i.e., latitude and longitude as well as altitude.

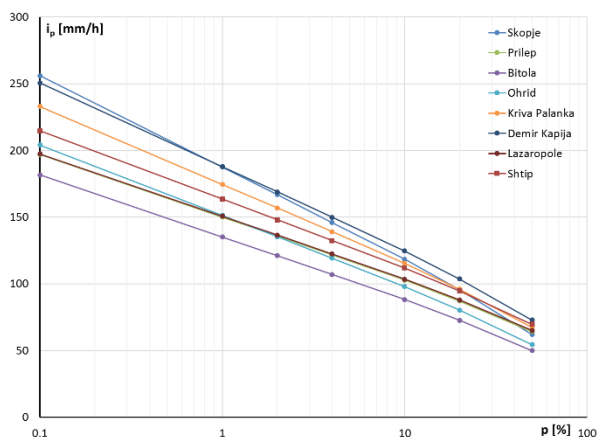


Figure 10. i-p curves for precipitation with duration of 5 minutes

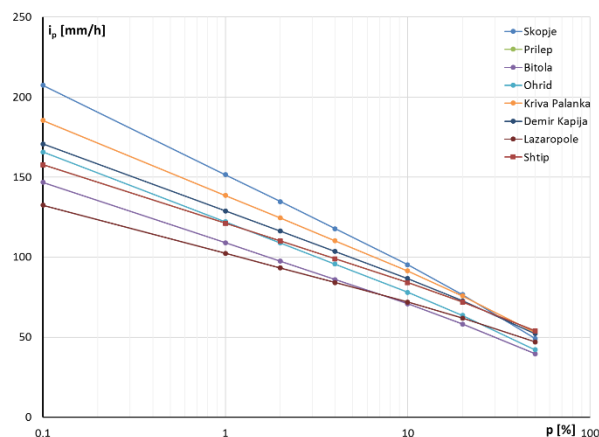


Figure 11. i-p curves for precipitation with duration of 10 minutes

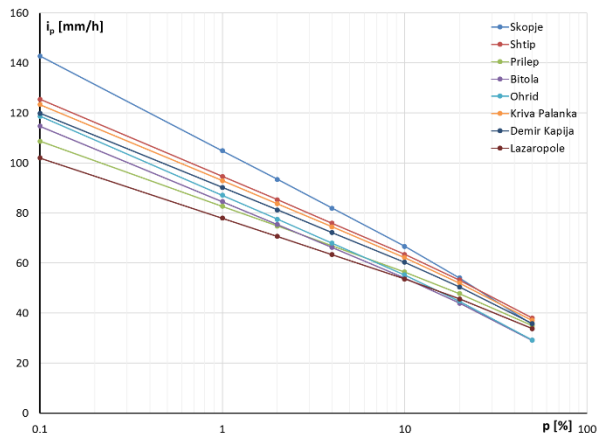


Figure 12. i-p curves for precipitation with duration of 20 minutes

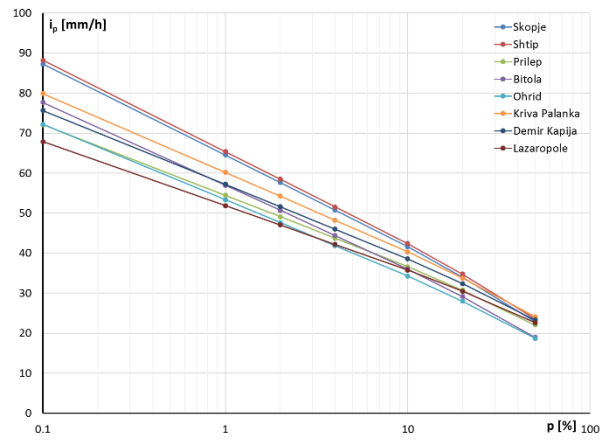


Figure 13. i-p curves for precipitation with duration of 40 minutes'

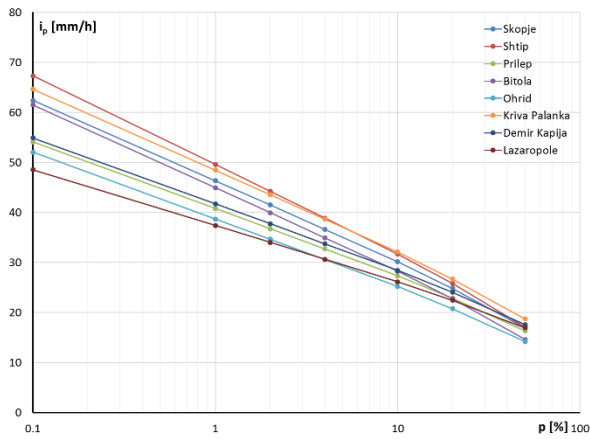


Figure 14. i-p curves for precipitation with duration of 60 minutes'

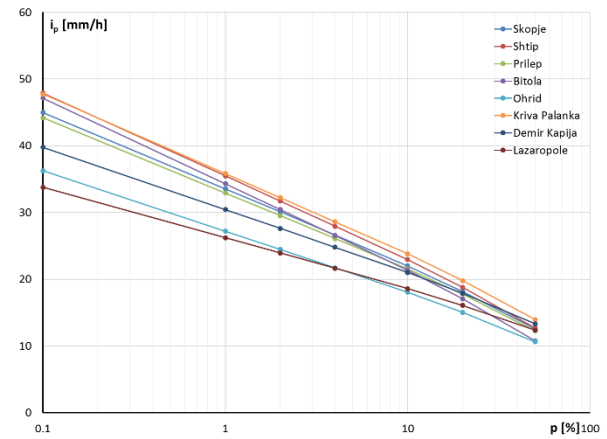


Figure 15. i-p curves for precipitation with duration of 90 minutes

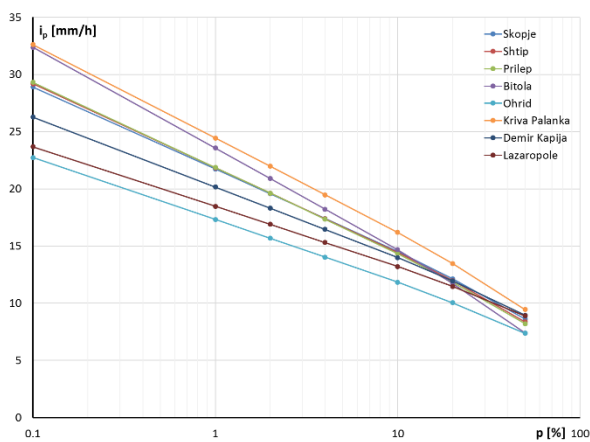


Figure 16. i-p curves for precipitation with duration of 150 minutes

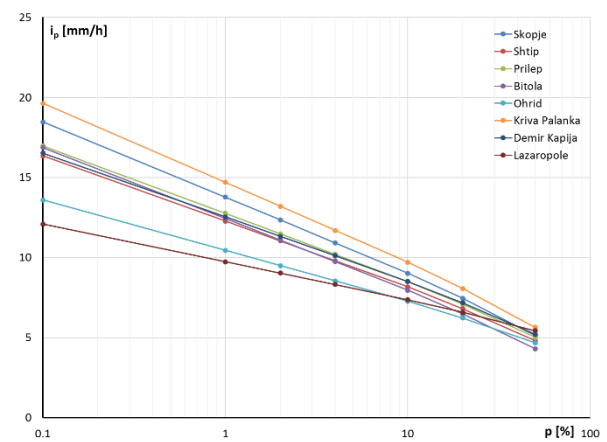


Figure 17. i-p curves for precipitation with duration of 300 minutes

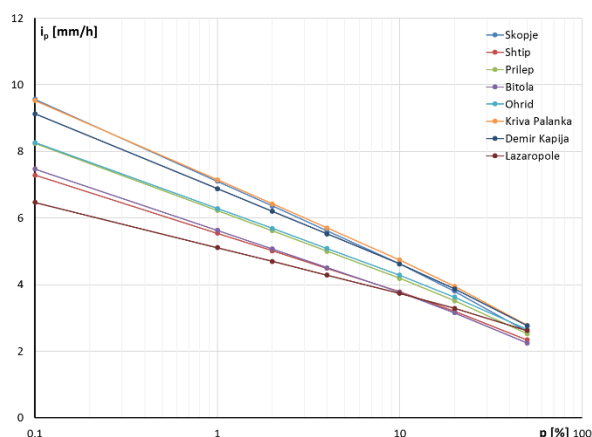


Figure 18. i-p curves for precipitation with duration of 720 minutes

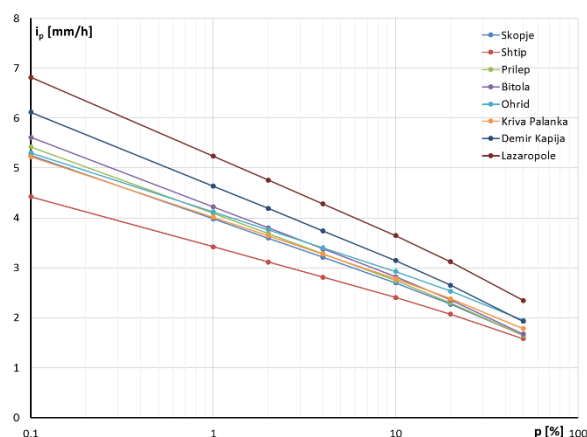


Figure 19. i-p curves for precipitation with duration of 1440 minutes

4. CONCLUSION

Short-term precipitation parameters are extremely important for hydrological analysis of small catchment areas, but also for the urban hydrology. Their application is justified and widely accepted in solving problems in hydrotechnics, water management, agriculture, etc. Recently, due to evident climate changes in all regions worldwide, there has arisen the need for innovation curves of intensity-duration and probability of occurrence i-T-p.

Based on available measured data on precipitation in the form of pluviographic tapes at eight measuring stations in the R.N. Macedonia, there has been established a series of data on maximum annual precipitation of different duration (5, 10, 20, 40, 60, 150, 300, 720, 1440 minutes) with a total of 65 data, for the period from 1956 to 2020. Based on this series of data, the probability of occurrence of maximum intensity of precipitation for all rainfall stations and duration of precipitation has been defined by applying the Gumble distribution.

Graphic dependencies between precipitation intensity, duration and probability of occurrence (i-T-p) for short-term precipitation (5, 10, 20, 40, 60, 150, 300, 720, 1440 minutes) have been established for all measuring stations and can be used for appropriate hydrological analyses to be performed for small catchment areas.

Due to the extremely stochastic nature of the precipitation, it is recommended that these curves are innovated in the next 10 to 15 years.

Acknowledgements

The analyzes and results presented in the paper were conducted within the scientific research project Analysis of intense rainfall in the Republic of North Macedonia, prepared by a team of scientists and collaborators from the Department of Hydraulics, Hydrology and River Engineering at the Faculty of Civil Engineering-Skopje, funded by University Ss. Cyril and Methodius-UKIM, Skopje. Data provided by the UHMR are also highly appreciated.

REFERENCES

- [1] V. Gjesovska, G. Tasevski, P. Pelivanoski, K. Donevska and all. (2022), Analysis of intense rainfall in the Republic of North Macedonia, Scientific research project, Faculty of Civil Engineering-Skopje, University Ss. Cyril and Methodius, Skopje
- [2] (1985), Methods of measurement and processing with computational examples, Yugoslav Hydrological Society
- [3] C.Popovska, V.Gjesovska, (2012), Hidrology-theory with solved problems, Faculty of Civil Engineering-Skopje, University Ss. Cyril and Methodius, Skopje
- [4] C.L. Chen, (1983), Rainfall intensity-duration-frequency formulas, J.Hyd.Div. ASCE109 (12): 1606-1621,
- [5] D.M. Hershfield, (1965), Estimating the probable maximum precipitation, J. Amer. Waterworks Assoc.57: 965-972,
- [6] O. Bonacci, (1981), Heavy rains in the catchment area of the city of Zagreb, Građevinar 3388):347-354

- [7] O. Bonacci, (1987), Correction of systemic precipitation measurement errors, Water management 19(8):193-204
- [8] O. Bonacci, (1994), Precipitation - the main input value in the hydrological cycle, University, Split
- [9] S.Prohaska, V. Ristic, (1996), Hydrology through theory and practice, University of Belgrade, Faculty of Mining and Geology, Belgrade
- [10] S.Prohaska, (2006), Hydrology 1, University of Belgrade, Faculty of Mining and Geology, Belgrade
- [11] S.Prohaska, (2006), Hydrology 2, University of Belgrade, Faculty of Mining and Geology, Belgrade
- [12] S.Prohaska, (1974), Stochastic hydrology, Yugoslav Hydrological Society -JDH, Belgrade
- [13] S.J. Prohaska, V.I. Bartoš Divac sa saradnicima,(2014), Intensity of heavy rains in Serbia, Institute of Water Management "Jaroslav Černi", Beograde
- [14] E. Zelenhasić, (1991), Engineering hydrology, Scientific book - Belgrade
- [15] V. Brutser, (2010), Introduction to hydrology, English translation, I.P. Tabernacule, Skopje
- [16] Ž. Shkoklevski, B. Todorovski, (1993), Intense rainfall in the Republic of Macedonia, Faculty of Civil Engineering, Institute of Hydraulic Engineering, Skopje
- [17] Hydrology Project Training Module # SWDP – 12, (2002), How to analyse rainfall data, New Delhi, 2002
- [18] Climate change strategy, (2017), City of Skopje, Sector for Environmental Protection and Nature of the City of Skopje

Gjorgji Gjorgiev

PhD, Associate Professor
University “Ss. Cyril and Methodius”
Faculty of Civil Engineering - Skopje,
N. Macedonia
gorgi.gjorgiev@gf.ukim.edu.mk

Vanco Gjorgiev

PhD, Full Professor
University “Ss. Cyril and Methodius”
Faculty of Civil Engineering - Skopje,
N. Macedonia
gjorgiev@gf.ukim.edu.mk

Natasa Malijanska

MSc, Teaching assistant
University “Ss. Cyril and Methodius”
Faculty of Civil Engineering - Skopje,
N. Macedonia
malijanska@gf.ukim.edu.mk

DEVELOPMENT OF REAL ESTATE MASS VALUATION MODEL FOR CONDOMINIUMS IN SKOPJE

Real estate mass valuation models of a market value have a tendency to generate real estate property values as close as to the real market values. The success of the mass valuation model is determined based on the differences in the appraised market value and the price a certain property has reached on the open market. In order to establish a model with satisfactory quality, the right factors that determined property value need to be considered in creating mathematical relations between property value and selected factors. Property valuation theory, as one of the primary factors influencing property value, considers location. The paper is striving toward establishing a mass valuation real estate property model considering the implementation of spatial data as a significant factor in determining the market value of condominiums in Skopje.

Keywords: Real estate valuation, mass valuation, Spatial data, GIS.

1. INTRODUCTION

The great importance of real estate, both in economic as well as in social life creates a need for trustworthy data about its own value, which will be helpful in making decisions during its management and usage.

The value, in the publication Uniform standards of professional appraisal practice by the Appraisal Foundation, is defined as “*the monetary relationship between properties and those who buy, sell, or use those properties*”. Value expresses an economic concept. As such, it is never a fact, that is, it is always an opinion about the value of the property at a given time in accordance with a certain definition of value. Real estate appraisal or property valuation is “*the act or process of developing an opinion of value of the property*” (USPAP, 2017).

According to international standards, more types of real estate value can be defined, depending on the situation and the needs for which the assessment is performed. The most common type of value that is estimated is the

market value of real estate. The market value by the International Valuation Standards Council in their publication International Valuation Standards is defined as *"the estimated amount for which an asset or liability should exchange on the valuation date between a willing buyer and a willing seller in an arm's length transaction, after proper marketing and where the parties had each acted knowledgeably, prudently and without compulsion"* (IVS, 2017).

It is important to distinguish the term market value from the term market price, which is the amount for which real estate is sold on a certain date. In addition to the market, investment, liquidation value, value according to the principle of continuity and many other types of real estate value can be also estimated.

Regarding the method of valuation, i.e., the number of real estates that are appraised, there is an individual and mass valuation. The individual valuation is an estimate of the value specifically intended for individual real estate, taking into account its specific characteristics and referring to a specific date. Unlike individual valuation, mass valuation is a process of valuing a group of real estate, on a given date, using common data, applying standardized methods and conducting statistical tests to ensure unity and equality in valuation. When assessing a large number of real estates, it is difficult to emphasize each of their qualities, so special attention is paid to defining what is common to all real estate that is valued, i.e., significant factors for their value. The mass valuation, by the Appraisal Foundation in their publication Uniform Standards of Professional Appraisal Practices, is defined as a *"process of valuing a universe of properties as of a given date using standard methodology, employing common data and allowing for statistical testing"* (USPAP, 2017).

1.1 DEVELOPMENT OF A MASS VALUATION MODEL

Mass valuation is based on the same basic principles as individual valuation. However, mass valuation includes many real estates for a certain date, which is why mass valuation techniques include equations, tables, and plans, collectively called models.

Mass valuation models attempt to represent the market for a certain type of real estate in a particular area. The structure of such models can be seen as a two-step process:

- Model specification and

- Model calibration.

The model specification provides a framework for simulating supply forces and real estate market demand. This step involves selecting the variables of supply and demand, that need to be considered and defining their correlation towards the value as well as their own correlation. Model calibration is the process of adjusting the mathematical model for mass valuation, the tables, and the estimates for the current market. The structure of the model can be valid for several years, but it is usually calibrated or updated each year. For longer periods, a complete market analysis is required (Eckert et al., 1990). The purpose of the mass valuation is to reflect the current conditions in the local market.

When specifying the mass valuation model, firstly the variables are identified (supply and demand) that can impact the value of the real estate and then they are defined as mathematical conversions such as logarithms, which are often used to transform nonlinear data. At the same time, the mathematical form of the model is defined. It can be used in linear (additive) and nonlinear (including multiplier) forms. Next, the model is calibrated, i.e., the data are analyzed so we can determine the adjustments or the coefficients that represent the contribution to the value of the real estate of the selected variables.

The construction of the models requires a good theoretical foundation, data analysis, and research methods. The best valuation models are expected to be accurate, rational, and explainable. Regression analysis is one of the most used methods in statistics, it is used for understanding, modelling, predicting, and explaining complex phenomena. In regression analysis, the predicted variable is called a dependent variable, and the variables used for prediction are called independent variables. Regression analysis allows the creation of a model for predicting the values of a dependent variable, based on the values of other independent variables or only one independent variable.

Building a regression model is an iterative process that involves finding effective independent variables to explain the dependent variable we are trying to model or understand. By repeating the regression procedure, we determine which variables are effective predictors, and then we constantly subtract and/or add variables until we find the best possible regression model. The process of building a model is a research process. It is

necessary to identify explanatory variables in consultation with theory, experts in the field, and based on common sense. We need to be able to state and justify the expected relationship between each explanatory variable and the dependent variable before the analysis, and we need to question the models where these relationships do not match.

Input data in the mass valuation models discussed in this paper are transactions that have occurred in the past, for real estate for what the model is built for, at locations within the area subject to processing, purified for transactions that bounce off the standard values and characteristics of the real estate subject to assessment.

For a long time now, the Republic of Northern Macedonia has been creating a basis for establishing a mass valuation system where the central institution that organizes and manages the system is the Agency for Real Estate Cadastre, which has established this mandate with the 2013 Real Estate Cadastre Act. (Official Gazette No. 55 from 16.04.2013). The infrastructure that is being built and on which the mass valuation system is based in the Register of Leases and Real Estate Prices, which was established on March 18, 2015, where for the first time the registration of real estate transactions by the Real Estate Cadastre Agency was created, the analysis and mass valuation models that result from this data are intended to be applied by researchers and professionals who need this data. The records that this database registers contain data on the characteristics of the real estate and the price for which the transaction or lease was conducted. All this explains the basis for establishing a sustainable system that will provide continuity in the assessment, increased uniformity and easy access to real estate transactions, and of course the value of the real estate.

2. OBJECTIVE / AIM OF THE RESEARCH

Based on the established infrastructure related to the mass valuation of real estate, the goal set before this research paper is defined as the first attempt to establish a model for mass valuation of real estate for parts of the city of Skopje, while explicitly incorporating the spatial factor. The research also focuses on the application of data that the Agency of Cadastre, registers as real estate transactions that take place within the state, and which are the only official and

relevant data source. Considering that in the value of the real estate, and consequently in the assessment of the value, the location has a great impact, the intention is to base the research on GeoInformation systems with which the spatial factor will be easily implemented in the model as well as the control of this component will be more extensive.

3. RESEARCH METHODOLOGY

For the needs of this research, the selected reference unit is the residential property in collective buildings, because this type of property has homogeneous characteristics compared to other types of property (for example, houses, retail properties), which means that characteristics that influence the value of the residential property can be better determined. Also, the market with residential properties (apartments) is quite active and a sufficient number of transactions can be provided, which allows the application of statistical models for mass valuation. In order to establish a model for mass assessment of real estate by applying GeoIS as a system that in the valuation itself explicitly carries the spatial component, an excerpt from the Register of Leases and Prices will be applied in order to test the power of the data, but also the power of the model that can be built on this data.

The empirical research was conducted on the basis of transactions for the purchase of apartments in five municipalities in Skopje, in the period from 2016 to 2017.

The research area covers a surface of about 30km². As the capital city of the country, Skopje has a dynamic real estate market, and the living market is particularly active. Urban areas are considered more dynamic real estate markets compared to rural areas, so the value of the property is determined by the forces of supply and demand. According to the annual reports of the Department of Mass Real Estate Valuation at the Real Estate Cadastre Agency, most of the purchase of apartments in the city of Skopje is in the municipalities of Centar, Aerodrom, and Karposh. In addition, the research includes the municipalities of Kisela Voda and Chair to make a more complete representation of the condominium market in the city of Skopje.

The regression model that will be used in the research is built on a spatially weighted regression (Geographically weighted regression, GWR) because the value of a real estate can vary considerably depending on its location, so the model needs to have the

characteristic of a local model that incorporates the variables obtained on the basis of regression in the valuation of specific real estate where the unknown values before the variables are obtained on the basis of real estate transactions that occurred near the real estate subject to valuation, not taking into account the transactions that took place in other parts of the city and which are at a greater distance than what is considered to be a limit of influence.

The data obtained from the *Register of Leases and Real Estate Prices* in one part will be used for calibration of the model i.e., determining the values before the variables while other part will be used to determine the quality of the developed model, i.e., it will be used as control transactions that will control how close the value of the real estate obtained from the valuation model and the prices of the real transactions are.

4. REGRESSION MODELS

4.1 LOCAL REGRESSION MODELS

In this particular research focused on creating a model for mass valuation of residential units in buildings for collective housing, taking into account the number of transactions with this type of real estate as well as the characteristics of this real estate market, a local regression model was chosen. Local models have been developed to capture spatial heterogeneity. If the nature of spatial relations is different in different places in the study area, these models allow the determination of coefficients, and thus predictions at the local level, so that the established relationships are limited to well-defined neighbourhoods, called windows. The window of local models can be in different shapes and sizes. Most suitable for real estate price modelling, however, are windows with an irregular shape with different sizes depending on the distribution of adjacent real estate that will be included in the window.

4.2 GEOGRAPHICALLY WEIGHTED REGRESSION

The often-applied regression model for real estate valuation is geographically weighted regression. Geographically Weighted Regression - GWR is a type of spatial analysis for the research of spatial non-stationary or spatial heterogeneous processes. The basic idea of GWR is that the parameters can be estimated anywhere in the field of study of a given dependent variable and a set of one or

more independent variables that have been measured in places whose location is known (Fotheringham, et al., 2002). The GWR expands the linear regression model by taking into account the spatial component and creates a separate model and local parameters for each data location, based on a local data set using a different weight scheme. Geographically weighted regression is the most popular local model. In each regression window, only a subgroup of observations that are closest to the point of regression is included in the regression. Nearby regression occurs with higher weights while observations beyond the regression point gain less weight. Due to the unequal valuation of the observations, it is used evaluation with WLS (Weighted Least Squares), instead of the method of OLS (Ordinary Least Squares). As a result of the application of GWR, a number of areas with the estimated parameters are obtained. The diversity of values of these parameters indicates the impact of local variations in the dependent variables of the explanatory variables, and thus the spatial heterogeneity of the considered phenomenon. It can be said that GWR is similar to a "spatial microscope" in terms of the ability to measure and visualize variations in relationships that are not seen in non-spatial, global models (Yang, et al., 2016).

The GWR expands the global regression model

$$y_i = \beta_0 + \sum_k \beta_k x_{ik} + \varepsilon_i \quad (1)$$

allowing local parameters to be assessed instead of global ones, so the model can be written as:

$$y_i = \beta_0(u_i v_i) + \sum_k \beta_k(u_i v_i) x_{ik} + \varepsilon_i \quad (2)$$

where $(u_i v_i)$ denotes the coordinates of the "i" point in space, and $\beta_k(u_i v_i)$ is the realization of the continuous function $\beta_k(uv)$ in point "i".

This means that there is a continuous surface of values of the parameters, and the measurements on this surface are taken at a certain point to indicate the spatial variability of the surface.

A very important part of GWR is its calibration. It is necessary to calibrate the GWR function for each independent variable x and in each geographical location i . The procedure for calculating GWR is as follows:

- 1) Drawing a circle with a given bandwidth, h around a certain location i (in the centre).

2) Calculate the weight for each measurement/observation according to the distance between the neighbour and the centre.

3) Calculate the coefficients using regression with weighted smallest squares (Weighted Least Squares - WLS) so that

$$\hat{\beta}_i = (X^T W_i X)^{-1} X^T W_i Y \quad (3)$$

where W_i is a spatially weighted matrix for centre i , so $W_i = f(d_i, h)$, where $f()$ is a function of a spatial kernel, d_i is a vector at a distance between centre i and all neighbours, and h is a bandwidth or a drop parameter.

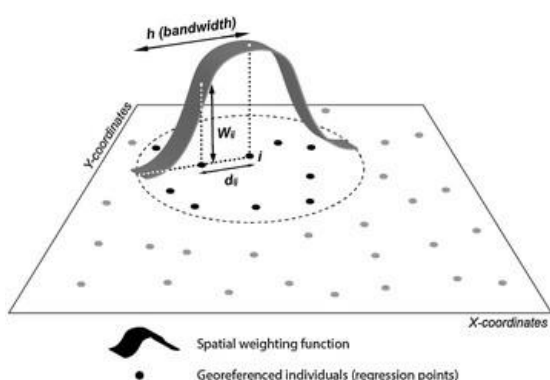


Figure 1. Spatial kernel, source: Fotheringham, et al., 2002

In the core of GWR, there are two kernel functions to achieve calibration, a fixed spatial kernel, and an adaptive spatial kernel. In general, in the calibration of the spatially weighted regression, regions described around the regression points i are used and all points in these regions are used to calibrate the model.

Each data point is weighted according to its distance relative to the regression point, i.e., the data points that are closer get more weight than the data points that are further away. For example, for a given data point, maximum weight is given when it shares the same location as the regression point. This weight decreases as the distance between the two points increases. The complete regression model is calibrated locally by moving the regression point across the region. For each location the calibration is different.

5. ANALYSIS OF THE RESULTS / OUTCOMES

According to the theoretical settings, experience, available research and data made available from the *Register of Leases and Real Estate Prices*, a set of proposed explanatory variables has been identified that are considered to determine the market value of the real estate. Despite the good reasons for including any available real estate data as variables in the model, it was found that some of the explanatory variables were statistically significant and some were statistically insignificant. For this reason, statistical tests have been conducted to make a number of possible combinations of proposed input explanatory variables, requiring models that best explain the dependent variable and thus perform the model specification. The analysis of the proposed explanatory variables gave the results shown in the table below. Also, through the statistical analysis, multicollinearity is calculated between the explanatory variables, i.e., VIF value. In which the value taken as a limit is the value 7.5, i.e., if the VIF value is less than 7.5 there is no multicollinearity between the explanatory variables.

The following table shows the result for significance and multicollinearity based on the analysis of the explanatory variables.

Table 1. Result of the analysis of variables

Summary of variable significance				Multicollinearity
Variable	Significant	Negative	Positive	VIF
Area	100	0	100	1.69
Garage (area)	100	0	100	1.19
Distance to closet mall	100	100	0	4.17
Age	98.07	100	0	1.67
Elevator	87.67	0	100	1.64
Distance to closest university	85.09	99.14	0.86	2.97
Distance to school	79.93	0	100	1.33
Balcon area	74.53	0.02	99.98	1.19
Floor number	73.79	0	100	1.21
High quality interior	69.43	0	100	1.03
Distance to closest park	65.00	62.99	37.01	3.71
Rooms	60.68	18.84	81.16	1.47
Own heating system	60.21	8.77	91.23	1.93
Distance to closest hospital	54.98	16.58	83.42	1.90
Distance to closest kinder garden	44.19	42.45	57.55	1.38
Distance to city centre	43.51	48.20	51.80	2.56
Basement area	39.99	77.79	22.21	1.30
Communal heating system	33.04	24.30	75.70	2.32
Distance to closest bus station	22.33	72.18	27.82	1.33

The results obtained from the analysis of the explanatory variables show that there is a high significance of certain structural, but also spatial characteristics for the real estate that is subject to transaction. It can also be noted that we do not have a redundant explanatory variable, i.e., there is no multicollinearity between the explanatory variables. In the process of defining an appropriate model, it is necessary to experiment with different variables to explain the value of the real estate. It is important to be aware that the coefficients of the explanatory variables (and their statistical importance) may change radically depending on the combination of variables we include in the model.

5.1 GEOGRAPHICALLY WEIGHTED REGRESSION

For the purposes of the research, two models were created with GWR, while for assessing the quality of the created models, the statistical parameters R^2 , adjusted R^2 and Akaike's Information Criterion (AICc) were used. R^2 and adjusted R^2 are statistically derived from the regression equation to quantify model performance. The value of R^2 ranges from 0 to 1. If the model explains the dependent variable perfectly R^2 is 1.0. As an example, if you get a value of R^2 of 0.49, it can be interpreted with the words: "the model explains 49 percent of the

variations in the dependent variable". Adjusted R^2 is always slightly lower than the value for R^2 , as it reflects the complexity of the model (number of variables). Consequently, the adjusted R^2 is a more accurate measure of model performance. The Akaike information criterion (AIC) is an estimator of prediction error and thereby the relative quality of statistical models for a given set of data. AIC estimates the relative amount of information lost by a given model: the less information a model loses, the higher the quality of that model.

Model 1 – GWR

For the purposes of the research, two models were created with GWR, while for assessing the quality of the created models, the statistical parameters R^2 , adjusted R^2 and Akaike's Information Criterion (AICc) were used. R^2 and adjusted R^2 are statistically derived from the regression equation to quantify model performance. The value of R^2 ranges from 0 to 1. If the model explains the dependent variable perfectly R^2 is 1.0. As an example, if you get a value of R^2 of 0.49, it can be interpreted with the words: "the model explains 49 percent of the variations in the dependent variable". Adjusted R^2 is always slightly lower than the value for R^2 , as it reflects the complexity of the model (number of variables). Consequently, the adjusted R^2 is a more accurate measure of

model performance. The Akaike information criterion (AIC) is an estimator of prediction error and thereby the relative quality of statistical models for a given set of data. AIC estimates the relative amount of information lost by a given model: the less information a model loses, the higher the quality of that model.

Model 1 – GWR

Model 1 created with GWR is specified only with structural features of residential property. As explanatory variables for which statistical tests showed the greatest signification are as follows: Area, Garage (area), Balcony area and Age. Using these explanatory variables, the first model for which the following statistical indicators are obtained is formed in the table below, through which we can see the success of the model.

Table 2. Results of the analysis – Geographically Weighted Regression for Model 1

OID	VARNAME	VARIABLE	DEFINITION
0	Bandwidth	2137.860192	
1	ResidualSquares	54169319433	
2	EffectiveNumber	21.807198	
3	Sigma	8063.135068	
4	AICc	17821.981138	
5	R2	0.794736	
6	R2Adjusted	0.78961	
7	Dependent Field	0	PRICE_EU
8	Explanatory Field	1	AREA
9	Explanatory Field	2	AREA_BALCO
10	Explanatory Field	3	AREA_GARAG
11	Explanatory Field	4	AGE

The correlation analysis between the appraised market value of the residential property that has been sold, obtained with model 1 and the actual purchase price performed in transactions for the control group of transactions, calculated with Pearson the correlation coefficient in the SPSS software for this model is 0.899, i.e., 89.9 %.

Table 3. Result of determining the correlation coefficient between the projected prices by Model 1 and the actual purchase prices for the control group points

Correlations

		price_eu	Predicted
price_eu	Pearson Correlation	1	,899**
	Sig. (2-tailed)		,000
	N	95	95
Predicted	Pearson Correlation	,899**	1
	Sig. (2-tailed)	,000	
	N	95	95

** . Correlation is significant at the 0.01 level (2-tailed).

Model 2 – GWR

Model 2 created with GWR uses the same structural and explanatory variables as Model 1 and supplemented by three spatial explanatory variables that the analysis showed were statistically significant: Distance to the closest mall, Distance to the closest hospital and Distance to the closest university. By applying all these explanatory variables, the following statistical indicators shown in the following table are obtained:

Table 4. Results of the analysis – Geographically Weighted Regression for Model 2

OID	VARNAME	VARIABLE	DEFINITION
0	Bandwidth	2137.860192	
1	ResidualSquares	47401929637.900002	
2	EffectiveNumber	31.111344	
3	Sigma	7585.142586	
4	AICc	17724.392795	
5	R2	0.82038	
6	R2Adjusted	0.813815	
7	Dependent Field	0	PRICE_EU
8	Explanatory Field	1	AREA
9	Explanatory Field	2	AREA_BALCO
10	Explanatory Field	3	AREA_GARAG
11	Explanatory Field	4	AGE
12	Explanatory Field	5	DIST_MAL
13	Explanatory Field	6	DIST_HOS
14	Explanatory Field	7	DIST_UNI

The correlation analysis between the appraised market value of the residential property that has been sold, obtained with model 2, and the actual purchase price performed in the transactions for the control group points, calculated with Pearson correlation coefficient in the SPSS software for this model is 0.906, i.e., 90.6%.

Table 5. Result of determining the correlation coefficient between the projected prices by Model 2 and the actual purchase prices for the control group points

Correlations

		price_eu	Predicted
price_eu	Pearson Correlation	1	,908**
	Sig. (2-tailed)		,000
	N	95	95
Predicted	Pearson Correlation	,908**	1
	Sig. (2-tailed)	,000	
	N	95	95

** . Correlation is significant at the 0.01 level (2-tailed).

When calibrating mass valuation models where spatial regression models are used, they have a variable value that varies depending on the location. In order to register this variation, spatial data in raster data format is used. Hence, a significant advantage in using the GWR model and applying GeoIS is the ability to create a series of raster layers of variable coefficients. This allows the identification of

spatial variations within the research area, which can help in effective decision making. Such records can provide an excellent insight into the key parameters that affect the value of the property in a particular area. For example, the age of the property can have a significant negative impact on the value of the property in newly developed areas where most of the properties are completely new, and on the other hand it can have a positive impact in an old part of the city where older buildings have architectural features and historical significance. In order to emphasize the importance of these models, the results of the age factor of the building will be presented. As expected, the age of the building is inversely proportional to the value of the property, i.e., the older construction reduces the value of the property due to obsolescence, deterioration and depreciation. The analysis of the raster data model of the coefficient for the age of the building showed that the impact of this factor varies through the field of research and less impact (lower coefficients) this factor is observed in the central area of the city, while the impact of the age of the building increases as we move away from the central urban area, to the settlements of Karposh, Aerodrom, where new buildings are being built and the demand for new buildings is higher.



Figure 2. Value of the coefficient before the variable age

The analysis of the raster data model of the coefficient for the impact of the garage surface showed that this impact is greater in the municipalities of Centar and Karposh, while in the municipalities of Aerodrom and Chair, that impact is less, as expected, due to the existence of more and larger parking spaces.

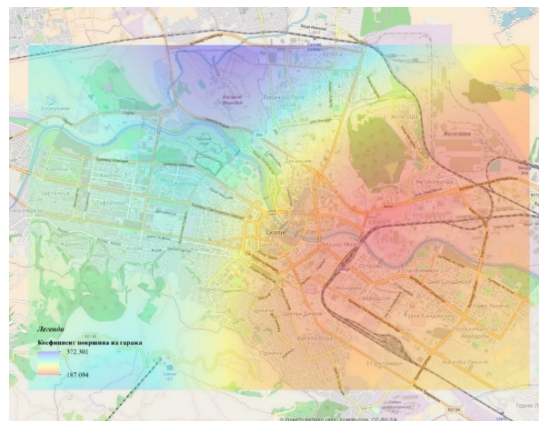


Figure 3. Values of the coefficient in front of the variable area of the garage

6. CONCLUSION

Based on the results obtained from quality control of the established models for mass valuation we can conclude that both models meet the statistical checks and have a satisfactory accuracy of market value prediction. However, although they have satisfactory accuracy, it is necessary to emphasize the difference between the number and type of explanatory variables that these models incorporate and how they affect the end result.

Table 6. Comparison of mass valuation models performance

	Model 1 - GWR	Model 2 - GWR
Coefficient of determination – R ²	79.5%	82.0%
Akaike Information Criterion – AICc	17822	17724
Pearson correl.	89.9%	90.8%
Input data	Non-spatial	Spatial
Number of explanatory variables	4	7

Model 2 has higher R² coefficient, which means that the created model fits much better in the data. A higher percentage shows that the dependent variable (the value of the residential property) is better explained by the selected independent variables, while this percentage is lower in Model 1. Also, the AICc value of the first model is lower than the one of Model 2.

As for the accuracy of the prediction, which is calculated as the correlation coefficient between the projected prices of the control transactions that were omitted from the creation of the models and the actual prices of their purchase, Model 2 has a higher Pearson correlation factor than Model 1.

The results show that the use of Geographically weighted regression (GWR) in predicting market real estate values is a great basis for developing mass valuation models. In doing so, the incorporation of spatial explanatory variables can have a positive impact on real estate mass valuation models.

REFERENCES

- [1] Appraisal Foundation (2016–2017), Uniform standards of professional appraisal practice (USPAP), Appraisal Foundation, Washington, D.C.
- [2] Eckert, J. (1990), Property Appraisal and Assessment Administration, International Association of Assessing Officers, Chicago, Illinois.
- [3] Fotheringham, A. S., Oshan, T. M. (2016), "Geographically weighted regression and multicollinearity: dispelling the myth", *Journal of Geographical Systems*, Vol. 18, No. 4, pp. 303-329.
- [4] Fotheringham, A.S., Crespo, R., Yao, J. (2015), "Geographical and temporal weighted regression (GTWR)", *Geographical Analysis*, Vol. 47, No. 4, pp. 431–452.
- [5] Fotheringham, S., C. Brunsdon and M. Charlton (2002), *Geographically Weighted Regression: the analysis of spatially varying relationships*, John Wiley & Sons Ltd., West Sussex, England.
- [6] Harris, R., Dong, G., Zhang, W. (2013), "Using contextualized geographically weighted regression to model the spatial heterogeneity of land prices in Beijing, China", *Transactions in GIS*, Vol. 17, No. 6, pp. 901–919.
- [7] IVSC (2017), *International Valuation Standards*, IVSC, London, United Kingdom.
- [8] Kauko, T., d'Amato, M. (2008), *Mass Appraisal Methods. An International Perspective for Property Valuers*, Wiley-Blackwell, West Sussex, United Kingdom.
- [9] Leung, Y., Mei, C.L., Zhang, W.X., "Statistical tests for spatial nonstationarity based on the geographically weighted regression model", *Environment and Planning A*, Vol. 32, No. 1, pp. 9–32.
- [10] Liu, J., Yang, Y., Xu, S. (2016), "A geographically temporal weighted regression approach with travel distance for house price estimation", *Entropy*, Vol. 18, No. 8, pp. 303.
- [11] Zhang, L., Ma, Z., Guo, L. (2009), "An Evaluation of Spatial Autocorrelation and Heterogeneity in the Residuals of Six Regression Models", *Forest Science*, Vol. 55, No. 6, pp. 533-548.



FACULTY OF CIVIL ENGINEERING



Faculty of Civil
Engineering - Macedonia



Foundation date



Years of tradition



Number of bachelor's
degree recipients



Number of master's
degree recipients



Number of doctoral
degree recipients



WWW.GF.UKIM.EDU.MK

Kerim Harapovic

EUR ING Bmstr. Dipl. Ing. Dr.

Kerim.harapovic@aon.at

SAFETY OF PEDESTRIANS AND CYCLISTS AT ROUNABOUTS

Abstract: The paper presents the basic settings for achieving a safe intersection with a roundabout in terms of pedestrian and bicycle traffic according to regulations and guidelines from Austria and Germany. The ways of directing bicycle traffic in the area of the roundabout are given, further the variant with underpasses for cyclists below the roundabout, which a priori excludes collision points between motor vehicles and cyclists, then the median traffic island for separating traffic flows at roundabouts according to and the location of public transport stations near the roundabout, as well as the road marking and traffic signing of the roundabouts, all in the context of pedestrian and cyclist safety as "weaker" traffic participant.

Keywords: roundabout, pedestrian, cyclist, traffic safety, median traffic island, underpass, pedestrian crossing.

1. INTRODUCTION

Roundabouts are not popular with all motorists, although they are much safer than "normal" intersections. In addition, roundabouts are more favourable in terms of environmental pollution than ordinary intersections (less traffic noise and exhaust emissions) and are cheaper than them. The roundabout has fewer points of conflict and is clearer than a regular intersection, and vehicles are moving at lower speeds on them. It is also important to say that it is easy to qualify roundabouts as "more favourable" in a certain traffic sense compared to "normal" intersections, but it is necessary to justify something like that with appropriate design solutions and the quality of construction. Large roundabouts should not be planned in front of schools and kindergartens as well as in front of institutions for the blind and visually impaired, in front of homes for the elderly, in front of hospitals and other health units, as well as in places where pedestrians do not I can cross the road safely. Special attention when planning, designing and building (constructive measures) of roundabouts should therefore be paid to non-motorized road users - pedestrians and cyclists as "weaker" road users, and we will say something about that here.

2. MEASURES TO ACHIEVE A SAFE ROUNDABOUT IN THE MEANING OF TRAFFIC - PEDESTRIANS AND CYCLISTS REFERENCES

2.1 DIRECTION OF BICYCLE TRAFFIC IN THE ZONE OF SMALL ROUNDABOUT

The safety of pedestrians and cyclists in traffic depends mainly on the appropriate road marking and traffic signing of the roundabouts, the median traffic islands for the separation of traffic flows as well as the applied methods of managing bicycle traffic in the area of the roundabout. There are basically two ways of directing bicycle traffic in the area of the roundabout (Fig. 1):

a) Parallel routing of bicycle traffic (along the outer edge of the roundabout) (Fig. 1a). Although this way of directing is found in both foreign and domestic literature, it is by no means recommended for security reasons!

b) Independent routing (parallel to curbs or in the form of a concentric circle outside the roundabout) (Fig. 1b).

Bicycle traffic as mixed traffic together with motor vehicles on the roundabout, recommended for traffic loads max. up to 15,000 vehicles per day. It is recommended that cyclists ride in the middle of the circular carriageway, which prevents them from being overtaken by motor vehicles (Fig. 2).

Therefore, the variant on a special bicycle path at the edge of the roundabout is not recommended (Fig. 3) because in this way the safety of cyclists is significantly endangered, as motor vehicles use the rest of the roundabout to overtake cyclists. just get out of the roundabout and turn right, overlook a cyclist (who, to make matters worse, "thinks" he is absolutely safe if he rides on this special and most likely coloured bike path) who is still riding in a roundabout and who is in at that moment in a dead end with the driver of the motor vehicle and thus a collision occurs!

In addition, vehicles entering the roundabout can notice a cyclist (compared to a motor vehicle) who is currently riding on that special track, especially if he is driving fast and "suddenly" is created in front of the car!

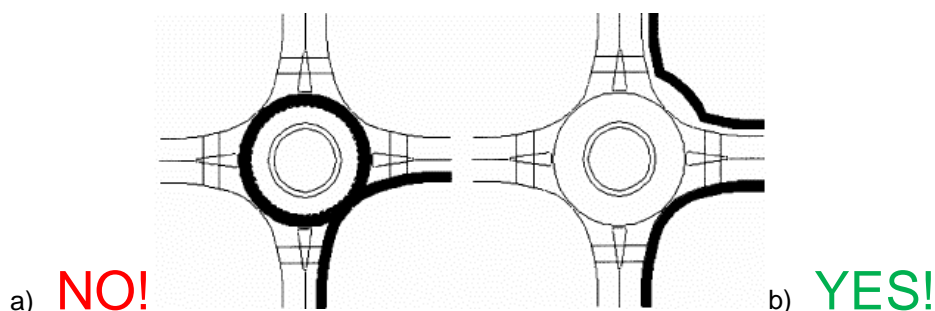


Figure 1. Two possible ways to direct bicycle traffic in the area of a small roundabout [1]



Figure 2. Bicycle routing in the area of a small roundabout on the circular carriageway - recommendation up to 15,000 vehicles / 24 h [1]



Figure 3. Directions of bicycle traffic on a special bicycle path on the roundabout - the safety of cyclists is significantly endangered! [1]

I can personally confirm that since I ride a bike a lot myself, that cyclists, for example with racing bikes they ride on the plain 35-40 km/h even faster. In addition, in recent years, E-Bikes or electric bicycles have become very popular in the West, so it is not uncommon for an older gentleman of the "sportier type" of at least 80 years of age to overtake me with such an electric bicycle! However, precisely because older people in particular underestimate the speed and power of these electric bikes, there has been a significant increase in traffic accidents with them in recent years!

According to the BMI - Bundesministerium für Inneres / Austrian Ministry of the Interior, in 2018, 40 cyclists were killed in traffic in Austria, of which 17 lost their lives on an electric bicycle - this is a new, so far the largest number! [3] Two-thirds of fatal traffic accidents with E-Bikes occurred outside populated areas and also two-thirds were fatal without the participation of other road users, through no fault of their own.

According to ÖAMTC - Österreichischer Automobil-, Motorrad- und Touring Club / Austrian Automobile Club, electric bicycles are especially attractive for the elderly. As many as two-thirds of all E-Bikes deaths are over 65, with an average age of 71. [3]

In Figures 4 and 5 we see two classic examples for directing bicycle traffic in the area of a roundabout using an independent method, i.e. a cycle path outside the carriageway of the roundabout.

All intersections of motor vehicles and pedestrians or cyclists must be at right angles, which as a result has the most correct shape of the field of view of all participants in the intersection. The result is also the fact that the points of conflict are only at the crossings over the arms of the roundabout, but that even there pedestrians and cyclists are (partially) protected by median traffic islands.



Figure 4. and Figure 5. Directions of bicycle traffic on special bicycle paths outside the roundabout [1]

2.2 UNDERPASSES FOR BICYCLISTS IN THE AREA OF THE ROUNDABOUTS

Another possibility regarding the safety of cyclists in the area of roundabouts is underpasses for cyclists. For this example, the roundabout "South" of the Lenzing bypass (Fig. 6) was chosen, a small town of only 5,159 inhabitants 5 km from Voecklabruck, the author's residence, in the construction of which the author himself participated while he was construction manager to a construction firm in Upper Austria.

The situation plan (Fig. 6) shows an underpass for cyclists, which is situated in a slight curve and which represents another possibility of conducting bicycle traffic at roundabouts: off-level crossing. In this way, all collision points are excluded on the one hand between motorized road users riding on the roundabout (above) and on the other hand by cyclists riding through the underpass (below).

The R6 - provincial cycling route, which is part of the international cycling route "Roman Cycling Route" (Roemerradweg), passes through this underpass (Fig. 7).

The Roman cycle path is 242 km long and leads from the German town of Passau in Bavaria (germ. *Bayern*), through the Innviertel area, further through the Salzkammergut (a beautiful part of Austria with several lakes translates to "salt demesne" or "salt domain"), where it passes through Lenzing and further through Voecklabruck and on to the oldest town of Enns in Austria, located east of the capital of Upper Austria Linz. From there leads the so-called. Donau-Radweg (Danube bike path) along the Danube back all the way to Passau. Whoever wants, can of course sit on the train or on the boat to Enns and return to Passau.

What this underpass for cyclists looks like can be seen in Figure 8 and its cross section in Figure 9. The light profile of the underpass is 2.5 m high and 3.5 m wide (Fig. 9).

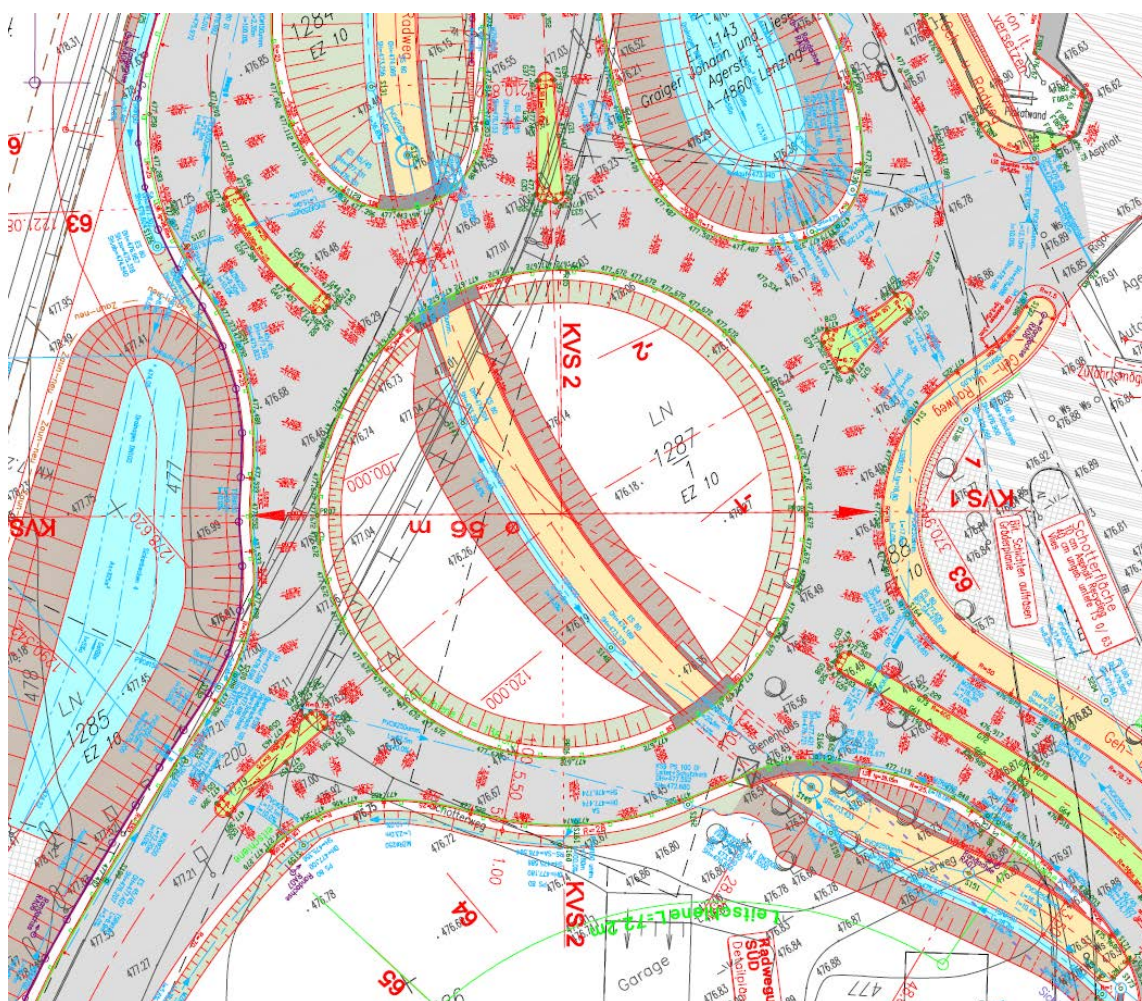


Figure 6. Situation plan of the roundabout "South" of the Lenzing bypass with an underpass for cyclists [5]



Figure 7. The international bicycle route marked "R6", the so-called "Roemerradweg" ("Roman Cycling Route") [6]



Figure 8. Underpass for cyclists KV „Lenzing South“ [author]

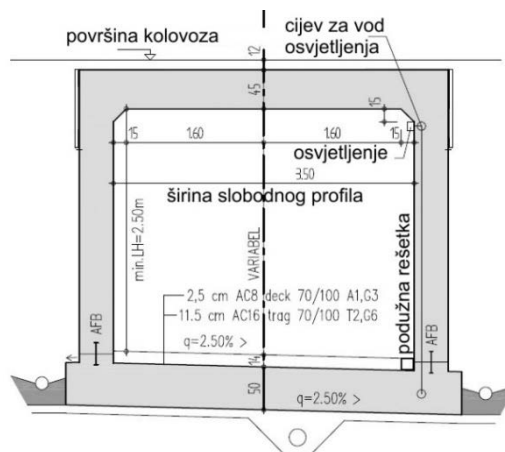


Figure 9. Underpass cross section [5]

3. MEDIAN TRAFFIC ISLAND ON THE ROUNDABOUTS

We can see in Figure 10 what the median traffic island for the separation of traffic flows should look like according to the guidelines for planning and construction of Upper Austria. The median traffic island should always be provided if possible and are also useful for mini roundabouts. They are placed between the entrances and exits at the roundabout arms to avoid wrong turns and to provide more traffic safety especially for pedestrians and cyclists. The width of the median traffic island is at least 1.60 m (RASt 06, 2006) [7] or 2.00 m (RVS 03.05.14, 2010) [2]. In the area of the crossing aid, the median traffic island must be constructed at least 2.50 m (Fig. 10). The median traffic island are to be bordered with kerbstones and lowered in the area of the

crossing point as a 2-3 cm high low kerb. The median traffic island is to be placed 0.25 m from the circular roadway and its length is 12.00 to 15.00 m depending on the local space conditions. The width of the median traffic island at its tip is at least 1.10 m (width of the guide angle + 2 x 0.30 m). The distance between the pedestrian crossing (zebra crossing) and the circular roadway should be 6.0 m, so that a car can remain inside until the circular roadway is clear, without preventing the crossing with its rear part. The width of the crossing should be at least 2.50 m, but 3.00 m is better [4]. In the lane divider it is also possible to place an exit sign, taking care not to obstruct the visibility of all road users (Fig.10). However, the pedestrian crossing (zebra crossing) should not be too far away from the roundabout road, as this creates longer paths for pedestrians or the speed of the outgoing traffic flow becomes too high, which poses a danger to pedestrians.

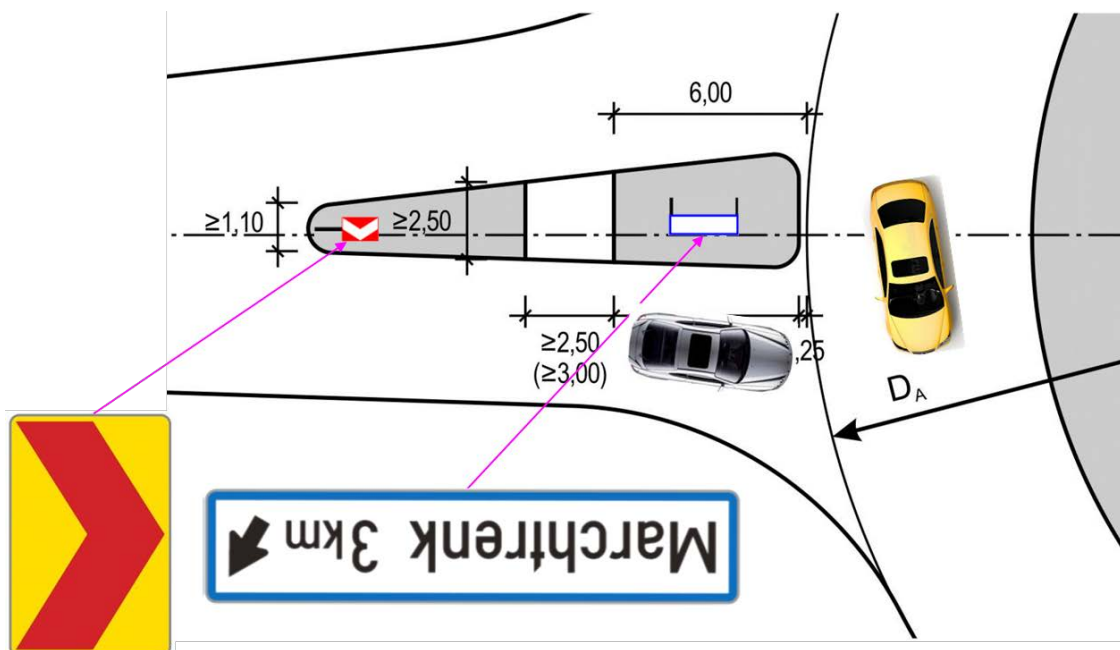


Figure 10. Dimensions of the median traffic island [4] (author's processing)

4. PUBLIC TRANSPORT STATIONS IN THE AREA OF ROUNDABOUTS

Public transport stations in the outgoing traffic flow should be located on a special traffic area outside the road (niche) (Fig. 11). Bus stops in the incoming traffic flow are situated according

to the Austrian guideline RVS 03.05.14 [2] in the form of stops on the road without the possibility of overtaking a stopped bus, which physically "protects" pedestrians crossing the pedestrian crossing in front of the bus, so this is one from pedestrian protection measures (Fig.11).

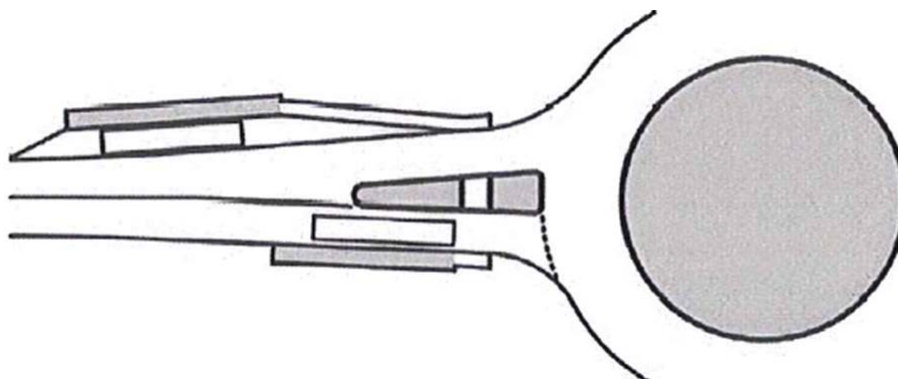


Figure 11. Situation of public transport stations near the roundabout [2]

5. THE ROAD MARKING AND TRAFFIC SIGNING OF THE ROUNDABOUTS

Figure 12 shows an example from the author's second book [16]: plan (original) scale 1: 500 horizontal and vertical signalization of the roundabout on the main road B10 Kugelkreuz in Lower Austria, where all signalling elements are represented roundabouts including hiking and biking trails and crossings. The same picture clearly shows the above-mentioned

method of conducting bicycle traffic outside the roundabout - on a special pedestrian-bicycle path (German: Geh- und Radweg) (Fig. 12). Another possibility of increasing the safety of pedestrians and cyclists in traffic at intersections with roundabouts, as well as at "normal" intersections, are the so-called three-dimensional zebras. One of the most beautiful cities in Austria, Salzburg is about a 50-minute drive from the author's residence Voecklabruck. Here we see the first three-dimensional zebra in that city at the roundabout in front of the large shopping centre "Europark". (Fig. 13).

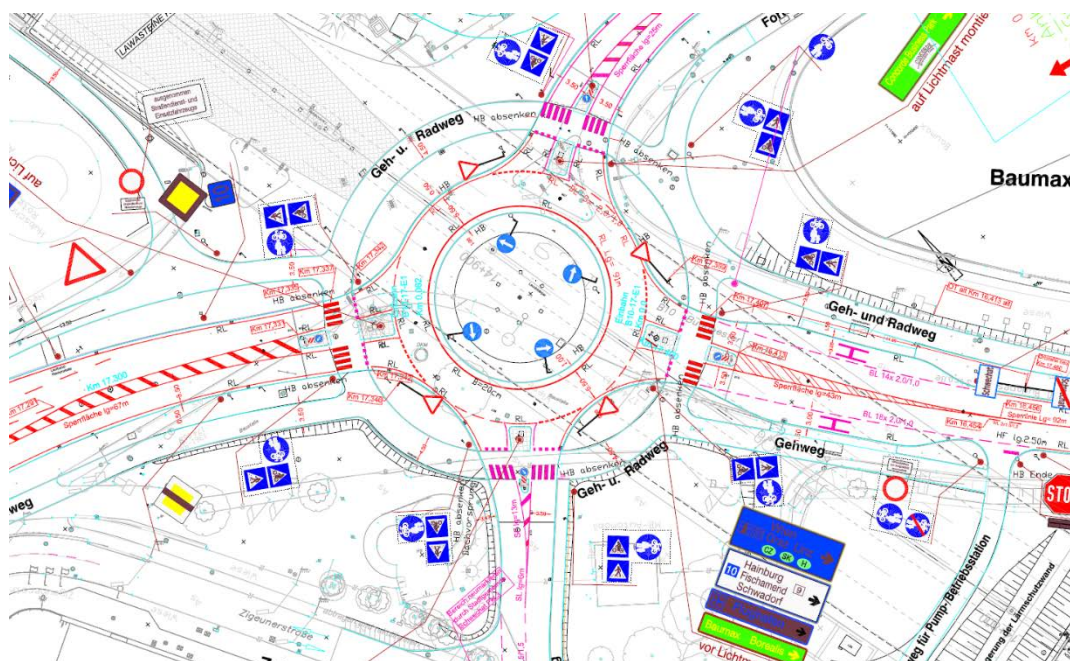


Figure 12. The road marking and traffic signing of the roundabout B10 Kugelkreuz B10 with special walking and cycling trail (germ. *Geh- und Radweg*) [8]



Figure 13. The first 3D pedestrian crossing in the city of Salzburg at the roundabout "Europark" [9]



Figure 14. 3D pedestrian crossing as a means to increase pedestrian safety on roads [10]

However, the full three-dimensional effect of this optical illusion is only achieved when the observer is a little further away from this 3-D zebra as in Figure 14. With the illusion, pedestrians seem to hover over white blocks ("normal" intersection) and thus contributes to even greater safety of pedestrians and cyclists in traffic.

6. CONCLUSION

All the above measures to achieve a safe roundabout in terms of pedestrian and cyclist traffic are very important when planning, designing and building roundabouts. Based on scientific research and statistics of pedestrian traffic accidents at roundabouts, the following can be concluded:

- Safety of pedestrians and drivers of motor vehicles on the so-called. "Mini-roundabouts" (roundabouts with inscribed circles with a diameter of 13 m to 22 m [12]) and "small roundabouts" (roundabouts with inscribed circles with a diameter of 26 m to 40 m [12]) compared to other intersections is especially large.
- Traffic accidents with injuries (pedestrians and cyclists) at roundabouts are rare because the speed of motor vehicles in roundabouts is low, traffic conditions are clear and simple and pedestrian and / or bicycle crossings over the arms of the roundabout are short and at right angles to the arm of the roundabout [11].
- Roundabouts significantly reduce the speed of traffic on sections of the road before and after those intersections in the length of 60 m.
- Urban roundabouts should have zebra crossings and / or bicycle crossings located on traffic separation islands at all ends of the roundabout where pedestrians and / or cyclists cross, thus contributing to unambiguous, simple and clear regulation of priority rights passage.
- One-lane roundabouts are safer for cyclists than two-lane ones, because the vehicle cannot overtake the cyclist or cross his path. Cyclists at one-lane intersections should ride in the middle of the roundabout and never along its edge.
- There is no need to situate special bicycle paths on the roundabout because practice has shown that and numerous studies, for example. [13] [14], as it is very dangerous for cyclists and it is better to even give up a roundabout than to use one such dangerous solution. One such bike path on a roundabout gives a false and deceptive sense of security to cyclists! In essence, this "adds" another "lane" on the

roundabout and thus doubles the number of conflicting points. Vehicles can thus overtake and intersect cyclists. In addition, one such bike path "forces" the cyclist to ride along the edge of the roundabout, which gives the impression that the cyclist wants to get off the roundabout even though he is still riding on it.

- The effect of reducing speed at less congested intersections can be further increased by partially paving pedestrian and/or bicycle crossings over the arms of the roundabout.

- A joint pedestrian and bicycle crossing should be designed, because this intensifies the optical interruption of the road even more.

For the author personally, roundabouts are an extremely important and above all interesting topic and that was the main reason why the author invested six full years of writing books in Montenegrin: Basics of Roundabout construction, Book I - General Part, Book II - Projects of Roundabouts Implemented in Austria, which show the design and construction of the same in German-speaking countries.

My new third book in Montenegrin printed in black and white and also in colour called: "Road constructions in German speaking countries - design, construction and maintenance". This reference book is meant to be like an encyclopaedia and it is intended for all those involved in highway engineering, such as universities, planners, designers, construction companies, experts and technical departments of municipalities and federal states. The book is a comprehensive guide to road construction in German-speaking countries and it is an extraordinary, very opulent and accomplished work with 934 pages, 1160 figures and 135 tables.

Open the link and scroll down:

<https://publish.bookmundo.de/site/?r=userweb site/index&id=kerimhrapovic/>

The book chapters are:

1. History of the road construction
2. Pavements in modern road construction
3. Flexible pavements construction
4. Rigid pavements construction
5. Paving blocks and paving flags, paving stones and paving slabs, curb stones and kerb units
6. Airfield pavements
7. Pavement condition assessment
8. Road maintenance

REFERENCES

- [1] Follman J.: Lehrveranstaltung Verkehrswesen SS 2012, Hochschule Darmstadt, Fakultät für Bauingenieurwesen, 2012.
- [2] FSV Österreichische Forschungsgesellschaft Straße-Schiene-Verkehr: RVS 03.05.14 – Richtlinien und Vorschriften für das Straßenwesen: Pangleiche Knoten-Kreisverkehre, Wien, 2010.
- [3] Niederösterreichische Nachrichten, www.noen.at, 15.11.2019
- [4] Land Oberösterreich: Standards für Kreisverkehre an OÖ Landesstraßen-Merkblatt, Linz, Juni 2007
- [5] Land Oberösterreich, Abteilung Straßenbau und Straßenerhaltung: Straßenprojekte in Oberösterreich, Linz, 2016
- [6] Römerradweg, www.roemerradweg.info/, 23.12.2019
- [7] FGSV e. V. Forschungsgesellschaft für Straßen- und Verkehrswesen RAS 06 - Richtlinien für die Anlage von Stadtstraßen, Köln, Jänner 2006
- [8] Land Niederösterreich, Straßenbauabteilung 2, Pribil W., Salat H.: Kreisverkehre in Niederösterreich – Zusammenstellung, Tulln, Jänner 2016
- [9] Salzburger Nachrichten, www.sn.at, 15.11.2019
- [10] Metro News, www.metro.co.uk, 15.11.2019
- [11] FUSS e.V. Fachverband Fußverkehr Deutschland: Merkblatt Kreisverkehre 2006: Kritische Auseinandersetzung mit dem Merkblatt, Berlin, Heft 1/2007
- [12] FGSV - Forschungsgesellschaft für Straßen- und Verkehrswesen e.V.: Richtlinie für die Anlage von Stadtstraßen, Ausgabe 2006, Köln, Stand 15. Dezember 2008
- [13] Daniels, S, et al: Injury accidents with bicyclists at roundabouts (Unfälle mit Verletzungsfolge mit Radfahrern im Kreisverkehr), Steunpunt verkeersveiligheid, Flanders, in Fietsvademecum, Brüssels, 2008
- [14] Schnüll et al: Sicherung von Radfahrern an städtischen Knotenpunkten, Bericht der Bundesanstalt für Straßenwesen zum Forschungsprojekt 8952, Bergisch Gladbach, August 2015
- [15] Hrapović K.: Osnove izgradnje kružnih raskrsnica, prva knjiga – opšti dio, Austrija, Vöcklabruck, 2016, E-Publi, 2020: <https://www.epubli.de/shop/buch/OSNOVE-IZGRADNJE-KRU%C5%BDNIH-RASKRSNICA-prva-knjiga-Kerim-Hrapovi%C4%87-9783752979404/101621>
- [16] Hrapović K.: Osnove izgradnje kružnih raskrsnica, druga knjiga – izvedeni projekti kružnih raskrsnica u Austriji, Austrija, Vöcklabruck, 2016, E-Publi, 2020: <https://www.epubli.de/shop/buch/OSNOVE-IZGRADNJE-KRU%C5%BDNIH-RASKRSNICA-druga-knjiga-Kerim-Hrapovi%C4%87-9783752979473/101628>



WWW.GF.UKIM.EDU.MK



WWW.GF.UKIM.EDU.MK

Ivan Mrdak

MSc, Teaching assistant
University of Montenegro
Faculty of Civil Engineering
ivanm@ucg.ac.me

Marina Rakocevic

PhD, Full Professor
University of Montenegro
Faculty of Civil Engineering
marinara@ucg.ac.me

EUROCODE-BASED SEISMIC ASSESSMENT OF FRAME STRUCTURE WITH NON-LINEAR DYNAMIC ANALYSIS

Nonlinear analysis enables engineers to control various aspects of seismic behavior. Utilizing nonlinear analysis, engineers can directly determine inelastic deformations of elements (e.g. rotation), as well as deformations of the structure (inter-storey drift). In addition, non-linear analysis can be used to check the bearing capacity of the elements that should remain in elastic region of deformations in order to prevent brittle failure. Subject of this paper is comparison of the results obtained from linear and non-linear seismic analysis of concrete frame structure designed and detailed according to principles of Eurocode 8 and capacity design method. Linear-elastic seismic analysis of multi-story frame structure was performed, with design and detailing of critical regions according to results and relevant requirements of Eurocode 8. Seismic analysis was performed for seismic zone which corresponds to $PGA=0.36g$ (peak ground acceleration) according to EC8, and for ground type C. Assessment of structure performance during strong ground motions was performed with non-linear time history (dynamic) analysis using software PERFORM 3D (Nonlinear Analysis and Performance Assessment of 3D Structures). Non-linear dynamic analysis was performed for four groups of seven ground motion records that were chosen in order to comply with spectrum defined by Eurocode 8 for analyzed frame structure. Comparison of characteristic results is presented at the end of paper, with conclusions, recommendations and critical assessment of regulation.

Keywords: Eurocode 8, non-linear time history analysis, capacity design method, frame structure.

1. INTRODUCTION

Design process for earthquake-resistant structures is pursuit of balance between the seismic capacity of structures and the expected seismic demand they may be subjected. Seismic excitation is an accidental natural phenomenon, which is manifested through alternating movements of the ground, and thus the movement of the supports-foundations of

the structure. Determining the impact in the structure due to this load is much more complex than in the case of other types of loads. An additional complication is cost-effectiveness to design structures to the full value of seismic impacts for strong earthquakes, taking into account the probability of occurrence. For these reasons, the concept of seismic analysis with reduced seismic forces was adopted. Reference methods for the seismic analysis of new buildings in Eurocode 8 [1] (hereinafter EC8) are linear-elastic methods. Linear-elastic methods are based on elastic response spectrum with 5% viscous damping reduced with behavior factor. The behavior factor takes into account the ductility capacity of the structure and the energy dissipation capacity. EC8 prescribes also application of capacity design method for the detailing of critical regions. The main feature of the capacity design method is to determine critical regions that will enter into plastic area of deformation during strong earthquakes and the regions that will remain in the elastic area. In that sense, when designing, special attention is to be paid on detailing of the connections between the structural elements and the areas where nonlinear behavior is predicted. Also it is necessary to provide sufficient load bearing capacity of elements that should remain in elastic region in order to prevent brittle failure [2-3]. Calculation algorithm in EC8 also prescribes an analytical criterion for taking into account (P- Δ) effects.

In order to perform a detailed evaluation of the expected seismic response of a structure designed in accordance with linear analysis and estimate deformations and displacements, EC8 recommends use of nonlinear analyses. These analysis can directly determine inelastic deformations of the element (e.g. rotation), as well as deformations of the structure (interstorey drift). In addition, this analysis can be used to check the bearing capacity of the elements that should remain in the elastic region in accordance with the capacity design. EC8 prescribes use of non-linear static (pushover) analysis and non-linear time history (dynamic) analysis (NDA). [4-5]

2. MODELING AND BUILDING DATA FOR LINEAR ANALYSIS

The analyzed example is a 6-storey spatial reinforced concrete frame structure shown on figure 1. Columns and beams are modeled as prismatic 3D beam elements. Stiffness properties were taken as one-half of the

corresponding stiffness of the uncracked elements. For the adopted return period of 475 years, the reference peak ground acceleration is equal to $a_{gR} = 0.36g$. The ground type at the structure location is C. The structure is designed for high ductility class DCH.

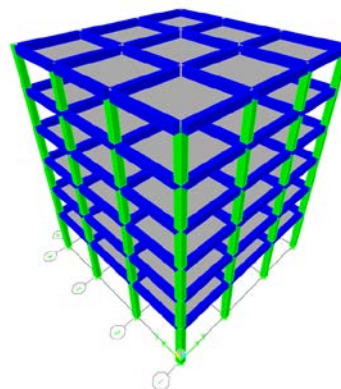


Figure 1. Spatial model of frame structure

The base of the building is rectangular in shape, measuring 16.8×16.8 m. In the X and Y directions layout has 3 bays, with dimensions 5.4, 6, 5.4 m respectively. The floor height of the ground floor is 5m, and the other floors 3.2m. The load from the reinforced concrete slab, thickness $d = 15$ cm, is transferred to the beams with dimensions $b / d = 40 \times 60$, and from the beams to the columns. The columns have square cross section: the outer columns are 50×50 cm and the inner columns are 60×60 cm. The concrete strength class according to EC2 is C30/37. Transverse and longitudinal reinforcement is B500 class C. The building is modelled in the ETABS software package. Self-weight of the structure is automatically determined in the software package. The adopted behavior factor is 5.85. The total mass includes the dead load, 15% of the live load and 30% of the snow load. The total mass of the inner frame with the corresponding load on the surface of the slab is $M = 5285$ kN.

The linear analysis was done with lateral force method. In addition, second-order effects had to be taken because the value of the interstorey drift sensitivity coefficient θ was calculated with a value of 0.17 according to the article 4.4.2.2.3 EC8 [1]. Second order effects were taken approximately by scaling the effects according to the calculation below.

$$\frac{1}{1 - \theta} = \frac{1}{1 - 0,17} = 1.205 \quad (1)$$

Based on the results of the calculation, taking into account (P- Δ) effects, detailing was done in accordance with capacity design, and the adopted reinforcement is presented on figure 2.

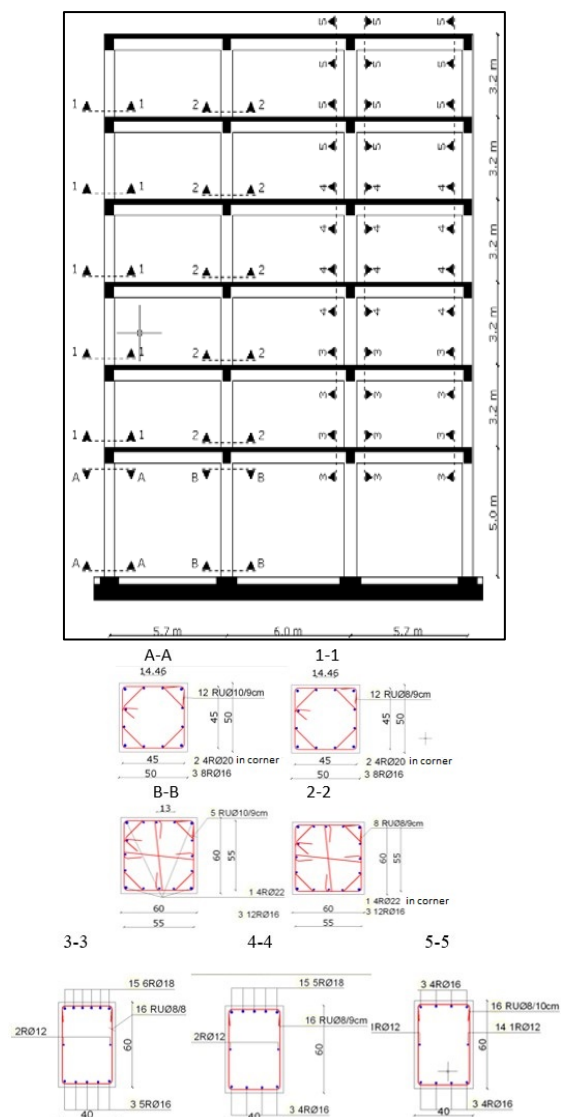


Figure 2. Reinforcement of beams and columns for frame 2-3-B-C

3. MODELING FOR NON-LINEAR ANALYSIS

PERFORM 3d software package [7-9] was used for non-linear modelling. On the location of every slab rigid diaphragm slaving was modelled with masses concentrated on each floor.

In practical modelling for nonlinear seismic analysis, static or dynamic, the reinforced concrete structure is modelled at the element level, and then the element connections are defined. The beam element consists of rigid zone, plastic hinge zone and a central elastic part. Rigid zones are modelled as “default end zones” that are pre-defined in the software and have ten times greater stiffness of the beam and a length equal to 1/2 the width of the column.

The central part of the beam is modelled as an elastic section with defined load-bearing characteristics in order to be able to control the influences during the seismic action. When modelling, a bilinear moment-curvature model was adopted for beam plastic hinge in accordance with the results obtained in the Xtraxt software (cross sectional analysis of components) for the adopted reinforcement. A model that takes into account the interaction of axial force and moment during an earthquake was chosen for the columns. The elastic-ideal plastic (EPP) moment-curvature model for hinges has been adopted and defined through the component "P-M2-M3 hinge". In addition, for beam and column elements strength sections were assigned (bending and shear) as well as the deformation capacities of plastic hinge to be controlled during the analysis. Beam column joints are modelled as elastic zones ("Elastic panel zone" elements), to behave elastic during earthquake. In accordance with this, the stiffness and load-bearing capacity of every joint was defined. Perform model of joint, beam and column are given on figures 3, 4 and 5.



Figure 3. Beam compound component in PERFORM 3D



Figure 4. Column compound component for ground storey and other storeys in PERFORM 3D

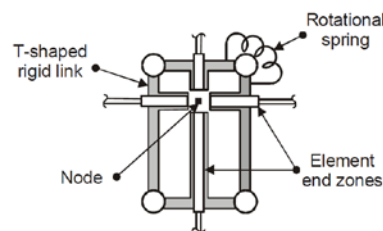


Figure 5. Model of joint with beam and column

Total damping is the sum of elastic and inelastic damping. In nonlinear dynamic analyses, inelastic hysteresis damping is modelled directly, while viscous damping defines elastic damping. PERFORM ("Perform components and elements-Defining the standard for practical performance based design") [7-9] defines two types of viscous damping, namely: modal damping and Rayleigh damping. In this analysis 5% modal damping was combined with

Rayleigh damping and a small amount of β_k damping in order to include "higher" modes damping. Second order effects were taken as $(P - \Delta)$ effects.

Following limit states were defined for structure:

- Curvature on the corresponding length of the beam and column plastic hinge in accordance with the no collapse limit state [1]. The curvature capacity of hinge was calculated with Xtraxt software (cross sectional analysis of components) utilising confinement models defined in EC2 and EC8;
- Load capacity of the joint in accordance with the no-collapse limit state. The capacity of the joint is checked for the transmission of moments from the beams on both sides of the joint;
- Shear force capacity for beams and columns in accordance with the no-collapse requirement. The shear capacity of beams and columns is checked whether the elements remain in the elastic area regarding shear during the seismic action;
- Inter-storey drift relative to the damage limitation request is checked;

4. NONLINEAR TIME-HISTORY (DYNAMIC) ANALYSIS

Earthquake records were selected in accordance with EC8 recommendations [1]. One-way records were used considering that the analysed nonlinear model is planar. For analysis with a single earthquake component, EC8 requires that the response due to records does not fall below 90% of the damped elastic spectrum in the $0.2T_1$ to $2T_1$ periods.

REXEL v.3.3 (beta) software was used to select the earthquake records. The software was developed at the University of Naples (*Università degli Studi di Napoli Federico II*) by *Iervolino I., Galasso C., Cosenza E* [11]. The subject software enables the selection of records from the database that are compatible with response spectrum. In addition, other seismographic conditions that need to be met by an earthquake (magnitude, epicentral distance, earthquake intensity, type of soil on which the earthquake was recorded) can be defined during the selection. The software includes the *European Strong-motion Database (ESD)*, the *Italian Accelerometric Archive (ITACA)* and selected records for the assessment and design of buildings in accordance with the *Selected Input Motions for*

Displacement-Based Assessment and Design (SIMBAD) [11].

The response of the structure was calculated for four groups of 7 earthquakes. As a representation, one of 7 record groups is shown on figure 6 and in table 1. This group is selected from Selected Input Motions for Displacement-Based Assessment and Design (SIMBAD), magnitude $6.5 < M < 7.5$, soil type C, maximum epicentre distance from earthquake 30km and within 90% to 130% of the spectrum value.

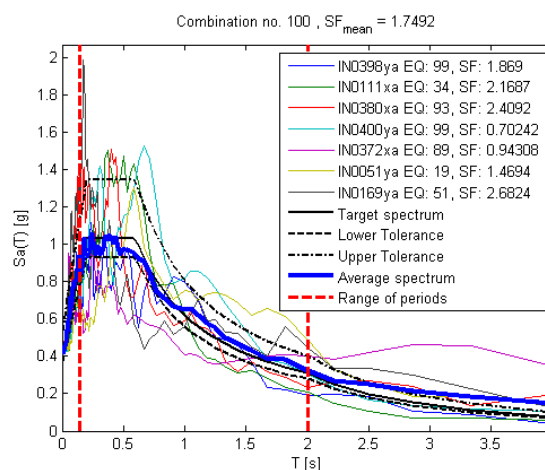


Figure 6. Selection of records in accordance with response spectrum for ground type C

Table 1. Group of selected records from SIMBAD base, ground type C, magnitude 6.5-7.5

ID	Name	ED [km]	PGA [m/s ²]
398	Northridge	20	2.17
111	Hyogo - Ken Nanbu	17.45	1.87
380	Superstition Hills	19.51	1.68
400	Northridge	20	5.78
372	Imperial Valley	27.47	4.31
51	NW Off Kyushu	26	2.76
169	Iwate Prefecture	27	1.51
mean		22.49	

5. RESULTS AND DISCUSSION

Presentation of results for four groups of 7 earthquake records are compared in order to verify the basic design objective and defined limit states. As a representation of software output, response of the structure due to the earthquake record "Imperial Valley" which caused largest response from structure was presented. Deformations of plastic hinge did not exceed the fracture limit X defined in F-D diagrams in PERFORM 3D [7-9]. The figures 7

and 8 presents the frame after the earthquake with the D/C ratio of plastic joints, as well as the frame with all the components that entered the plastic area during the earthquake. It can be concluded that plastic hinges appeared in defined locations. Plastic hinges appeared on top of the columns on the second, third and fourth story. Hinges didn't appear on the other end of the columns so "soft story mechanism" was avoided. The maximum D/C factor ratio of 0.83 was recorded in the beams at the first floor.

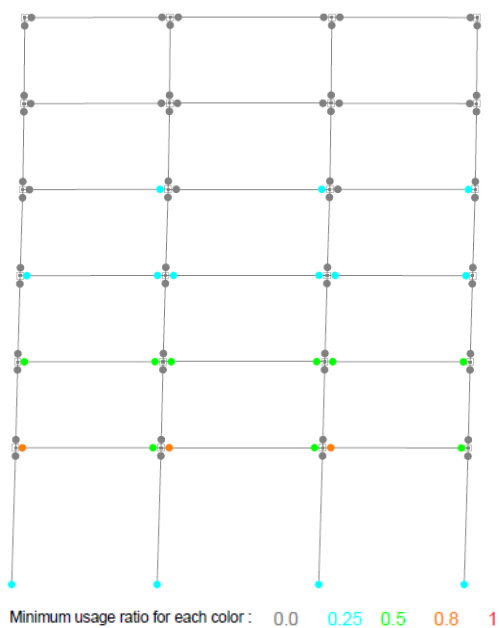


Figure 7. D/C ratio for plastic hinges for „Imperial Valley“

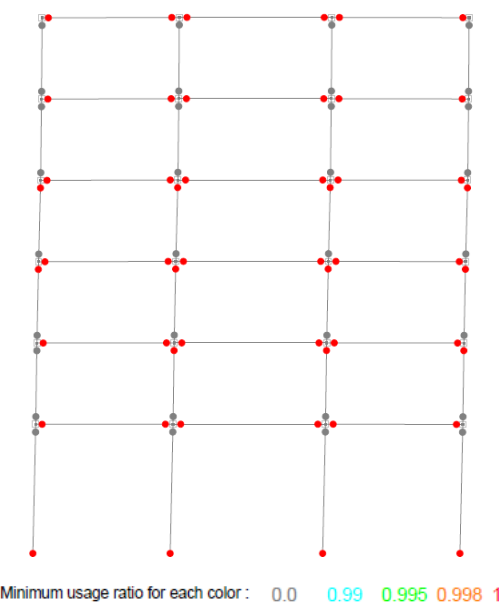


Figure 8. Hinges that have yielded „Imperial Valley“

The table 2 gives the maximum value of D/C ratio for rotation capacity of plastic hinges four groups of 7 records in accordance with the "no collapse" requirement.

Table 2. Overview of maximum values of D/C ratio for the limit state of deformation of plastic joints of beams and columns

Hinge rotation capacity – D/C ratio	Beam	Column
1. group of 7 records	0.60	0.34
2. group of 7 records	0.65	0.34
3. group of 7 records	0.84	0.40
4. group of 7 records	0.82	0.35
Medium value of 28 records	0.73	0.37

Load capacity of the beam-column joint was defined via moment which joint can transmit and load capacity of beam and column was defined for shear strength of cross section. Results of analysis for example earthquake shown on figure 9 and 10 present that load bearing capacity of elements was sufficient.

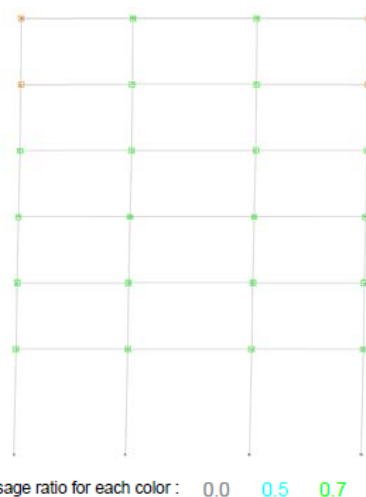


Figure 9. D/C ratio joint capacity „Imperial Valley“

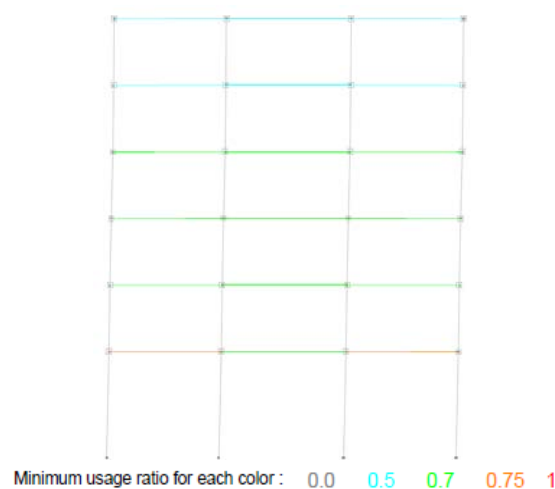


Figure 10. D/C ratio shear strength capacity of beams „Imperial Valley“

The table 3 provides information on the maximum value of D/C ratio (demand/capacity) for shear capacity of joints, beams and columns for four groups of 7 records in accordance with the “no collapse” requirements.

Table 3. Overview of maximum values of D/C ratio for the limit state of load bearing capacity of beams, columns and joints

Load bearing shear capacity – D/C ratio	Joint	Beam	Column
1. group of 7 records	0.87	0.71	0.34
2. group of 7 records	0.88	0.72	0.34
3. group of 7 records	0.89	0.72	0.34
4. group of 7 records	0.89	0.72	0.34
Average value of 23 records	0.88	0.72	0.34

The “damage limitation requirement” stipulates that the structure must be designed and constructed to withstand a seismic action that are more likely to occur than the design seismic action corresponding to the "no-collapse requirement”, without the damage and restrictions in use. This requirement is fulfilled if inter-storey drifts are checked in accordance with article 4.4.3.2. (a, b, c) [1]. The control of inter-storey drifts were checked and results are presented on figure 11.

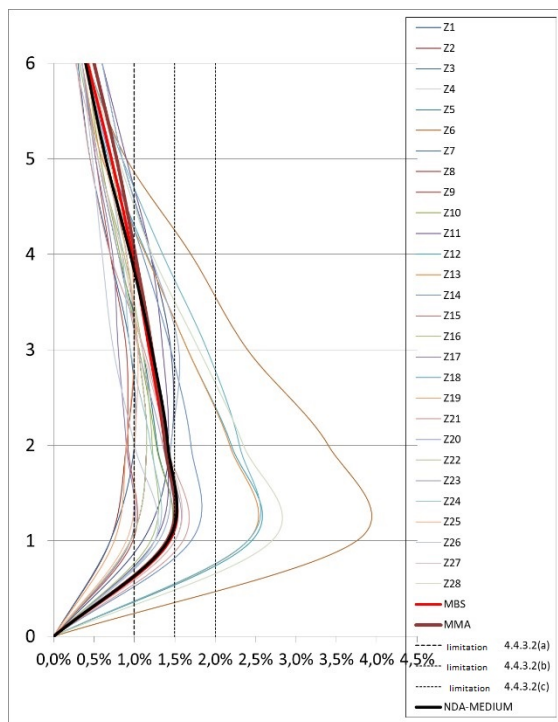


Figure 11. Inter-storey drift from linear and non-linear NDA analysis

In the figure 11 representation of inter-storey drifts are given for linear analysis and NDA for all 28 records including mean diagram from all 28 records. In all NDA analysis the maximum inter-storey drift occurred on the first floor. NDA analysis have large dispersion of results. The maximum NDA drift exceeds 150% value obtained from to linear static analysis. On the other hand the mean diagram of all 28 NDA deviate $\pm 10\%$ from the values obtained by linear analysis. It must be clarified that diagrams shown in Figure 11 for NDA are determinate for the design seismic action and are not suitable for controlling the damage limitation requirement explicitly because NDA results cannot be linearly scaled.

5. CONCLUSIONS

Based on the results presented in this paper, the following conclusions can be drawn:

- EC8 requires that beams and columns are safe for unfavourable brittle failure due to shear in plastic hinges, which in the case of a analysed structure, was satisfied in each section. In addition, with a larger amount of transverse reinforcement, a higher capacity of rotation of plastic joints is enabled, i.e. ductility of curvature.
- Provided load-bearing capacity of the joints as a result of the capacity design was sufficient in each joint of the frame in accordance with the results of the NDA analysis. The joint reinforcement calculation model from EC8 recommends a higher amount of reinforcement compared to the Paulay and Priestley model which provides additional joint protection [6].
- The rotational capacities for plastic hinges of the beams and columns were satisfied. D/C ratio ranged up to 83%. This way, the EC8 recommendation that the D/C ratio for deformation was met with the appropriate safety coefficients for constituent materials.
- Damage limitation state defined in EC8 for inter-storey drift was met in linear-elastic analysis for limit b and c, and for NDA with 3% margin. It can be concluded that the structure has met the “damage limitation requirement“ for buildings with ductile non-structural elements. NDA analysis have large dispersion of results. The maximum NDA drift exceeds 150% value obtained from to linear static analysis. On the other hand, average value of drift, considering that more than min 7 EQ ground motion are used for NDA, correspond to the values obtained from linear analysis.

In accordance with all the results and conclusions, the linear-elastic seismic analysis of reinforced concrete frames regular in plan and elevation very well describes the behaviour of the structure under the action of the design seismic load. Further research on this subject should be performed on the RC structures with other structural types and structures classified irregular in plan and elevation in order to provide critical assessment of regulation.

REFERENCES

- [1] Eurocode 8 (EN 1998-1:2004), "Design of structures for earthquake resistance, part 1: General rules, seismic actions and rules for buildings".
- [2] Michael N. Fardis (2009), "Seismic design, assessment and retrofitting of concrete buildings", Springer, Dordrecht, ISBN 978-1-4020-9841-3, pp. 120-155.
- [3] Ahmed Y. Elghazouli (2017), "Seismic design of buildings to Eurocode 8", Taylor & Francis Group, Boca Raton, LLC ISBN-13: 978-1-4987-5159-9, pp. 135-170.
- [4] Matjaž Dolšek (2010), "Development of computing environment for the seismic performance assessment of reinforced concrete frames by using simplified nonlinear models", *Bulletin of Earthquake engineering*, <https://doi.org/10.1007/s10518-010-9184-8>, pp. 1309–1329.
- [5] Peter Fajfar (2000), "A nonlinear analysis method for performance-based seismic design. *Earthquake spectra* [online]. 2000. Vol. 16, no. n 3, pp. 573–592.
- [6] Paulay T., Priesley N (1992), "Seismic design of reinforced concrete and masonry buildings", , John Wiley & Sons, Inc. West Sussex, PO19 8SQ United Kingdom. ISBN:9780470172841, pp 300-361.
- [7] Computers & Structures Inc, Berkeley (2006), "CSI PERFORM-3D user guide" Computers and Structures, Inc. Berkeley, California 94704 USA
- [8] Computers & Structures Inc, Berkeley (2006), "CSI PERFORM-3D Components and Elements " Computers and Structures, Inc. Berkeley, California 94704 USA
- [9] Graham Powell (2007) " Nonlinear dynamic analysis-Capabilities and Limitations", *The Structural Design of Tall and Special Buildings*, John Wiley & Sons, Inc. West Sussex, PO19 8SQ United Kingdom 15(5): 547- 552 <https://doi.org/10.1002/tal.381>
- [10] Iervolino I., Galasso C., Cosenza E.. (2010) " REXEL: computer aided record selection for code-based seismic structural analysis. *Bulletin of Earthquake Engineering*", *Bulletin of Earthquake Engineering* 8, Springer Switzerland, pp 339–362.

HOW WOULD YOU TAKE YOUR STUDYING?

STAY IN



TAKEOUT

ON THE GO



Harmut Pasternak

Chair of Steel and Timber Structures,
Brandenburg University of Technology,
Germany
h.pasternak@web.de

Zheng Li

Institute of Civil Engineering,
Technical University of Berlin,
Germany

DESIGN OF STEEL FRAME WITH VARIABLE CROSS- SECTION CONSIDERING STABILITY USING GENERAL METHOD ACCORDING TO EN 1993-1-1

Summary: In this paper, the advantages of the general method for verification of the lateral torsional buckling are demonstrated through the calculation of a real steel frame with variable cross-section in Germany. According to the Eurocode 3, the minimum load amplifier of the design loads and the minimum amplifier for the in plane design loads to reach the elastic critical load with regards to lateral or lateral torsional buckling are determined with the linear buckling analysis and the geometrically and materially nonlinear analysis using finite element method. The results show that shell models can create arbitrarily complex cross-sections and obtain more accurate results comparing to beam elements. Finally, the practical implementation of the reinforcement of steel frame is shown.

Keywords: steel frame, stability, variable cross-section, general method, numerical simulation.

1. INTRODUCTION

Welded frames with variable cross-section are commonly used in some steel structures, to save material and reduce costs. However, on the other hand, due to its complicated changes of cross-section along the length direction, it is difficult to accurately calculate the buckling resistance of frames using conventional methods (according to EN 1993-1-1 [1], Section 6.3.3) with hand calculation. In other words, the calculated buckling resistance of frames is an approximate result obtained by many simplifications. Of course, it is also possible to calculate the frame held by purlins and wall beams using the **Geometrically and Materially Nonlinear Analysis with Imperfections included (GMNIA)**. But this requires a wider knowledge of **Finite Element Method (FEM)**. An early example is given in [2].

The so-called "general method" is provided in EN 1993-1-1, Section 6.3.4 to carry out load-bearing capacity verifications against overall spatial failure, namely lateral torsional buckling. This approach can be used to analyze the spatial stability of steel frames with complicated

thin-walled, predominantly open profiles and to determine the global individual solutions of overall frames and structures at risk of bending torsion [3]. Since there are no analytical solutions available for the exact calculation of elastic critical load and associated eigenmodes, an FE-based method of stability analysis and verification is optimal and easy to use in practice.

2. GENERAL DESCRIPTION OF REAL CASE STUDY

There is an industrial single-story steel building with a dimension of $48 \times 36 \times 6 \text{ m}^3$ [LxBxH], which built at 1990s in Berlin, Germany. Recently, according to the owner's request, this steel hall should be demolished as a whole and rebuilt in northern Germany. However, the new site is located in the "Norddeutsches Tiefland" area of Germany, which requires calculation of exceptional snow (accidental) loads with a partial safety factor 2.3. Therefore, the entire steel building needs to be re-calculated. Fig. 1 shows a sketch of one of the frames.

3. NUMERICAL MODEL

In this case study, the numerical analysis of steel frame with variable section made from steel S335 was conducted using the general-purpose commercial finite element software Abaqus® [4]. First, each part of the frame (such as flange and web) is built using the shell model, and then all the parts are merged into a

whole frame model in 3-dimension, as shown in Fig. 2. The bottom of the two frame columns is coupled with a central reference point with an all degrees of freedom fixed coupling connection. Then these two reference points are defined as fixed bearings. To simplify the influence of the connection and support between the frames, the out-of-plane direction support is defined at every 6-meter at the upper flange of the rafter, as displayed in Fig. 3.

In this example, the snow load and the roof weight are defined as linear load loading with a value 11.2 kN/m at the middle of upper flange of the frame rafter. In order to add linear load to the shell element, a circular beam element with a diameter of 1 mm is defined at the middle of the upper flange, as shown in Fig. 2. To consider the self-weight of the frame, a gravitational field along the opposite direction of Y is defined as 1.0×9800 , where 1.0 is safety factor for permanent load and 9800 is the product of the earth's gravitational constant 9.8 and the dimensional conversion factor. In this model, mm, N, ton and s are used as the unit of consider the self-weight of the frame, a gravitational field along the opposite direction of Y is defined as 1.0×9800 , where 1.0 is safety factor for permanent load and 9800 is the product of the earth's gravitational constant 9.8 and the dimensional conversion factor. In this model, mm, N, ton and s are used as the unit of length, force, mass and time respectively. Because the steel building is relatively low, the influence of wind load and welding residual stress is ignored in this study.

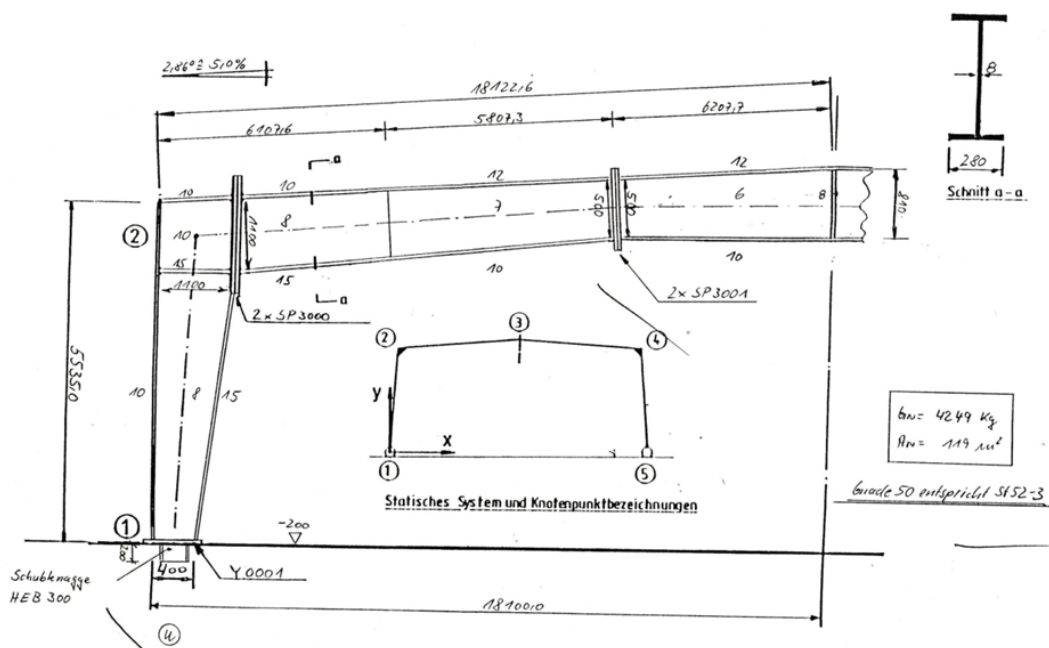


Figure 1. Sketch of a steel frame

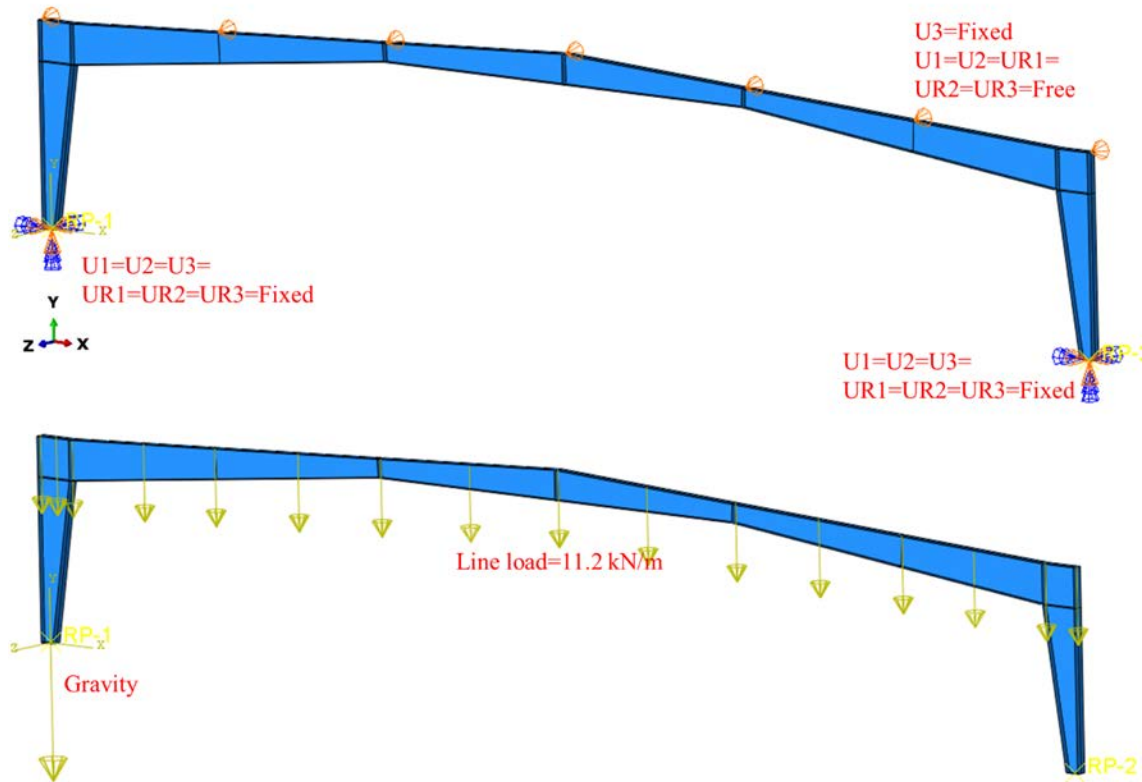


Figure 2. Numerical model and boundary conditions of the steel frame

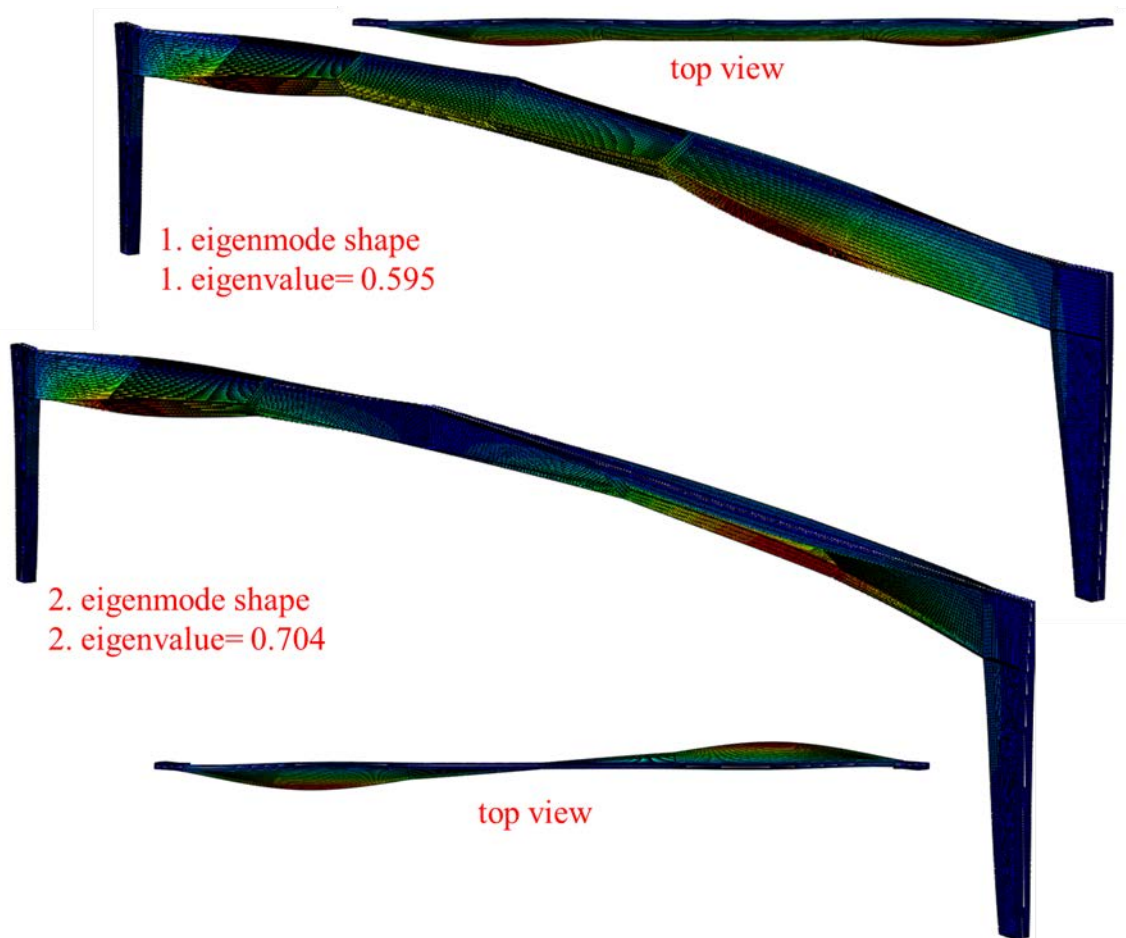


Figure 4. First two eigenvalues and eigenmode shape

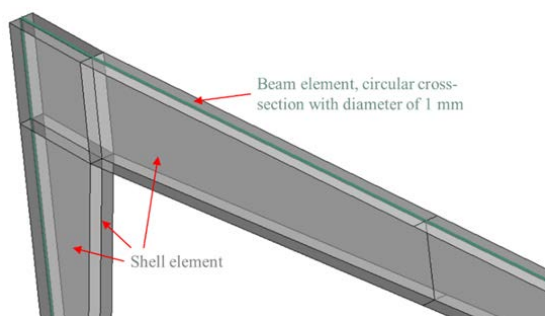


Figure 3. Element type of the steel frame

The non-linear elasto-plastic material model is employed and defined according to the corresponding design standard with a Young's modulus of 210 GPa and a yield stress of 355 MPa. The hardening property of the steel is not considered, or in other words it is simplified as zero. According to the convergence study, the element size of 50 mm was used and the total number of shell element for whole frame is about 28 thousand.

In this study, the subspace iteration eigensolver is employed to analyze the eigenmodes and eigenvalues for Linear Bifurcation Analysis (LBA), as shown in Fig. 4. The nonlinear static problem is solved for geometrically and materially nonlinear analysis using Riks (arc-length) Method. Since the Riks approach allows you to find static equilibrium states during the unstable phase of the response. The minimum load amplifier $\alpha_{ult,k}$ of the design loads to reach the characteristic resistance of the most critical cross section without taking lateral or lateral torsional buckling and the minimum amplifier $\alpha_{cr,op}$ for the in plane design loads to reach the elastic critical load with regards to lateral or lateral torsional buckling can be determined with the LBA and GMNA. In this study, the min. eigenvalue or the 1. Eigenvalue is used as the load amplifier $\alpha_{cr,op}$ and the ratio of max. moment of the frames based on GMNA and the design bending moment is defined as load factor $\alpha_{ult,k}$, as shown in Fig. 5. It is worth mentioning that local imperfections are not considered here, as it is not a decisive factor. Hence, these two values are determined with numerical approach as $\alpha_{ult,k}=1.990$ and $\alpha_{cr,op}=0.595$, respectively.

4. DESIGN USING GENERAL METHOD

According to the regulations of general method in EN 1993-1-1, section 6.3.4, this approach can be used for the verification of the resistance to lateral and lateral torsional buckling where the conventional methods are not applicable.

Base on the Formula 6.64 in [1], the global non-dimensional slenderness $\bar{\lambda}_{op}$ can be calculated as following:

$$\bar{\lambda}_{op} = \sqrt{\frac{\alpha_{ult,k}}{\alpha_{cr,op}}} = \sqrt{\frac{1.990}{0.595}} = 1.829 \quad (1)$$

Therefore, the corresponding reduction factor for the non-dimensional slenderness χ_{op} can be determined with the formula of Lateral torsional buckling curves base on $\bar{\lambda}_{op}=1.78$,

$$\chi_{op} = \frac{1}{\Phi_{op} + \sqrt{\Phi_{op}^2 - \bar{\lambda}_{op}^2}} \quad (2)$$

where, $\Phi_{op} = 0.5 * [1 + 0.76 * (\bar{\lambda}_{op} - 0.2) + \bar{\lambda}_{op}^2]$
It can be determined that $\chi_{op} = 0.204$.

Hence, the overall resistance to out-of-plane buckling of these frames can be verified by ensuring with the formula 6.63 in EN 1993-1-1,

$$\frac{\chi_{op} \alpha_{ult,k}}{Y_{M1}} = \frac{0.204 * 1.990}{1.1} = 0.37 < 1.0 \quad (3)$$

where Y_{M1} means partial factor for stability, which is equal to 1.1 according to German National Annex [5]. Therefore, the steel building needs to be reinforced during the reconstruction at the new location.

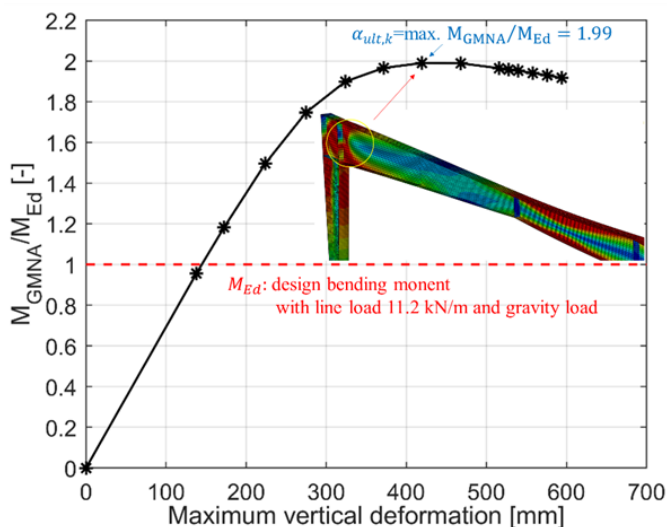


Figure 5. Moment vs max. deformation curve with GMNA

5. CONCLUSION AND DISCUSSION

The examples show that the steel frames with variable cross-section can be ensured by the verifications according to the general method for lateral torsional buckling with numerical approach. The shell model used can not only easily create complex arbitrary cross-sections, but also provide more accurate results



Figure 6. Reinforcement of steel frames

compared to the beam element. Such as, when the flange width of the frame beam is increased from 280 mm to 440 mm without changing other conditions in this example, local buckling will occur according to the first eigenmode and the 1. branch point load is not suitable for the subsequent overall buckling analysis of the steel frame. While using beam elements may ignore these issues.

Moreover, for the practical engineering problem, the flexural capacity of the frame columns is strengthened by the use of triangular additional structural members. Fig. 6 shows the implementation of the reinforcement.

Acknowledgements

The calculations were carried out by the authors. The client arranged the reinforcement of the structure.

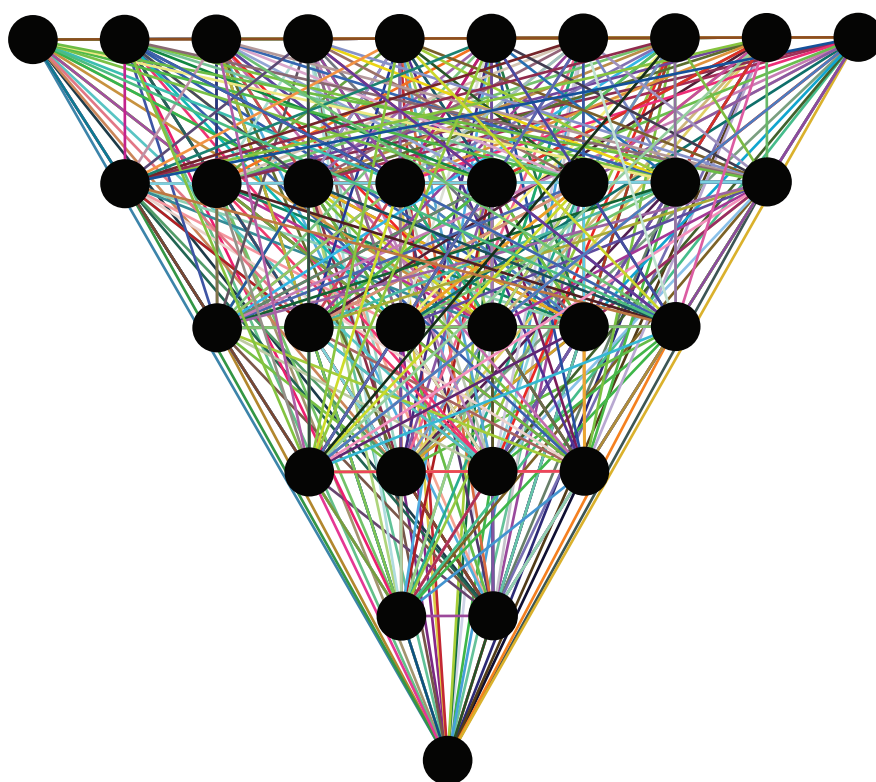
REFERENCES

- [1] EN 1993-1-1 (2005) + AC:2009 Eurocode 3: Design of steel structures – Part 1-1: General rules and rules for buildings. Berlin: Beuth.
- [2] Pasternak, H.; Müller, L (2001). Zur FE-Modellierung leichter Hallenrahmen, Stahlbau 70 (2001), Vol. 1, pp. 53-58.
- [3] Papp, F. (2016) Buckling assessment of steel members through overall imperfection method in: Engineering Structures (106), pp. 124– 136.
- [4] Smith, M. (2009) ABAQUS/Standard User's Manual, Version 6.9.
- [5] DIN EN 1993-1-1 National Annex (2010) - Nationally determined parameters - Eurocode 3: Design of steel structures - Part 1-1: General rules and rules for buildings. Berlin: Beuth.

THE AII4R&D PLATFORM HAS PUT US ON THE MAP



WE IMPROVE THE KNOWLEDGE TRIANGLE
AND JOINTLY ACCELERATE INNOVATION



35 INNOVATIVE TEACHING PRACTICES

8 RESEARCH PROJECTS LINKED TO REAL SECTOR

50 PROFESSIONAL COURSES WITH 500 PARTICIPANTS

DIVERSE NETWORK OF 6 COUNTRIES AND 14 PARTNERS



Promoting academia-industry alliances
for R&D through collaborative and
open innovation platform - AII4R&D
www.platform.all4rd.net

Co-funded by the
Erasmus+ Programme
of the European Union



Elena Popovska

MSc, Civil Engineer
e-popovska@hotmail.com

Mile Partikov

PhD, Assistant Professor
University "Ss. Cyril and Methodius"
Faculty of Civil Engineering – Skopje
partikov@gf.ukim.edu.mk

Denis Popovski

PhD, Associate Professor
University "Ss. Cyril and Methodius"
Faculty of Civil Engineering – Skopje
popovski@gf.ukim.edu.mk

STIFFNESS COMPARISON OF UNSTIFFENED AND STIFFENED T - JOINTS OF HOLLOW SECTIONS

Structural analysis is performed on 12 models of T-joints from hollow cross sections reinforced with welded flange plate on the chord. Cross sections used for the verticals are sized from 40 to 70mm square section while the chord has size of 100mm square hollow section. For each vertical three different thickness are analyzed, also considering the thickness of the chord is same as the thickness of the vertical in the respective model. Joints are loaded with maximal in-plane bending moment. The results are drawn in a form of moment – rotation diagram and table result and compared to results obtained for same unstiffened models. Reinforcement used is based on the assumption that all the models comply with chord face failure mode, which is expected for the geometry used for these types of joints. It is concluded that the type of reinforcement is properly chosen since in all models there is an increase of the initial stiffness. Additionally, is summarized that the increase of the stiffness relies greatly of the solidness of the used sections.

Keywords: stiffness analysis, T-joints, moment connections, reinforced connections, hollow sections.

1. INTRODUCTION

The behavior of a Vierendeel beam markedly relies on the stiffness of the joints. This type of beam is consisted exclusively of T-joints that are loaded with a combination of a bending moment, shear force and certain axial force. Since it is very complex to do and properly interpretate separate analysis of such joint when all three internal forces are present in the joint usually is recommended studies to be done of joint loaded with in-plane bending moment as a the most influential force. According to stiffness classification joints can either be found as pins, semi rigid or rigid and while rigids are rarely used due to economic reasons, mostly we are talking either about pins or semi-rigids. According to the Eurocodes few parameters are highly important for the definition of a T-joint geometry. Factor ' β ' which is ratio of the mean width of the brace members, to that of the chord: factor ' γ ' which

is the ratio of the chord width to twice its wall thickness and factor ' β_p ' which is the ratio of the width of the brace members, to that of the stiffening plate. Expressions for these factors point out the limits where joints change classification, as well define the mode of failure. For models loaded with in – plane bending moment two modes of failure are expected: if $\beta \leq 0,85$ plastic failure of the chord face is applicable, while when $\beta > 0,85$ failure of the side wall of the chord by yielding, crushing or instability is expected.

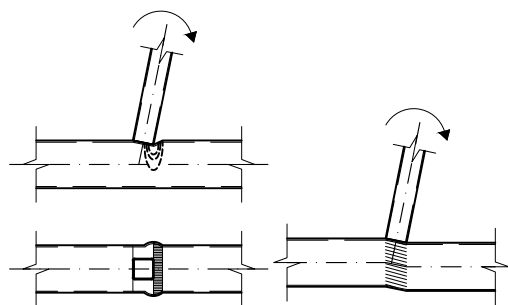


Figure 1. Chord plastification mode of failure on the left; chord side wall failure mode on the right

Another factor to distinguish pins and semi rigid is the value of ' γ ' where bigger values lead to thicker chords and stiffer joints.

Provided the fact that the Vierendeel is greatly depending on the stiffness of its joints pinned joint in this type of member will lead to increase in the internal forces of the chord and considerable increase of the global deformation, which not always will be bearable. So, when increase of a cross section is not an option next step is to select proper type of reinforcement. This also relies on the mode of failure.

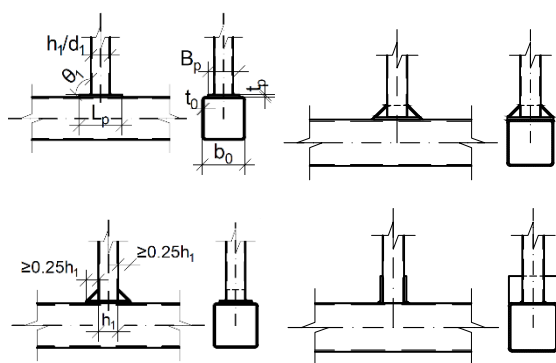


Figure 2. Recommended types of reinforcement in joints where chord plastification failure is expected

Reinforcements when a failure due to plastification of the face of the chord is expected can be in a form of haunch welded between the chord and the vertical, welded ribs aligned with the webs of the vertical to the

chord, angles positioned in between the vertical and the chord to avoid direct welding between the two elements, and most used plate welded to chord's face.

All these reinforcements will secure this weak spot in the joint and move the failure to another section by also increasing the general stiffness.

Another important factor when obtaining stiffness of a joint is to perform correct classification. Every geometry of joint has values of limit where pins end and limit where rigid starts. Everything in between is semi rigid. These values can be pointed on a diagram of moment - rotation. The diagrams are obtained in an iterative calculation with incremental increase of the moment to obtain the representative rotation and the curve of the correlation $M-\phi$. Also, from the value of the stiffness of the connection, value of the initial stiffness of the joint is derived.

This research focuses on the analysis of T-joints classified as pins, whose geometrical factor $\beta \leq 0,85$ and factor $2\gamma > 16$. Reinforcement is performed by welding a stiffening plate $\beta_p < 0,85$ on the face with of the chord what is according to the recommendations of Eurocode 1998, chapter 8, annex E table 7.17. The behavior of these models is compared to the behavior of the same unstiffened models and conclusions about the factors that influence the stiffness are drawn.

2. NUMERICAL ANALYSIS

Analysis is performed in software IDEA StatiCa where two separate calculations are performed. First a design capacity analysis is done for all models to obtain the maximal value of the bending moment and next the main stiffness analysis is run with this bending moment. With these more accurate values for the secant stiffness are obtained.

2.1 SOFTWARE THEORETICAL BACKGROUND

Software IDEA StatiCa is designed for calculation of steel joints (connections). Four types of analysis can be performed: stress/strain analysis where plates and connectors are checked, stiffness analysis, design resistance analysis, and capacity analysis. The calculations are based on the component based philosophy where this method (CM) solves the joint as a system of interconnected items – components. Each component is

checked separately using corresponding formula derived from the codes. To avoid the generality of the component-based method the internal forces in the components are calculated by FEA. Elastoplastic behavior with hardening of the material is considered. The welds are designed as a multipoint constraint that relate the finite element nodes of one plate edge to another. This way of modeling is conservative and leads to the fact that the resistance of the weld along the length will rely on the stress peaks that appear at the end of plate edges, in corners and rounding. To eliminate these effects, a special elastoplastic element is added between the plates that redistributes the stress peaks along the length of the weld and real values are obtained.

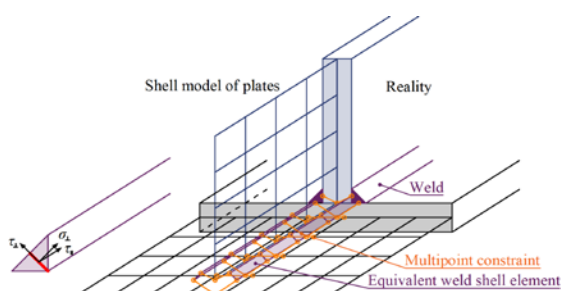


Figure 3. Multipoint constraint weld model

2.2 MATHEMATICAL MODELS

The geometry of each model is given in the table 1. Material used for all elements is S275JR. The welds of each model are one-sided filed weld with thickness same as the thickness of the plates they connect. The cross sections used are cold formed square hollow sections.

Table 1. Models geometry

Model	chord	vertical	reinforcement
1.1	□100.100.3	□40.40.3	≠90.6...110
1.2	□100.100.3	□50.50.3	≠90.6...110
1.3	□100.100.3	□60.60.3	≠90.6...115
1.4	□100.100.3	□70.70.3	≠90.6...115
2.1	□100.100.4	□40.40.4	≠90.8...110
2.2	□100.100.4	□50.50.4	≠90.8...110
2.3	□100.100.4	□60.60.4	≠90.8...115
2.4	□100.100.4	□70.70.4	≠90.8...115
3.1	□100.100.5	□40.40.5	≠90.10...110
3.2	□100.100.5	□50.50.5	≠90.10...110
3.3	□100.100.5	□60.60.5	≠90.10...115
3.4	□100.100.5	□70.70.5	≠90.10...115

In the software the appropriate cross sections are selected. For the chord length of 1000mm is used in all models while the vertical is 400mm. The connection between the elements is done by using predesigned layouts where

values for the geometrical characteristics of the stiffening plate and welds are specified, and relations of the connecting plates with welds are assigned. In the design resistance analysis bending moment of 1kN is applied on the vertical and the analysis is started. The analysis finishes with a factor which multiplied by 1kN will give the value of the maximal bending moment the joint can bear. This is done separately for each model.

These moments are next used in the main stiffness analysis. For this analysis the member of the vertical is assigned as analyzed member, on which the bending moment is going to be applied. For the software to do a classification of the joint also the theoretical buckling length should be inputted. The chord is considered as continuous beam with two supported endings while the vertical is loaded on one ending and connected on the other.

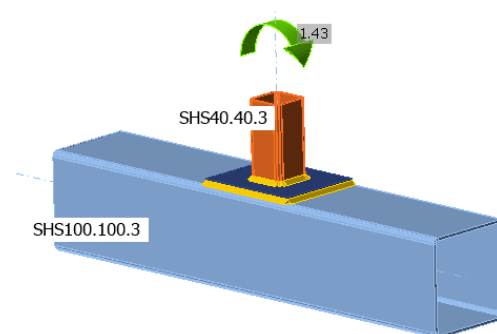


Figure 4. 3D model of model 1.1.

The stiffness analysis is run, and results are requested in both diagrams and table representation.

2.3 RESULTS AND DISCUSSIONS

From the analysis diagrams of the curve moment - rotation correlation is drawn. Apart from this, information can be got about the plastic moment. To obtain this curve the program applies load steps and evaluates the rotation of the connection. Additional information can be gotten about joints ultimate resistant moment $M_{j,Rd}$, the ultimate plastic moment of the cross section of the analyzed member or the vertical $M_{c,Rd}$, value of the initial stiffness $S_{j,ini}$, value of the secant stiffness $S_{j,s}$, rotation deformation and rotational capacity φ and φ_c , boundary where rigids start $S_{j,R}$, boundary where pins end $S_{j,P}$ and class.

The model 3.1 with vertical □40.40.5 displayed biggest difference of the stiffness between stiffened and unstiffened model while smallest difference happened in model 1.4 with vertical □70.70.3. Models of vertical with width 40mm

display nonlinear rapid increase of the initial stiffness after reinforcement. Similar behavior, display models of vertical with width 50mm, while the ones of wider verticals display linear increase by the increase of the stiffness. Their lines are almost parallel. Same applies to the thickness of the models, in the models with thickness of 3mm the increase is somewhat same, but there is great difference in the stiffness after reinforcing the models of 5mm. All models after reinforcement change class from pins to semi-rigid. The model 3.1 with vertical [40.40.5 is closest to the boundary of rigids. By comparing the diagrams of unstiffened and stiffened joint can be assumed that the reinforced joints display smaller changes in the rotation. Also, the angle between the horizontal and the M-φ curve is bigger compared to the unstiffened ones.

Table 2. Stiffness difference after applying reinforcement

Model	Stiffness increase	Increase in %
1.1	6.55	655%
1.2	4.64	464%
1.3	3.82	382%
1.4	2.81	281%
2.1	10.06	1006%
2.2	6.27	627%
2.3	4.97	497%
2.4	3.85	385%
3.1	22.87	2287%
3.2	9.36	936%
3.3	5.89	589%
3.4	4.97	497%

Table 3. Class boundaries and initial stiffness

Model	Sj,P [kNm/rad]	Sj,R [kNm/rad]	Sj,ini [kNm/rad]
1.1	24,47	1223,25	87,20
1.2	51,19	2559,38	126,39
1.3	92,14	4606,88	106,89
1.4	150,94	7546,88	333,23
2.1	29,14	1456,88	281,59
2.2	62,21	3110,63	308,18
2.3	114,45	5722,50	435,64
2.4	189,26	9463,13	672,09
3.1	35,18	1758,75	1083,16
3.2	70,88	3543,75	756,14
3.3	132,56	6628,13	912,22
3.4	222,08	11103,75	1288,65

Table 4: Results of calculated stiffness of model [40.40.3 - [100.100.3 + #90.6...110

Name	Comp.	Loads	Mj,Rd [kNm]	Sj,ini [kNm/rad]	Φc [rad]	L [m]	Sj,R [kNm/rad]	Sj,P [kNm/rad]	Class.
SHS40.40.3	My	LE1	1.44	87.20	0.08	0.40	1223.25	24.47	Semi-rigid

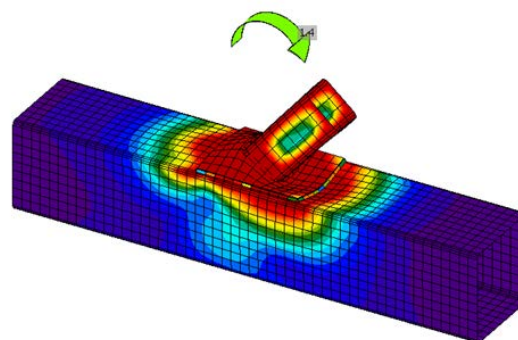


Figure 5. Results of loaded model 1.1 [40.40.3 - [100.100.3 + #90.6...110

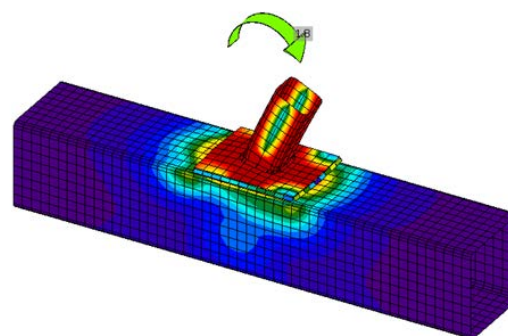


Figure 6. Results of loaded model 1.2 [40.40.4 - [100.100.4 + #90.6...110

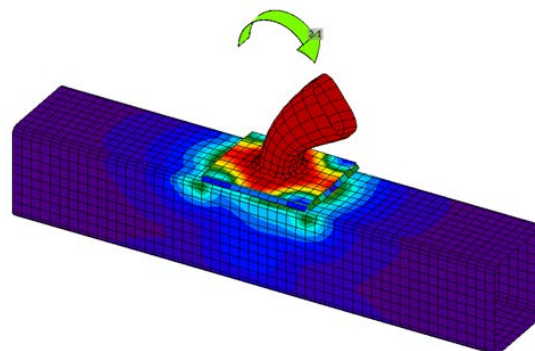


Figure 7. Results of loaded model 1.3 [40.40.5 - [100.100.5 + #90.6...110

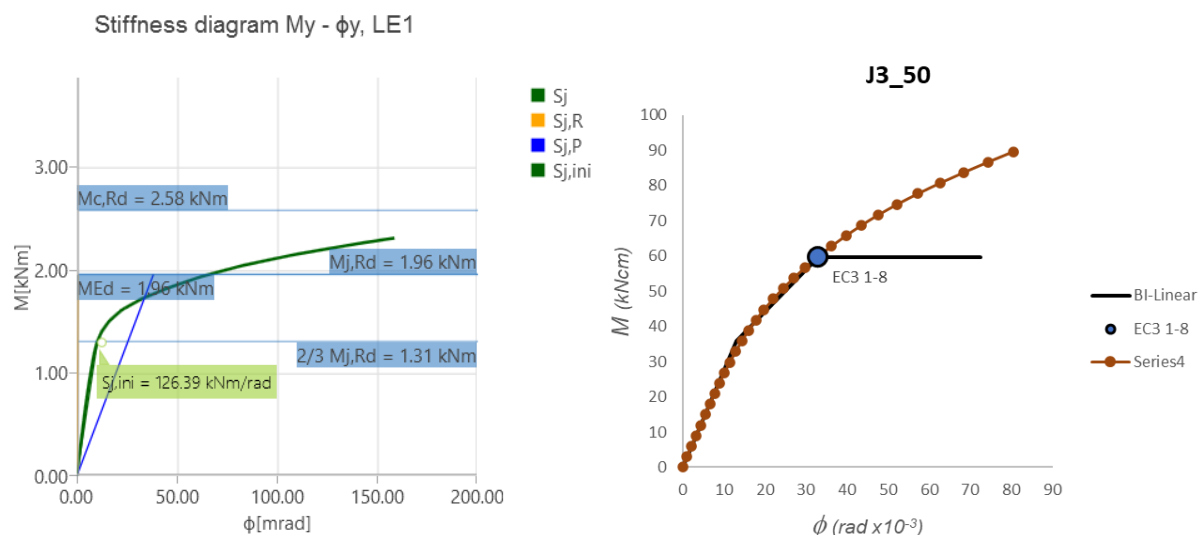


Figure 8. Moment rotation curve of a reinforced joint on the left; moment- rotation curve of the initial joint

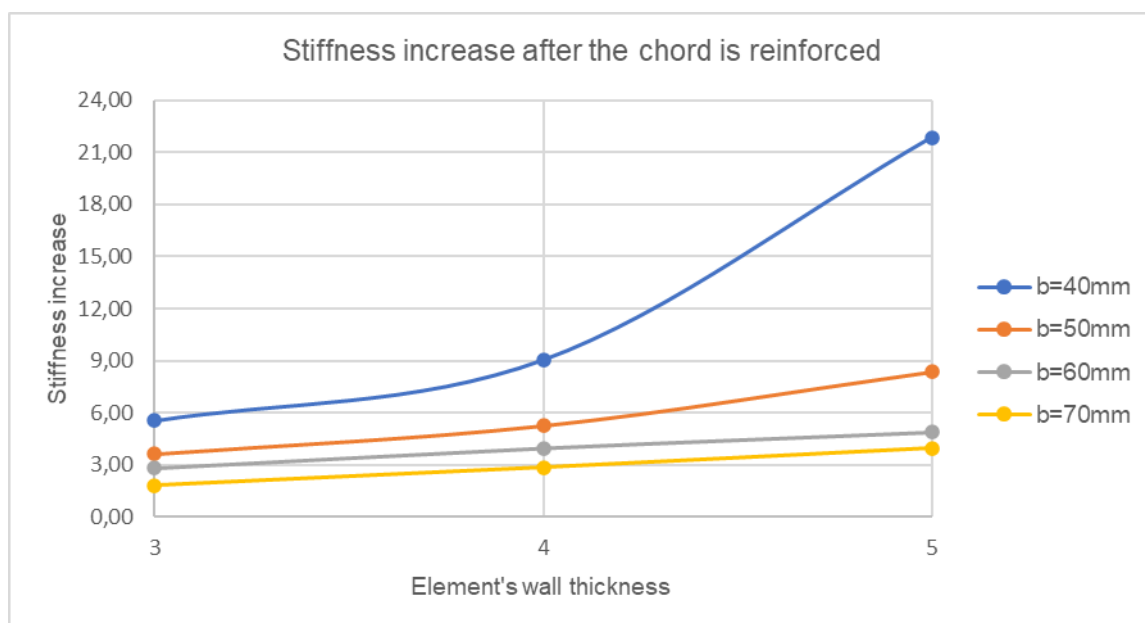


Figure 9. Diagram of the increase of the stiffnesses to vertical geometry

4. CONCLUSION

Based on the numerical results the following can be concluded:

- (1) All joints after reinforcement increase their stiffness leading to conclusion that the initial assumption of failure due to plastification of the face of the chord is correct. This increase varies from 2,81 to 22,87 times the initial stiffness. Additionally, all models change class from pin to semi rigid, meaning that while the reinforcement does help in

the stiffness none of the models reaches rigid class. This indicates that other factors considerably influence the stiffness of a T-joint. Model 3.1 with a vertical of a SHS40.40.5 is closest to the boundary with an initial stiffness of 1083kNm/rad in comparison to the 1758kNm/rad where rigids start. Also, the initial stiffness is 60% of the value where rigids start, while in model 1.4 with a vertical of a SHS70.70.3 the initial stiffness is 4% of the value for rigids limit.

- (2) Reinforcement has a great benefit in the models with thicker walls and

smaller size vertical. Models 1.1, 1.2 and 1.3 all with a vertical of 3mm have almost similar increase in the stiffness from 6,55 in the smallest vertical to 2,81 times in the largest vertical. Contrary to this the models with thick verticals have increase starting from 4,27 to 22,87 times the initial stiffness. Taking all these factors in account leads to a conclusion that the effects of thin-walled elements which persist after reinforcement of the chord will influence the general stiffness of the global system.

- (3) Models with large sized verticals don't have rapid increase of the stiffness like the small sized. This can be because these models have β ratio closer to the boundary of 0,85 which indicates that although their primary mode of failure is plastification of the chord they are also influenced of the side wall failure specific for models with β ratio bigger than 0,85.
- (4) T-joints with smaller sized verticals depict more drastic increase of the stiffness with the increase of their wall thickness, while this is not the case with the joints with wider verticals. On the joined diagrams for the stiffness it can be seen that the models 1.1, 2.1 and 3.1 all with a vertical of a SHS40.40.3 have a rapid increase in the stiffness especially the leap between model 2.1 and 3.1 where from 9 times it will reach 22 times in the next one. This is also happening in models 1.2, 2.2 and 3.2 but with lower impact where the increase starts with 4,6 to 6,27 and ends with 9,36 times increase. In the other models the increase is almost linear. It can be concluded that an increase of 1mm thickness makes significant difference of the ratio width to thickness of the vertical which leads to thicker cross sections, while this increase is not that remarkable in the big sized cross sections of the vertical bracing. This also confirms the theory that the stiffness is greatly influenced by the thin-walled effects of the cross sections used.

REFERENCE

- [1] Packer J. A., Henderson J.E. (1997); Hollow structural section connections and trusses; Canadian Institute of Steel Construction
- [2] Packer J.A.; Wardenier J., Zhao X.L. et al; (2009 god.); Design guide for rectangular hollow sections (RHS) joints under predominantly static loading; CIDECT
- [3] Партиков М.; (2020 год.); Експериментално и теориско истражување на влијанието од крутоста на јазлите кај Виренделови носачи од затворени профили; Градежен факултет, Универзитет „Св. Кирил и Методиј“; Скопје
- [4] Simoes da Silva L., Lamas A., Jaspart J.P. et al; (2016 god.); Design of Joints in Steel and Composite Structures; European Convention for Constructional Steelwork; Portugal
- [5] The European Union; (2005 year.) Eurocode 3: Design of steel structures – Part 1-1: General rules and rules for buildings; Management Centre: rue de Stassart, 36; B-1050 Brussels
- [6] The European Committee for Standardization; (2005 year.) Eurocode 3: Design of steel structures –Part 1-8: Design of joints; Management Centre: rue de Stassart, 36; B-1050 Brussels
- [7] Wardenier J. , Packer J.A., Zhao X.L. et al; (2010 god.); Hollow sections in structural applications; Geneva Switzerland
- [8] Partikov M., Cvetanovski P.; (2019); Model calibration of welded SHS to SHS T-joints under moment loading; Scientific Journal of Civil Engineering, Volume 8, Issue 2.
- [9] Партиков М., Цветановски П., Поповски Д.; (2015 год.); Проектирање на решеткаст носач со К јазли според Еврокод 3; ДГКМ, 16. Симпозиум; Охрид.
- [10] Филиповски А.; (2000 год.) Основи на челични конструкции; АД Печатница „НАПРЕДОК“ –Тетово; Скопје.

Denis Popovski

PhD, Associate Professor
University “Ss. Cyril and Methodius”
Faculty of Civil Engineering – Skopje
popovski@gf.ukim.edu.mk

Mile Partikov

PhD, Assistant Professor
University “Ss. Cyril and Methodius”
Faculty of Civil Engineering – Skopje
partikov@gf.ukim.edu.mk

Ivan Micevski

MSc, Civil Engineer
micevskivan@gmail.com

PULL-OUT TEST FOR CHEMICAL ANCHORS

The task of connecting building components is as old as building itself. Modern technology for fastenings is getting more applied worldwide. Fastenings must be designed in such a way that they do the job for which they are intended, are durable, robust and exposed to external loads. This study deals with the identification of chemical anchors embedded in reinforced concrete slab under tension load. The anchors are embedded according to rules and recommendations given from anchor manufacturer. The axial load capacity and the failure mode are observed for each test. Results from conducted tests are given in form of load – displacement diagram curves which defines the type of anchor failure. Conducted tests in this paper are basis for further experimental researches for chemical anchors under tension load while changing the parameters of concrete, reinforcement, edge and axis distances, embedment depth and other parameters that define the behavior of chemical anchors and ultimate failure loads.

Keywords: chemical anchors, post-installed anchors, pull-out test, load-displacement, ultimate failure loads.

1. INTRODUCTION

Design of construction and construction elements have to comply with the current norms and standards. In case when the design of structure or detail cannot be in accordance to national norms and standards, then technical approvals should be used. Every type of anchor is designed for use in special conditions such as different type of concrete, different type of load, frequency of load, position of installment, etc.

The technical approvals are based on results from qualifications tests conducted by independent laboratories. Modern technology for fastenings is more applied worldwide and every type of anchor is designed for use in special (individual) conditions, such as different type of concrete, load, frequency of load, position of installment etc. If the anchor is not properly installed in conditions which is suitable for, then the safety of the detail is suspected, even the safety of the whole structure. Due to the complexity and diversity of post – installed

anchors, all attempts to standardize anchor products have failed.

In the countries in the European Union, calculation of load capacity of anchors is carried out according to Annex C of ETAG001 (Guidelines for European Technical Approval of Metal Anchors for use in concrete) until implementation of CEN/TS 1992-4 (2009) as part of Eurocode 2 (2005) – Part 4. In United States calculation for load capacity of anchors is regulated from 2002 in Appendix D from ACI318 (2002), revised and supplemented in 2011. Recommendations given in guidelines strictly defines the conditions and the manner in which tests for approval of anchors will be carried out.

2. EXPECTED BEHAVIOR AND TYPES OF FAILURE FOR ANCHORS LOADED WITH TENSION FORCE

Several failure modes are possible for post – installed adhesive anchors loaded in tension and all of the failure modes are characterized with different load – displacement curve in function of different types of factors.

Expected types of failures under external tension load are:

- Steel failure,
- Concrete cone failure,
- Splitting failure,
- Pull – out failure (concrete/adhesive interface),
- Pull – out failure (adhesive/anchor interface)
- Pull – out failure (mixed interface)

Apart from the type of the anchor, the failure and behavior also depend on cleanliness of the drilled hole, adhesive type, embedment depth, concrete class, cracked or non – cracked concrete and the way force is applied. Total measured displacement (extraction) of the anchor is compiled of the slip of the anchor, local deformation in concrete zone where the transfer of the friction load occurs, and the deformation of the anchor itself. Every type of failure occurs after characteristic tension force is reached.

At small embedment depths ($h_{ef} \approx 3d$ to $5d$) concrete cone failure is characterized by a cone – shaped concrete breakout originating at the base of the anchor. It occurs when full tensile capacity of the concrete is utilized. Splitting failure is characteristic failure when anchor is installed near the edge of the concrete

embedment or when dimensions concrete cone is limited. For greater embedment depths, the concrete failure mode usually transitions to a mixed – mode (bond/concrete breakout) type of failure. A concrete cone with a depth of approximately $2d$ to $3d$ forms at the top end of the anchor and the bond fails over the balance of the embedment depth. Bond failure occurs either at the boundary between concrete and mortar or at the boundary between the mortar and anchor rod. Often a failure between concrete and mortar occurs in the upper part of the embedment, with the failure of the bond between mortar and anchor rod confined to the deeper end. For large embedment depths the bond resistance developed over the length of the anchor can exceed the rupture strength of the steel rod, leading to steel failure. The minimum embedment depth of a single anchor rod depends on the grade of the steel, the concrete mechanical properties and the properties of the mortar.

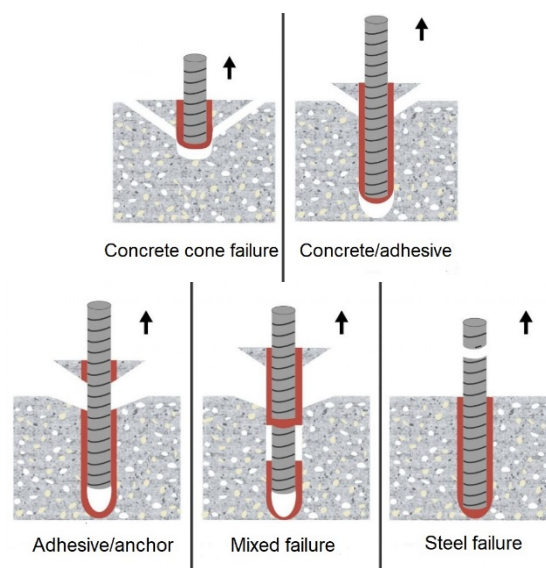


Figure 1. Types of failure due to tension load

3. TEST PREPARATION

3.1 PREPARATION, DRILLING AND INSTALLATION OF ANCHORS

In the foundation slab 4 types of anchors from same manufacturer were installed with different type of chemical injection.

All parameters for installation of anchors are previously measured and approved. After drilling of the holes, before installation of the anchors, every hole was cleaned from drilling dust. Scheme of the procedure for installation of chemical anchors is shown in figure 2 and figure 3.

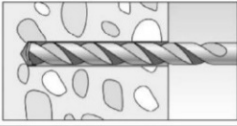
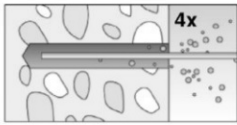
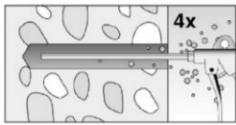
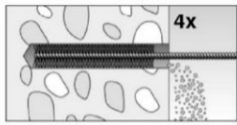
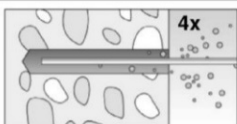
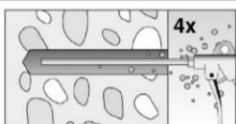
Installation instructions	
Drilling and cleaning the hole (hammer drilling with standard drill bit)	
1	 <p>Drill the hole. Nominal drill hole diameter d_0 and drill hole depth h_0</p>
2	 <p>4x Clean the drill hole: For $h_{ef} \leq 12d$ and $d_0 < 18$ mm blow out the hole four times by hand</p>  <p>4x For $h_{ef} > 12d$ and / or $d_0 \geq 18$ mm blow out the hole four times with oil-free compressed air ($p \geq 6$ bar)</p>
3	 <p>4x Brush the drill hole four times. For deep holes use an extension.</p>
4	 <p>4x Clean the drill hole: For $h_{ef} \leq 12d$ and $d_0 < 18$ mm blow out the hole four times by hand</p>  <p>4x For $h_{ef} > 12d$ and / or $d_0 \geq 18$ mm blow out the hole four times with oil-free compressed air ($p \geq 6$ bar)</p>

Figure 2. Drilling and cleaning the hole

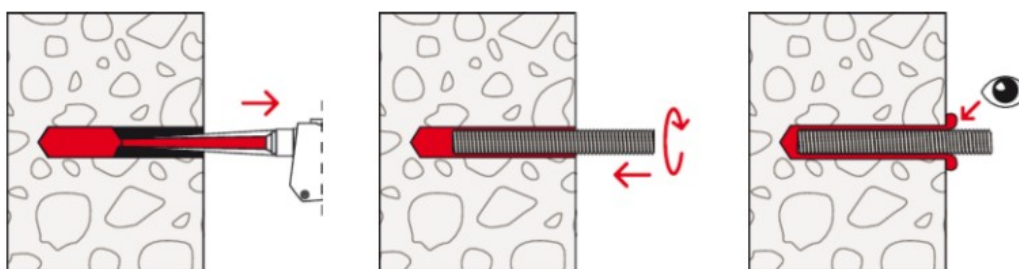


Figure 3. Application of adhesive and installation of anchor

3.2 QUALITY CONTROL OF CONCRETE

As mentioned before, the pull-out test conducted for chemical anchors embedded in non-reinforced concrete, presented in this paper, is not standard procedure, which differs from procedures stated in ETAG. To control the quality of concrete from which foundation slab is made, samples from concrete in phase of concreting are taken for further laboratory tests. Samples are taken for cubes with standard dimensions 15/15/15cm in accordance with EN12390-1 (Testing hardened concrete – Part1: Shape, dimensions and other requirements for specimens and molds). According to recommendations, many samples are taken in phase of concreting. Samples were stored in controlled laboratory conditions in accordance with EN12930-2 (Testing hardened concrete – Part2: making and curing specimens for strength tests). To determine the class of

concrete and compressive strength, all of the cubes were tested after 28 days from concreting the foundation slab. Obtained results from concrete tests are processed in accordance with EN 13791. From measured results concrete class C25/30 was achieved.

3.3 EQUIPMENT FOR MEASURING TEST RESULTS

The electronic equipment is connected to HBM Quantum data acquisition system amplifier, directly connected to computer, with measuring in real time. Results are given in form of vertical deformation of anchor (extraction) in proportion to the applied tension force. Scheme for installation of measuring equipment is shown in Figure 4.

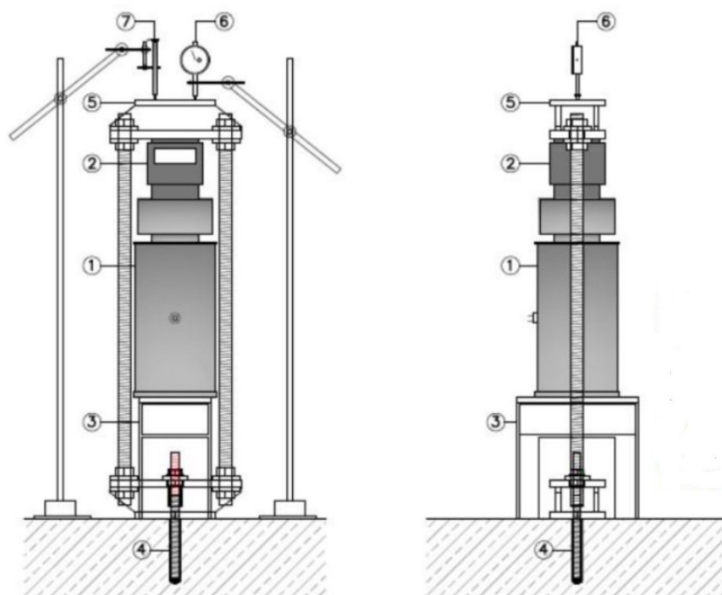


Figure 4. Scheme for installation of the equipment

Where,

- 1) Hydraulic press
- 2) Dynamometer
- 3) Concrete cone support construction
- 4) Installed chemical anchor
- 5) Tension load construction
- 6) Inductive deformer (comparator)
- 7) Electronic deformer (comparator)

All of the selected anchors were with similar installation procedure, steel quality, equal diameter and same thread M16, but with different load capacity defined by the manufacturer as a result of different type of adhesive.

Tension force for the anchor was applied through special designed system with hydraulic press positioned on steel construction which does not affect the concrete cone failure. Application of tension load on anchors was continuously monitored through the electronic dynamometer. Installed anchors were loaded in one phase until failure occurs. Measurement of vertical displacement of the anchors was carried out by two positioned deformers (electronic and inductive).

4. RESULTS FROM CONDUCTED PULL-OUT TEST FOR CHEMICAL ANCHORS

With the conducted experimental tests of the chemical anchors installed in foundation slab,

the obtained data was used for the analysis of the behaviour of the anchors. All gathered data was processed in form of load – displacement diagrams. The following are the results for each anchor group from the experimental research. The anchors were loaded until the failure occurs. During the experimental examination maximum force that was occurred was 108.8 kN and maximum vertical deformation of the anchor was 10.8 mm.

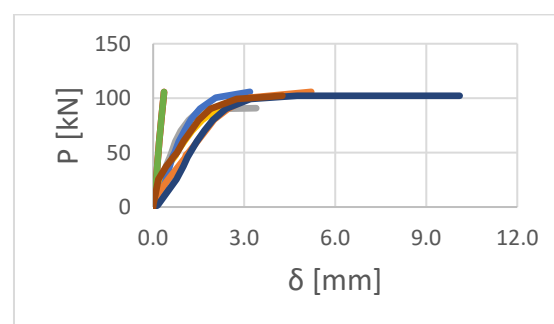


Figure 5. P-δ diagram for anchor type 1

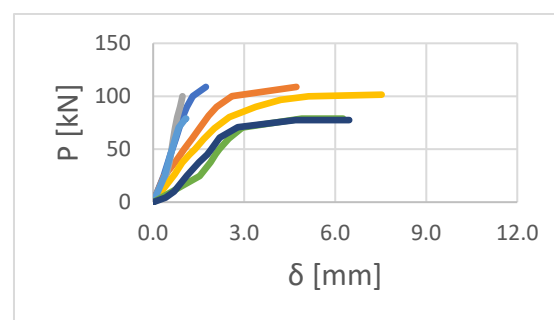


Figure 6. P-δ diagram for anchor type 2

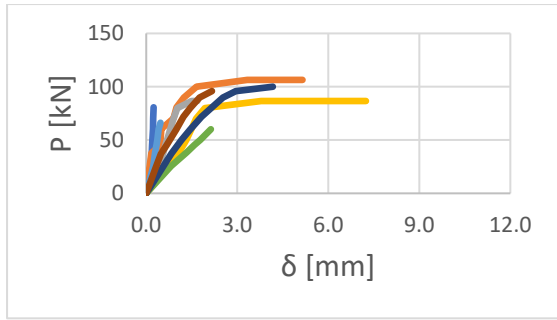


Figure 7. P-δ diagram for anchor type 3

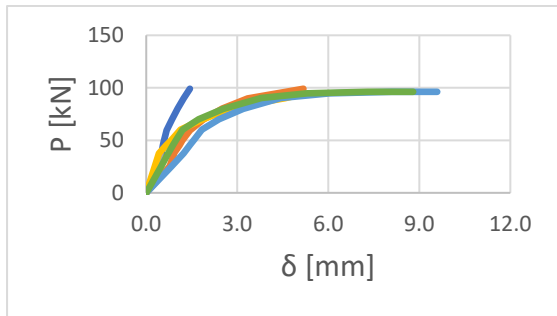


Figure 8. P-δ diagram for anchor type 4

In all cases of the tested anchors, the failure was different. There was concrete cone failure in most of the cases, but there were also steel failure and mixed failure (failure between concrete/adhesive/anchor).



Figure 9. Failure of anchor type 1



Figure 10. Failure of anchor type 2



Figure 11. Failure of anchor type 3



Figure 12. Failure of anchor type 4

This paper gives the results from the tested anchors that are embedded in accordance to the manufacturer recommendations. The testing was conducted so at least four anchors of each type fully developed failure occurs.

Anchor type 1, with double component epoxy injection, average value of the tested anchors 101.12kN. Anchor type 2, with epoxy resin injection, average value of the tested anchors 91.67kN. Anchor type 3, with mortar-based injection, average value of the tested anchors 89.80kN. Anchor type 4, with double component mortar injection, average value of the tested anchors 96.47kN. Manufacturer tension load for all 4 anchor types 55.19kN.

5. CONCLUSION

From the occurred data for this experimental research can be concluded that the behavior of the chemical anchors depends on many different factors, which always vary for each situation.

By obtaining the results and creating the load – displacement diagrams, the behavior of the mechanical anchors as elements for connection gives opportunity for ease of analysis. Conclusions from conducted pull-out test of mechanical anchors are that:

- The load-bearing capacity obtained from the experimental test is much higher than the calculated design load-bearing capacity of the anchors. The difference between the design and tested loads of tension anchors is not only due to the revised global and partial reliability coefficients, but additionally the design loads are reduced due to a number of parameters that in practice can not be precisely defined. With further analysis of the results and comparison with the given design and allowed tension loads from the manufacturers for each type anchor, can be concluded that maximum bearing capacity of the anchors is underestimated (62-83%).
 - Different based injection filler (epoxy-based or mortar-based), during static loads, have similar bearing capacity, with maximum difference around 12%.
 - Double component injection filler (epoxy-based or mortar based), during static loading, gives higher bearing capacity than the single component injection, with difference around 7-10%.
 - The type of chemical used as adhesive has little effect on the tensile strength of the anchor. While the process of drilling, cleaning the opening and the way of installing the anchor has a huge impact on the load capacity of the chemical anchor.
- [7] European Organization for Technical Approvals (2012): „ETAG 001-Guideline for European Technical Approval of Metal anchors for use in concrete, Part two: Torque-controlled expansion anchors “.
 - [8] European Organization for Technical Approvals (2012): „ETAG 001-Guideline for European Technical Approval of Metal anchors for use in concrete, Part three: Undercut anchors “.
 - [9] European Organization for Technical Approvals (2012): „ETAG 001-Guideline for European Technical Approval of Metal anchors for use in concrete, Part four: Deformation-controlled expansion anchors “.
 - [10] European Organization for Technical Approvals (2012): „ETAG 001-Guideline for European Technical Approval of Metal anchors for use in concrete, Part five: Bonded anchors “.
 - [11] European Organization for Technical Approvals (2012): „ETAG 001-Guideline for European Technical Approval of Metal anchors for use in concrete, Annex A: Details of tests “.
 - [12] European Organization for Technical Approvals (2012): „ETAG 001-Guideline for European Technical Approval of Metal anchors for use in concrete, Annex B: Tests for admissible service conditions detailed information “.
 - [13] European Organization for Technical Approvals (2012): „ETAG 001-Guideline for European Technical Approval of Metal anchors for use in concrete, Annex C: Design methods for anchorages “.

REFERENCES

- [1] Australian Engineered Fasteners and Anchor Council (2015): „Test and Evaluation Procedure for Concrete Screw Anchors “.
- [2] Cannon R.W. (1981): „Guide to the Design of Anchor Bolts and Other Steel Embedments “, Concrete International.
- [3] Damjanovski Vladimir (2015): „Testing the extraction of anchors in existing concrete slab“, MASE16 proceedings.
- [4] Denkovski Damjan (2019): „Experimental and analytical research of behavior of mechanical anchors“, master thesis, Skopje.
- [5] Dr. S.S.H Cho, „Guide on Design of post-installed anchor bolt systems in Hong Kong “, The Hong Kong Institute of Steel Construction
- [6] European Organization for Technical Approvals (2013): „ETAG 001-Guideline for European Technical Approval of Metal anchors for use in concrete, Part one: Anchors in general “.

Jovana Topalić Marković

MSc, Research Assistant
Faculty of Technical Sciences,
University of Novi Sad, Serbia
jovanatopalic90@uns.ac.rs

Vladimir Mučenski

PhD, Associate Professor
Faculty of Technical Sciences,
University of Novi Sad, Serbia
mucenskiv@uns.ac.rs

Igor Peško

PhD, Associate Professor
University of Novi Sad, Serbia
igorbp@uns.ac.rs

ONE EXAMPLE OF CIVIL ENGINEERING RESEARCH CONDUCTED WITH THE DELPHI METHOD

In this work one example of civil engineering research conducted with the Delphi method is shown. The Delphi method is one of the most popular scientific methods for research of problems with lack of known data. For this research, researcher must form the team of experts and analyze their answers on questions asked during the research with controlled feedback. In this article researcher wanted to prove hypothesis for making risk assessment model for planning and design processes of wastewater treatment plants. This research was conducted with Classical Delphi method is shown step by step.

Keywords: Delphi method, civil engineering, research, risk assessment model.

1. INTRODUCTION

The Delphi method or Delphi technique is specific type of research used in various scientific disciplines. Development of this method started in early 50s of the last century in Research and Development Corporation (RAND) in Santa Monica. It can be defined as a method that enables the process of group communication so that the process is effective and allows a group of individuals, as a whole, to agree on a solution to a complex problem, i.e. to reach a consensus [1].

For finding a solution of some unexplored problem the Delphi method implies sending questionnaires, which are structured or partially structured, to the examinee who are most often defined as experts or panel of experts. Replies are collected and in the following circles either the original or changed questionnaire is sent to the participants. Participants need to confirm or customize previous responses after the data from the last round has been processed. This procedure repeats until a consensus is reached, i.e., confirmation of the starting hypothesis. Often, panelists can explain their answers or give a certain confirmation. The research itself is anonymous, which is suitable for participants because they respond without pressure [2].

This research method is used in different areas of scientific research. In September 2008, a

review of the Scopus database was conducted, and out of the 15.000 articles published by 4.000 publishers, 105 articles were based on the Delphi method [3].

The Delphi method is highly suitable for research precisely because the participants are anonymous and feel that they can freely provide their opinion. When designing any research, the most important thing is to carefully select individuals for the team of participating experts. Depending on the method of research, one can clearly define a specific group of individuals who stand out in a certain field or choose participants who can help discover new ideas related to a certain field. This approach involves understanding a concept that is part of a much larger theory that the researcher plans to develop during the research [4]. In this research is shown implementation of the Delphi method in specific civil engineering research. The Delphi method is used for making risk assessment model for planning and design processes of wastewater treatment plants [5].

There are published research about implementation of the Delphi method in civil engineering research. In [6] is said that there are 7 studies up to 2008. implementing of the Delphi method in civil engineering research. Also, they concluded that structure of this method is suitable in different areas of research.

According to the research [7], the construction project management and planning were processed in 29 out of 88 papers based on the Delphi method, where this method was used to obtain and evaluate the risk data. It is also important to note that between 3 and 93 experts participated in the research based on the Delphi method, in the field of construction, and the number of rounds of research varied between 3 and 6. In [8], there is a description of the research engaging 14 experts: professors, engineers, contractors and experts in the field of international development.

If a researcher wants to use the Delphi method for research, there are some things to consider: type of the Delphi research, sample size, defining criteria for experts, anonymity and controlled feedback.

There are three types of the Delphi method [9]:

1. The Classical Delphi: This type of study is characterized by features: anonymity, iteration, controlled feedback, statistical group response and stability in responses among those with

expertise on a specific issue. Participants in this type of Delphi have expertise and give opinions to arrive at stability in responses on specific issues.

The Policy Delphi: The aim in this research is not to reach stability in responses among those with expertise but to generate policy alternatives by using a structured public dialogue. Here the Delphi is an instrument for policy development and promoting participation by obtaining as many divergent opinions as possible. It is characterised by 'selective anonymity', iteration, controlled feedback, polarised group response and structured conflict. Selective nonymity may mean that participants answer questions individually but may also come together in a group meeting.

The Decision Delphi: This type of Delphi is used for decision making on social developments. Reality is created by a group of decision-makers rather than from the ad-hoc decision of only a small number of persons. Crucial to this type is that decision-makers involved in the problem participate in the Delphi. They are selected according to their position in the hierarchy of decision-makers and the aim is to structure thinking so that consensus can be achieved. The characteristic is 'quasi-anonymity' (where people with expertise are mentioned by name and known to everybody from the beginning but questionnaire responses are anonymous).

Sample size for the Delphi method could be from 3 to 50, or more examinee [7]. The most of the research (71 percent) had less then 20 experts. The recommended number of participants in scientific research is 10 to 50. It is likely that the results will be suitable for analysis and that sufficient data will be obtained if the number of experts is up to 50.

In [10,11,12,13, 14] are defined different types of criteria to choose who can be an expert. After analyzing, there is a conclusion that every research is unique and criteria also. It means that researcher need to realize which results want and in accordance with that make criteria for experts.

The most obvious advantage [9] of guaranteed anonymity in responding to individual questions is that it is likely to encourage opinions that are free of influences from others and is therefore more likely to be 'true'. It has been suggested that anonymity encourages experts to make statements based on their personal knowledge and experience, rather than a more 'cautious institutional position' [15]. By adopting an

iterative approach to data collection through questionnaires and feedback however, the 'collective human intelligence capability' found in groups of people with expertise can be harnessed [1].

The research presented in this article was performed as a theoretical experiment. This article is focused on making of this theoretical experiment step by step. In research there were 35 experts consisted of engineers of various professions, chemists and spatial planners from the Republic of Serbia and Bosnia and Herzegovina.

The Delphi method was conducted in three rounds (zero, first and second round), the zero one of which represented the selection of experts based on their education and expertise influencing the research, whereas the remaining two involved risk analysis and assessment by the selected first round expert team [5].

2. STRUCTURE OF THE DELPHI RESEARCH

This research started with hypothesis that it is possible to obtain a risk assessment model for the construction process using the Delphi method.

The researcher chose this scientific method after analysis of suitable methods. Making of risk assessment model was the main goal of this research and Delphi method was adequate because of lack of data about civil engineering risks in design of wastewater treatment plants. After research of literature, there is a conclusion that Delphi method is suitable for civil engineering research. In this research there was a need to include experts from different areas connected with wastewater treatment and that was also a reason for using the Delphi method for research. Therefore, it was necessary to perform identification, analysis, and evaluation, i.e., the assessment and evaluation of the risk significance of WWTP construction [5].

As it is said for using of Delphi method, the researcher had to consider type of the Delphi research, sample size, defining criteria for experts, anonymity and controlled feedback.

For this example of civil engineering research conducted with the Delphi method, the Classical Delphi was used. Team of experts is selected, because in this type of Delphi, participants have expertise and give opinions to

arrive at stability in responses on specific issues. For them, it is important that they are multidisciplinary, available and experts in the field of research [15].

To participate in the research, potential experts were selected based on experience in the planning and design processes of wastewater treatment plants. The number of experts with experience in this field is small because the topic itself is not sufficiently represented in Serbia. Therefore, the researcher decided to include experts from the state of Bosnia and Herzegovina in the research. On the territory of this state, planning and design laws are like laws in Serbia, and experts themselves have experience in both Serbia, and Bosnia and Herzegovina.

Sample size for this research was 35 experts, and this is number of experts which fits the suggested number of participants in the method. Thirty-five experts with experience in planning, designing, or constructing a wastewater treatment plant were selected to participate in the research. The team of 35 experts consisted of engineers of various professions, chemists and spatial planners from the Republic of Serbia and Bosnia and Herzegovina.

Researcher made specific criteria for expert's identification relying on literature instructions. Criteria is shown in Table 1.

Table 1. Criteria for experts

Number	Criteria	Explanation
1	Original scientific work	The expert has published scientific work in the field of risk management or wastewater treatment
2	Conference experience	The expert has participated in conferences or scientific meetings in the field of risk management or wastewater treatment
3	Experience in urban planning	The expert was involved in the development of two or more spatial or urban plans, defining the location of wastewater treatment plants

4	Experience in topic of research	The expert participated in the development of two or more previous studies or feasibility studies for the construction of wastewater treatment plants
5	Work experience	The expert has five or more years of experience in planning or designing or running wastewater treatment plants
6	Scientific experience	The expert works at the University
7	Professional associations	The expert is member of some professional associations
8	License	The expert is licensed engineer

The requirement to define the research participant as an "expert", was to meet 3 out of 8 criteria. Only two participants didn't meet this requirement.

The author himself, as a research facilitator of the method, fully respected the anonymity of the experts and their conclusions. Examinee felt free to express their opinion on certain risks and why they evaluated risks in that way. This approach has great benefit to the research.

The research was conducted through several phases in the Delphi method by forming a questionnaire given to the experts, specific analysis and systematization of the obtained data and forming a model for preliminary risk assessment (with quantified risks) [5].

Controlled feedback was the most important part because, after each round, there was need to analyze data proceeded from the experts. The Delphi method was conducted in three rounds (zero, first and second round), the zero one of which represented the selection of experts based on their education and expertise influencing the research, whereas the remaining two involved risk analysis and assessment by the selected first round expert team. After three rounds and statistical analysis the risk assessment model was made. This proved hypothesis from the beginning of the research.

3. CONCLUSION

In this research is shown one example of civil engineering research conducted with the Delphi method. This scientific method is very used in different areas of research, but in civil engineering research isn't implemented as in other areas of research. After literature review there was conclusion that this method can be used for civil engineering research. This research started with hypothesis that it is possible to obtain a risk assessment model for the construction process using the Delphi method. By selecting experts based on defined criteria and implementing an anonymity with controlled feedback, the researcher obtained the desired result – risk assessment model planning and design processes of wastewater treatment plants. This model was the proof for possibility of using this method in civil engineering research.

Acknowledgements

The paper presents the part of research realized within the project "Multidisciplinary theoretical and experimental research in education and science in the fields of civil engineering, risk management and fire safety and geodesy" conducted by the Department of Civil Engineering and Geodesy, Faculty of Technical Sciences, University of Novi Sad.

REFERENCES

- [1] Linstone, H. A., Turoff, M. (1976), "The Delphi Method: Techniques and Applications", Journal of Marketing Research, 13(3), pp. 317–318,
- [2] Mullen, P. (2003), "Delphi: myths and reality, Journal of health organization and management", 17(1):37-52, DOI:10.1108/14777260310469319
- [3] Gordon, T. J. (2009), "The Delphi Method", [pdf] The Millennium Project, Washington, DC, USA, Available at: <http://www.millennium-project.org/wp-content/uploads/2020/02/04-Delphi.pdf>
- [4] Creswell, J. W. (2012), "Planning, conducting and evaluating quantitative and qualitative research", 4th ed., Pearson, Boston, MA, USA,
- [5] Topalić Marković J., Mučenski, V., Savić, D., Velkovski, T., Peško, I., Tomaš, L. (2020), „Risk Assessment Model for Planning and Design Processes of Wastewater Treatment Plants“, Periodica Polytechnica Civil Engineering, Available at: <https://doi.org/10.3311/PPci.16740>
- [6] Hollowell, M.R., Gambatese, J.A. (2010), „Qualitative Research: Application of the Delphi Method to CEM Research“, Journal of Construction Engineering and Management,

- Volume 136, Issue 1, Available at: <https://ascelibrary.org/doi/abs/10.1061/%28ASCE%29CO.1943-7862.0000137>
- [7] Ameyaw, E. E., Hu, Y., Shan, M., Chan, A. P. C., Le, Y. "Application of Delphi method in construction engineering and management research: a quantitative perspective", *Journal of Civil Engineering and Management*, 22(8), pp. 991–1000, 2016. Available at: <https://doi.org/10.3846/13923730.2014.945953>
- [8] Kaminsky, J., Javernick-Will, A. (2013), "Contested Factors for Sustainability: Construction and Management of Household On-Site Wastewater Treatment Systems", *Journal of Construction Engineering and Management*, 139(12), Available at: [https://doi.org/10.1061/\(ASCE\)CO.1943-7862.0000757](https://doi.org/10.1061/(ASCE)CO.1943-7862.0000757)
- [9] Hanafin, S. (2004), „Review of Literature on the Delphi Technique“, The National Children’s Office, Dublin, Ireland
- [10] Hsu, C.C., Sandford, B.A. (2007), “The Delphi Technique: Making Sense of Consensus“, *Practical assessment, research and evaluation*, volume 12, article 10
- [11] Tersine, Richard J.; Riggs, Walter E. (1976), „The Delphi Technique: A Long-Range Planning Tool“, *Business Horizons*, 19, 2, 51-56, Apr 76
- [12] Rogers, M. R., Lopez, E. C. (2002), „Identifying critical cross-cultural school psychology competencies“, *Journal of School Psychology*, 40, 115–141
- [13] Veltri, A. T. (1985), „Expected use of management principles for safety function management“, (PhD thesis) West Virginia University, Morgantown, West Virginia
- [14] Rajendran, S. (2006), „Sustainable Construction Safety and Health Rating System“, Oregon State University, Corvallis, USA
- [15] Gupta, U.G., Clarke, R.E. (1996), *Theory and Applications of the Delphi Technique: A Bibliography (1975-1994)*
- [16] Meyer T., Reniers G. (2013), „Engineering risk management“, De Gruyter



MACEDONIAN TEAM IN THE BUNDESLIGA



Chair of concrete and timber structures

BE PART OF THE TEAM!



Joint activities in research projects, international conferences and publication of journal papers



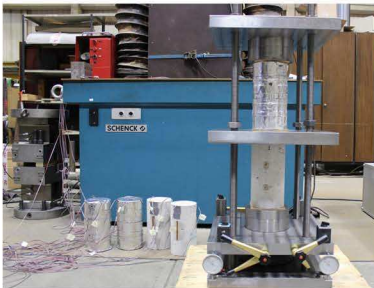
CONCRETE STRUCTURES

Prof. Dr.-Ing. habil. P. Mark



RUB
RESEARCH SCHOOL

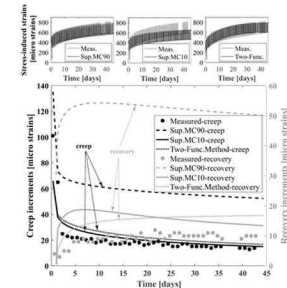
Scholarships for our young researchers provided by the RUB Research School, Germany



Experimental investigation of concrete creep and creep-recovery phenomenon, Structural testing laboratory KIBKON, RUB-Germany



Long-term experiments on reinforced concrete elements subjected to real load histories, Laboratory for concrete and structures, FCE-Skopje



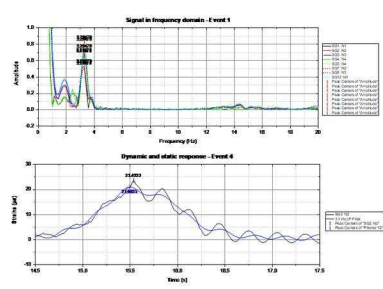
Analytical models for prediction of long-term deformations of concrete elements



Static and dynamic proof loading tests on roadway concrete bridges



Measurements of strains and deflections during the proof loading tests of concrete bridges



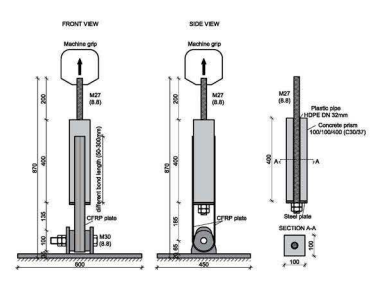
Determination of dynamic amplification factor (DAF) using Fast Fourier Transform and low-pass filtering



Time-dependent behavior of rc elements under sustained loads with various intensity, Laboratory for concrete and structures, FCE-Skopje



Long-term experiments on reinforced concrete elements strengthened by carbon strips, Laboratory for concrete and structures, FCE-Skopje



Short-term tests of concrete-carbon strips bond, Structural testing laboratory KIBKON, RUB-Germany

Marija Vitanova

PhD, Associate Professor
University “Ss. Cyril and Methodius”
IZIIS, Skopje, N. Macedonia
marijaj@iziis.ukim.edu.mk

Julijana Bojadjeva

PhD, Associate Professor
University “Ss. Cyril and Methodius”
IZIIS, Skopje, N. Macedonia
jule@iziis.ukim.edu.mk

Slobodan Micajkov

Researcher
University “Ss. Cyril and Methodius”
IZIIS, Skopje, N. Macedonia
micajkov@iziis.ukim.edu.mk

REGIONAL INFRASTRUCTURE INVENTORY TOWARD SEISMIC NETWORK SAFETY

Bridges represent a critical facet when determining a community's resilience to a disaster and its ability to resume normal activities. The accurate prediction of the future condition of bridges is an important part of any bridge management system. Past bridges inspection data along with information on any repair and/or retrofit can provide a baseline for predicting their future conditions. To develop a reasonable estimate for future bridge safety, this paper describes a creation of the information system that get insight into the critical infrastructure elements and can identify the losses that can be caused by earthquake. This system includes bridge infrastructure network elements from the N. Macedonian region. An extended database of bridge population (created for the Infra-NAT project www.infra-nat.eu) is developed through a data collection form and allows for a detailed exposure model of the bridge network to be compiled. The database is upgraded with retaining walls that are important parts of the regional transportation network. By considering the general characteristics of the bridge, a representative sample of bridges is chosen to develop fragility functions for bridges exposed to seismic hazard. To estimate the physical vulnerability and potential economic losses due to seismic hazards to all transportation network, seismic risk assessment toll is developed. The results enable a better understanding of the relevance of the vulnerability level of critical infrastructure in the analyzed region, correlating it to the corresponding levels of development, as well as other socio-economic variables.

Keywords: bridge inventory, seismic hazard, exposure, fragility curves.

1. INTRODUCTION

The resistance of the transportation infrastructure systems is of a primer importance, particularly in the period after occurrence of any natural or man-made disaster. In an environment exposed to frequent natural disasters (earthquakes, floods,

landslides and alike) as is the case with N. Macedonian region, it is of a particular importance to monitor the conditions of the transportation infrastructure and all its elements for the purpose of obtaining timely information about their current conditions, conceiving and evaluating possible risks and their mitigation.

Although the occurrence of natural disasters is inevitable in numerous cases, considering their consequences, we are increasingly becoming aware of the importance of fulfillment of serious obligations of all entities within the system of action in conditions of crisis, related to establishment and development of systems and standards for prevention and mitigation of consequences for the purpose of proactive management of the risk through adequate prioritization and taking preventive measures. Pursuant to item 6.9 of the National Platform for Mitigation of Disaster Risks announced by the Government of RNM in September 2019, IZiIS is involved in the activities for prevention and early warning, performing: research of earthquake phenomena and their manifestation upon ground and consequences upon engineering structures; exploration of risks pertaining to natural disasters; development and improvement of methods of management of natural disasters and alike.

This paper presents part of the research activities in the framework of two projects “Upgrading and Improvement of Information System on Transportation Infrastructure and Seismic Risk Assessment for New Infrastructure Structure” [1] and international project Infra-NAT (783298 – INFRA-NAT – UCPM-2017-PP-AG, <http://www.infra-nat.eu/>). [2]. The projects are oriented towards particular contribution in definition of the regional infrastructure inventory and amendment of the already defined comprehensive frame for monitoring of the vulnerability of the bridge infrastructure in our country.

For the purpose of the analyzed inventory database, the analytically developed type of fragility curves were developed. The mathematical description facilitates their incorporation in computational environments for regional risk and resilience assessment of transportation networks such as introduced in MAEviz (Mid-America Earthquake Center 2006) [3], Hazus (Hazus-MH 2011) [4]. These analytical fragility models have received increased attention in the literature in the past decade given their ability to overcome limitations of subjective expert-based fragilities or empirical ones that are constrained by the lack of adequate data, as stated in Gidaris et al. (2017) [5].

2. INFRASTRUCTURE INVENTORY

Different countries have different institutions that maintains bridge inventory data systems. Illinois Highway Information System has data for 2,601 bridge [6]. In Serbia, predecessor of the ‘Roads of Serbia’ public enterprise, the Road Directorate of Serbia, began recording bridge inspection data in a database named BPM (in Serbian **B**aza **P**odataka o **M**ostovima) in 1990 [7].

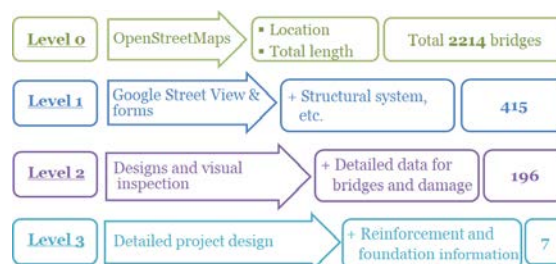


Figure 1. Schematic presentation of levels of data on the bridges

For the territory of N. Macedonia, an information system was created including data on a total of 679 bridge structures that are part of the existing motorways and main roads in our country, selected due to their extraordinary importance for the country and the region. A most up-to-date model of seismic hazard and the most reliable time histories for analysis of bridge structures, were also defined. For each of these bridge structures, different number and type of data are available. The information entered into the information system is divided into three sets: 1) Level 0, involving data on the location of the structure and its total length; 2) Level 1, data of level 0 + involve material, structural system and alike; 3) Level 2, level 1 + involves complete geometry and damage data; and 4) Level 3, level 2 + includes data on the reinforcement and foundation (Fig. 1).

Locations of the bridges with Level 0 and 1 data are given on Fig. 2 [2].

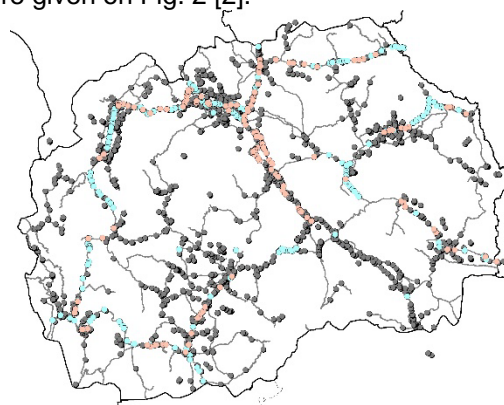


Figure 2. Bridge locations with Level 0 data (grey), Level 1 (blue) and Level 2 (pink)

Based on the data from the created information platform, a typological classification of the bridges was made as the basis for formulation of analytical models for definition of the vulnerability of different bridge typologies. For each typology, there were developed numerical models per 50 bridge structures with different geometrical parameters, including span length, height of central piers and width of superstructure. For each of these bridges, nonlinear dynamic analyses were performed using 30 time histories with 7 hazard levels, or more specifically, over 10000 analyses were done for each type. The used methodology is published in the literature [8]. The obtained results were used for development of vulnerability curves for each of the different typologies and these were entered into the web-based platform that has the possibility of identifying the critical parts of the infrastructure network (<http://www.infra-nat.eu/web-based-platform/>). For 2 span bridges results are given on Fig. 3, for 3 span on Fig. 4 and for 4 spans on Fig. 5.

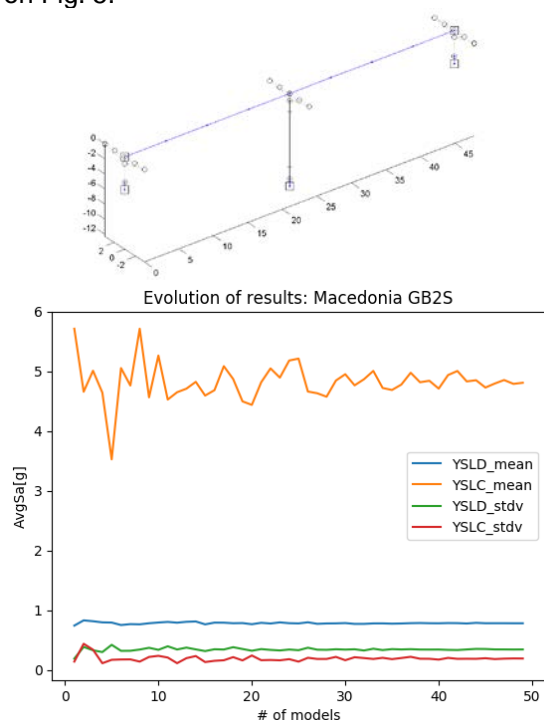


Figure 3. Numerical model and results from the vulnerability analyses for 2 span girder bridges (mean and standard deviation of damage and collapse limit state of risk indicator (Y) for whole system).

After the definition of the vulnerability curves, the infrastructure inventory is upgraded with information of other structures that are part of the transportation system and assessing the risk. The main activities involved three phases 1) acquisition, processing of data on structures

and definition of vulnerability; 2) analysis and integration of the seismic conditions and site soil conditions; 3) risk assessment which are explained below.

2.1 PHASE 1

The first phase of the research was upgrading the information system with data on new structures that are part of the Miladinovci-Shtip motorway, part of the Deve Bair – Kafasan motorway as well as part of the state roads A4 Shtip – Radovish and A1 Prilep-Gradsko. That includes bridge structures and retaining walls. The system is upgraded with 20 such structures. For all of these structures design documentation was provided, mainly bridges that are situated along the roads in the part bordering on Greece and Albania for the purpose of preparations for the international project financed by EU, namely, CRISIS (Comprehensive Risk Assessment of Basic Services and Transport Infrastructure) that just started and will be coordinated by IZiIS (www.crisis-project.org).

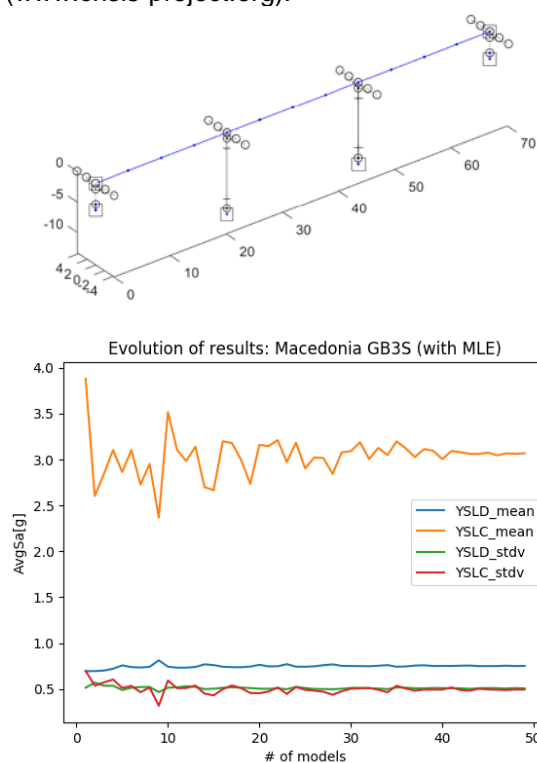


Figure 4. Numerical model and results from the vulnerability analyses for 3 span girder bridges (mean and standard deviation of damage and collapse limit state of risk indicator (Y) for whole system)

This first phase started with first part which included definition, i.e., selection of roads, i.e., railway corridors that have to be encompassed, selection of structures whose data have to be included in the information system, and finally,

providing safety to these structures. For all types of structures, a certain number of data are entered into the system. These data will refer to structures that are part of the new motorways, state roads. For most of these structures detailed data were available, encompassing level 3, meaning that, in addition to location and total length of the structure, these include data on the structural system complete geometry, data on the foundation and the reinforcement. Integrated in the system will be also data on the type of soil. In this phase data affecting the stability of the structures that are of a temporary character were included. Inspection of the conditions of the greater number of structures was done in 2007, while regular inspection on some of the structures was done in 2017.

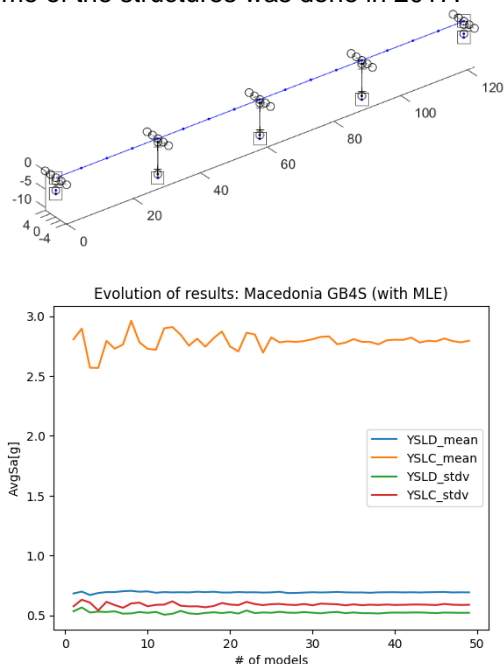


Figure 5. Numerical model and results from the vulnerability analyses for 4 span girder bridges (mean and standard deviation of damage and collapse limit state of risk indicator (Y) for whole system)

These data are the subject of inspection by institutions that manage the road and railway network and are of a particular importance for the stability of the structures as they affect their vulnerability and risk. With these information, the already existing information system was considerably upgraded and improved. In addition to the main geometrical data and data on damages, the information system integrates data referring to vulnerability of each of the structures that is the basis for definition of the seismic risk for each structure taken separately. Most of the structures that are part of the information system belong to one of the different structural typologies for which two

levels of vulnerability were already defined within the frames of the Infra-NAT project [9].

2.2 PHASE 2

With the completion of the first phase, the activities envisaged in the second were started within which the hazard conditions were defined for each structure, depending on the site soil conditions and the seismic hazard on the site. The hazard was defined through three parameters of expected seismic events: 1) location (where), 2) genesis and evolution (how much) and 3) intensity (degree). Mapping of the hazard consists of consistent and uniform discretization of the territory of Macedonia into smaller territorial units of a size suitable for reasonable monitoring of changes of all parameters referring to distribution and concentration of the hazard. These data were basic for the realization of the last phase of the project.

2.3 PHASE 3

The final, third phase, involved activities related to risk assessment. It represents a factor that is not constant, but changes in the course of time. The frame for risk management assessment provides the static current state of the risk at a certain time and place that is changed by following the dynamics of the hazard and the dynamics of the parameters affecting the vulnerability of structures. In this phase, assessment of the current risk was made for the structures included in the information system that also includes the newly built structures that are part of the Miladinovci – Shtip motorway and part of the Deve Bair Kafasan motorway as well as state roads A4 Shtip – Radovish and A1 Prilep – Gradsko. In the first part of this phase, the parameters to be used for risk assessment were defined. A methodology for monitoring and consideration of vulnerability by following the characteristic indicators or a group of indicators was applied, that recognized and indicated the conditions that are with a great probability of causing the occurrence of a certain hazard and realization of the corresponding risk. The information system offers the possibility of a multiple risk assessment, namely, when change of some characteristic indicators or a group of indicators affecting the vulnerability or definition of risk takes place, it will be possible to re-assess the risk. This system provides the possibility for temporary definition of the risk pertaining to the transportation network, which considerably contributes to high quality fulfilment of the obligations of the Institute as part of the National Frame, creating tools that can be used

by the institutions in charge of management of the transportation infrastructure and effectuation of the necessary controls for the purpose of mitigation of the consequences of possible risks and bringing the exposure to risk to an acceptable level. Fragility curves for the typical bridge structures in R.N. Macedonia, obtained from the analyses are given on Fig. 7, 8 and 9 [10].

3. TOWARD SEISMIC NETWORK SAFETY

The created system gives a great contribution to getting a better insight into the risk related to natural hazards pertaining to the critical infrastructure by development and refinement of a comprehensive frame for evaluation of vulnerability, with a special focus on the seismic hazard and the effects of ageing/deterioration of the transportation infrastructure network that can be used independently by a number of countries. The results of this research are double: greater knowledge and increased awareness.

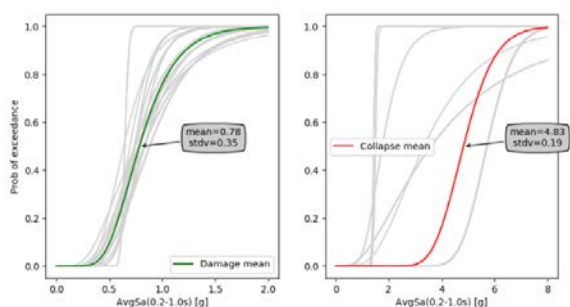


Figure 7. Fragility curves for the 2 spans girder bridges

By synthesis of the data on the exposure and the vulnerability of the critical infrastructure in the territory of a country, one can obtain new knowledge and better insight into the current number, location and conditions of existing elements of the considered critical infrastructure.

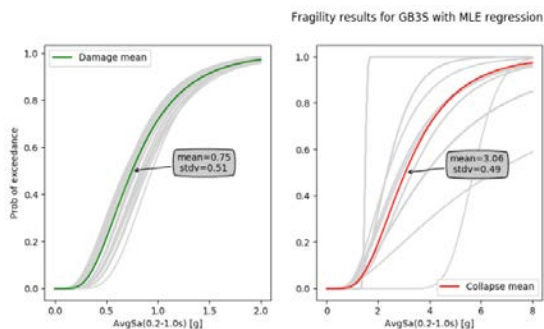


Figure 8. Fragility curves for the 3 spans girder bridges

Increased awareness about natural hazards and changes of existing critical infrastructure facilities is necessary for the success of the strategies of response to emergency situations and definition of the level of resistance of the European (and neighboring) societies.

By realization of all the activities realized in this research, the following is achieved:

- Integration and harmonization of data in the information system with data on the entire
- Exposure of the structures that are part of the main roads and motorways in our country, including bridges, retaining walls and alike. These data will provide all relevant information about the structures at regional level;
- Combination of existing seismic hazard models and their including into the information system;
- Characterization of the direct physical vulnerability and indirect losses through existing methods from former studies of seismic risk and through an innovative approach to fast consideration of reduced capacity due to deterioration of structures;
- Monitoring of the risk will be enabled through relevant factors of monitoring, parameters and data for identification of the efficiency of the existing frames of risk management;
- The application of the information system in using prevention measures, effective management of resources and prioritization, with a focus on seismic hazard and effects of ageing of bridges, will contribute to the increase of resistance of the critical infrastructure;
- For the local and regional bodies, there will be provided the necessary tool for risk assessment through definition of the vulnerability of the critical infrastructure, providing thus instructions for optimal distribution of available resources. This tool can also be used in other European countries.

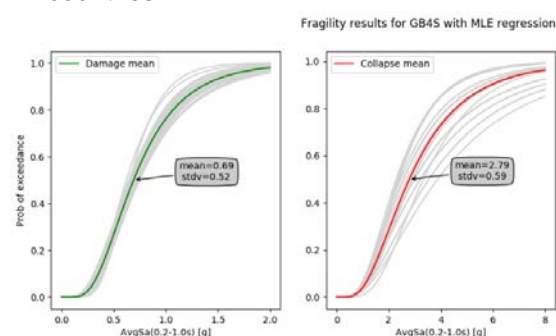


Figure 9. Fragility curves for the 4 spans girder bridges

4. CONCLUSIONS

This paper deals with research which anticipated to enable upgrading and improvement of the information system that was created within the international project Infra-NAT (783298 – INFRA-NAT – UCPM-2017-PP-AG, <http://www.infra-nat.eu/>) with structures that are part of the infrastructure network on the territory of N. Macedonia. In addition to bridges, the system includes newly built retaining walls that are part of the state roads and motorways that are under construction. Presented here are the results from the performed nonlinear analyses of bridge samples and calculation of the fragility curves.

To estimate transport network vulnerability, seismic assessment tool is developed based on bridge inventory system. Of particular importance is the including of parameters that are of a temporary nature and refer to the conditions of the structural and non-structural elements that directly affect the stability and vulnerability of the structures. These data can be collected in a certain time period and then integrated into the system and processed. As a result of their analysis, one can get an insight into the critical infrastructure elements and identify losses to be caused by an earthquake event. These could contribute to the process of optimization of the distribution of resources by public and private stakeholders.

The creation of this tool was based on systematic approach through integration of national and international practice and theoretical and methodological soundness whereby practical usability of the offered system solution was achieved. In this sense, this system can be used as a referent model for a consistent approach to prevention, early warning and management of a large number of risks and possible seismic disasters. The main advantage of this system is that it can easily be upgraded and adapted in order that it could also be used beyond the boundaries of our country. By application of this tool, the process of management of infrastructure elements can be systematized and made practical and simple by which it can significantly contribute to the improvement of the conditions for its use for the purpose of development of the country and improvement of the lives of its citizens.

Acknowledgements

The authors would like to acknowledge the financial support of the INFRA-NAT project (www.infra-nat.eu) co-funded by European Commission DG-ECHO – Humanitarian Aid and Civil Protection.

Project reference: 783298 – INFRA-NAT – UCPM-2017-PP-AG.

REFERENCES

- [1] Vitanova, M. (2020). Upgrading and Improvement of Information System on Transportation Infrastructure and Seismic Risk Assessment for New Infrastructure Structures. Application for a proposal of a scientific research project financed by IZIS
- [2] D 2.3 Final Database of Bridge Data and Summary Report, Increased Resilience of Critical Infrastructure under Natural and Human- induced Hazards (INFRA-NAT), <http://www.infra-nat.eu/>
- [3] Elnashai, A. S., & Hajjar, J. F. (2006, December). Mid-America Earthquake Center Program in Consequence-Based Seismic Risk Management. In *8th US National Conference on Earthquake Engineering 2006* (pp. 8624-8630).
- [4] Schneider, P. J., & Schauer, B. A. (2006). HAZUS—its development and its future. *Natural Hazards Review*, 7(2), 40-44.
- [5] Gidaris, I., Padgett, J. E., Barbosa, A. R., Chen, S., Cox, D., Webb, B., & Cerato, A. (2017). Multiple-hazard fragility and restoration models of highway bridges for regional risk and resilience assessment in the United States: state-of-the-art review. *Journal of structural engineering*, 143(3), 04016188.
- [6] Bolukbasi, M., Mohammadi, J. and Arditi, D., Estimating the Future Condition of Highway Bridge Components Using National Bridge Inventory Data. *Practice Periodical on Structural Design and Construction*, ASCE, 2004.
- [7] Masovic, S.&Hajdin, R. Modelling of bridge elements deterioration for Serbian bridge inventory, *Structure and Infrastructure Engineering*, 2014 Vol. 10, No. 8, 976–987,
- [8] Borzi, B., Ceresa, P., Franchin, P., Noto, F., Calvi, G. M., & Pinto, P. E. (2015). *Seismic Vulnerability of the Italian Roadway Bridge Stock*. *Earthquake Spectra*, 31(4), 2137–2161. doi:10.1193/070413eqs190m
- [9] Deliverable D3.2. *Portfolio of bridge technology numerical models and fragility functions*, Increased Resilience of Critical Infrastructure under Natural and Human- induced Hazards (INFRA-NAT). <http://www.infra-nat.eu/deliverables/>
- [10] Deliverable D6.2. *Case Study Application in R.N.Macedonia*, Increased Resilience of Critical Infrastructure under Natural and Human- induced Hazards (INFRA-NAT), <http://www.infra-nat.eu>